8-2022

Characterization of Kinases and Hypothetical Proteins in the Entamoeba Species

Heather Andrews Walters
Clemson University

Characterization of kinases and hypothetical proteins in the *Entamoeba* species

A Dissertation

Presented to

the Graduate School of

Clemson University

In Partial Fulfillment

of the Requirements for the Degree

Doctor of Philosophy

Biological Sciences

by

Heather Andrews Walters

August 2022

Accepted by:

Dr. Lesly Temesvari, Committee Chair

Dr. Lukasz Kozubowski

Dr. Zhicheng Dou

Dr. James Cardelli

ABSTRACT

Entamoeba histolytica is a protozoan parasite that causes amebic dysentery and amoebic liver abscess. This pathogen possesses a two-stage life cycle consisting of an environmentally stable latent cyst and a pathogenic amoeboid trophozoite. Since infection is acquired by ingestion of cysts from contaminated food and water, this parasite is prevalent in underdeveloped countries. A reptilian pathogen, *Entamoeba invadens*, which can encyst in culture, has long-served as a surrogate to study stage conversion. Much remains unclear about stage conversion and the stress response in these parasites and current treatments for amoebiasis are lacking, as they cause severe side effects. Ultimately new therapeutic strategies are needed and the parasite stress response and stage conversion mechanisms may represent targetable vulnerabilities. To gain insight into these cellular processes, we characterized two hypothetical proteins, EIN_059080 (in *E. invadens*), and EHI_056700 (in *E. histolytica*). We also characterized two putative eIF2 alpha kinases in *E. invadens*. In all cases, we used an RNAi-based silencing system to reduce expression of the genes. Reduction of EIN_059080 expression resulted in a decreased rate of encystation and an increased rate of erythrophagocytosis, an important virulence function. Additionally, these mutants were more susceptible to oxidative stress. Similarly, reduction of EHI_056700 resulted in increased susceptibility to oxidative stress and glucose deprivation, but not to nitrosative stress. Interestingly, parasites with decreased expression of EHI_056700 also exhibited decreased erythrophagocytosis and adhesion to host cells. We authenticated the two eIF2α kinases using a heterologous yeast system. Parasites with decreased kinase expression exhibited decreased phosphorylation of eIF2α and increased sensitivity to oxidative stress. Diminished kinase expression also correlated with an increased rate of encystation, a decreased the rate of excystation, and an increase in several virulence functions, erythrophagocytosis and adhesion to host cells. Taken together, these data suggest that these hypothetical proteins and

kinases may play a role in various aspects of stage conversion, virulence, and the response to stress.

DEDICATION

       To Henry and your future siblings- As I worked tirelessly to finish these projects, I dreamt of you and the family that your father and I would build. You will never have to wonder how much I adore you and how I cherish every moment that I spend with you. While I am proud and excited about the career that I am building, you are my greatest dreams come true.

ACKNOWLEDGEMENTS

I'd like to thank Dr. Temesvari for being an incredible mentor. Her passion and enthusiasm for research and teaching has been truly inspiring. She is the scientist that I will always inspire to be. I would also like to thank Dr. Lukasz Kozubowski, Dr. Zhicheng Dou, and Dr. Jim Cardelli for their support and guidance during this project. Their advice has been invaluable.

Thank you to Brenda Welter for your never-ending support and advice, for all the answered phone calls and text messages, and for teaching me everything you know!

Finally, I would like to thank my husband, Joshua. Your support and encouragement during the last 5 years have been instrumental in my success. Thank you for taking true joy in my work and for picking up the slack when science took up 100 percent of my time. I couldn't have accomplished this without you.

TABLE OF CONTENTS

Page

LIST OF FIGURES

LIST OF TABLES

CHAPTER ONE

LITERATURE REVIEW

I.   Introduction

Entamoeba histolytica is the causative agent of amebic dysentery and amebic liver abscess. In the late 1990's the World Health Organization (WHO) estimated that 50 million people worldwide were infected with *E. histolytica*, which causes over 100,000 deaths annually (1). Infection occurs when the infectious cyst form of the organism (see Figure 1.1) is ingested from contaminated food and water. According to a 2020 report published by the WHO, approximately 2 billion people lacked access to safely managed drinking water services, while 670 million people lacked access to hand washing stations. Four hundred and ninety-four million people continue to defecate in the open (2) . In 2015,10% of the world's population consumed crops that had been irrigated with contaminated water. Therefore, there is considerable global risk for acquiring infection and it is not surprising that this disease is prevalent in developing countries where sanitation is substandard, such as the middle east and sub-Saharan Africa (3).

This pathogen not only affects indigenous populations, but also poses great risks to American travelers, soldiers, and aid-workers (4,5). In March 2018, USA Today reported that American soldiers were deployed in countries where this parasite is highly prevalent, including Afghanistan, Iraq, Syria, Niger, Yemen, and Somalia (6). *E. histolytica* is classified as a category B bioterrorism pathogen by the National Institute of Allergy and

Figure 1.1: Life Cycle of *Entamoeba Histolytica*
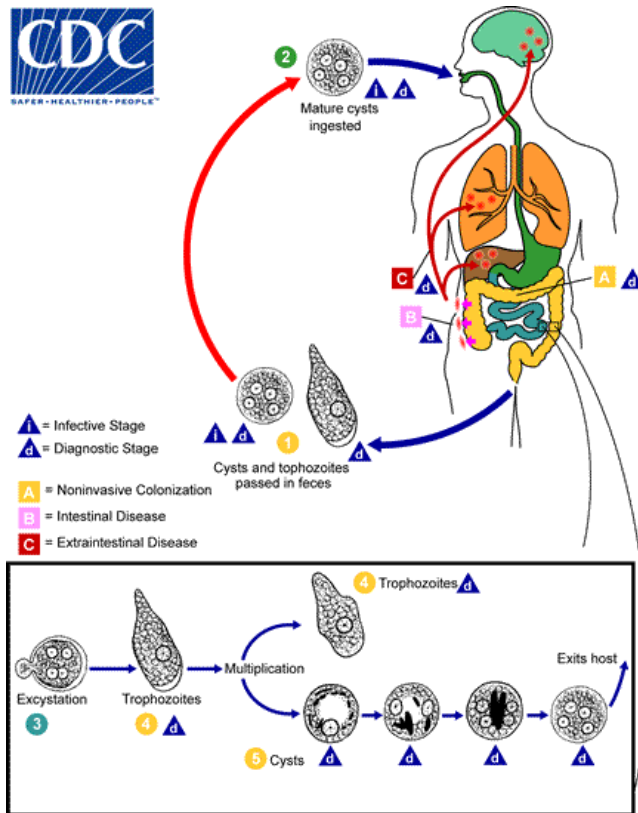
The infective stage of the parasite is the latent cyst, which can persist in the environment for extended periods of time. Quadrinucleated cysts are ingested through contaminated food or water. As the cysts pass through the digestive system unharmed, unknown signals trigger excystation in the small intestine, where each cyst can release 8 mature trophozoites. The motile trophozoites travel to the large intestine, where trophozoites feed on the mucosal lining or on natural gut flora. Unknown cues trigger encystation of a small percentage of trophozoites, and cysts and trophozoites are passed back into the environment through feces. Trophozoites are vulnerable outside of their human host, while the cysts can persist and continue the life cycle. Image modified from the Centers of Disease Control, 2019.

Infectious Disease for several reasons. First, the organism can be manipulated genetically. Thus, it is conceivable that a hyper-virulent strain of the parasite could be developed. Second, the cysts can persist in harsh environments for long periods of time due to their chitinous cell wall. For example, this form of the parasite is resistant to heat, desiccation, low pH, and disinfectants, such as chlorine (5,7). Third, infection can be acquired by ingesting a relatively low dose of cysts (5). Fourth, symptoms mimic those of other enteric infections making diagnosis difficult. Ultimately, *E. histolytica* continues to pose a considerable threat to public health.

 Life Cycle

This microaerophilic parasite has a simple two-stage lifecycle (See Figure 1.1), comprised of the infective latent cyst and the pathogenic trophozoite. Cysts can persist in harsh conditions for long periods of time due to its chitinous cyst wall. Once ingested, quadrinucleated cysts travel through the digestive system, where unknown cues trigger excystation in the small intestine. Each cyst can release 8 mature trophozoites. Motile trophozoites travel to the colon and adhere to the protective mucin layer via a galactose and N-acetyl-D-galactosamine (Gal/GalNAc)–specific lectin, which resides on the surface of the parasite (8). In the large intestine, infection proceeds via two non-mutually exclusive routes: trophozoites can either feed on the mucosal lining and natural gut flora, establishing an asymptomatic infection or trophozoites can degrade the mucin and invade the underlying intestinal epithelium, establishing an invasive infection.

During symptomatic infection, trophozoites may completely degrade the intestinal epithelium and enter the bloodstream, allowing the parasite to establish extra-intestinal infections in organs such as the liver, lungs, and rarely, the brain (9,10). In both types of infections, trophozoites reproduce by binary fission and continue feeding on host cells and gut-dwelling bacteria until unknown signals trigger trophozoite aggregation and subsequent encystation. Mature trophozoites and cysts are then passed through the feces and back into the environment (1). Recently, encystation of E. *histolytica* has been observed *in vitro* in cultures lacking glucose

and seeded at high densities (50,000 cells/mL) (11) *Entamoeba invadens,* a parasite that causes amebiasis in reptiles, is routinely used as a model organism. Synchronous encystation of *E. invadens* can be triggered *in vitro* by a combination of glucose starvation, serum starvation, and osmotic shock (12).

Treatment

Current treatment for amebiasis is metronidazole, an antibiotic from a class of drugs known as nitroimidazoles. These drugs function by passively diffusing into anaerobic cells as an inactive prodrug. Once in the cytoplasm, the drug is reduced into a short-lived nitroso free radical, which damages DNA, ultimately leading to cell death. This drug has been used to successfully treat amebiasis, trichomoniasis, giardiasis, and anaerobic bacterial infections for over 55 years (13). However, high toxicity and severe side effects have been observed when treating amebiasis. Metronidazole is highly absorbed in the small intestine and *E. histolytica* colonizes the large intestine. Therefore, treatment of amebiasis typically requires a high dosage of metronidazole, which in turn, leads to side effects like liver toxicity (14,15). Additionally, there are concerns that the parasite could quickly develop drug resistance. While drug resistance is not prevalent in *E. histolytica*, occasional reports of metronidazole failures, not attributable to patient non-compliance, suggest the possibility for the development of clinical resistance (16–18). Furthermore, metronidazole-resistant strains have been produced in the laboratory (18). One way in which resistance could occur is through re-oxidation of the drug in the presence of molecular oxygen, converting the drug back to its inactive form (13). Finally, metronidazole is thought to be carcinogenic (19). Since metronidazole is presently the only treatment for invasive amebiasis, there is an urgent need to develop a more efficient drug or a vaccine (5).

II.   Stress Response in *Entamoeba histolytica*

Beside the environmental stresses experienced by the cyst form of the parasite, the amoeba encounters harsh conditions in the host. These include low pH (as the parasite passes through the stomach) heat shock (due to fever), and glucose starvation (in the large intestine), and immune modulators such as reactive oxygen and reactive nitrogen species produced by neutrophils and macrophages (10). It has been hypothesized that nitrosative stress may also induce endoplasmic reticulum (ER) stress in this parasite (20). ER stress is characterized by a buildup of misfolded proteins and disturbances in ER function. Despite facing these various stressors while invading its human host, *E. histolytica* can ultimately persist and establish infection (21). Therefore, this amoeba must be able to adapt to its ever-changing environment. Exploring the stress response of this pathogen could be critical in revealing new drug targets.

Heat shock

Heat shock for any organism can be caused by a temperature change of just a few degrees, as proteins and cellular enzymes are highly temperature-dependent. Minor temperature changes can induce protein unfolding, entanglement, and aggregation, which ultimately perturbs cellular organization, nuclear processes, and cell cycle. Since a change in protein homeostasis is detrimental to the cell, unfolded proteins are an indicator for needed counter measures (22). Most organisms have developed sophisticated stress response mechanisms to combat unfolded proteins caused by heat stress, known as the heat shock response, which is managed by 7 classes of heat shock proteins (Hsp) (22). The heat shock response is a rapid and transient gene expression program that is modulated by molecular chaperones, proteolytic enzymes, RNA- and DNA-modifying enzymes, metabolic enzymes (most variation between species here), regulatory proteins such as transcription factors and kinases, cytoskeleton maintenance proteins, and lastly, transport, detoxifying, and membrane-modulating proteins, which are required for restoring membrane stability (22). Heat shock proteins are recruited in response to heat stress and other stresses that induce protein damage (23).

To invade and colonize the human host and withstand various external environments, *E. histolytica* must be able to respond to heat shock. *E. histolytica* possesses conserved homologs of several Hsp and molecular chaperones. Microarray analysis of *E. histolytica* parasites exposed to heat stress (42℃ for 4 hours), showed that of 1,131 unique transcripts, 471 were downregulated, while 40 were upregulated. Downregulated genes included proteins of unknown function (29%) and virulence-related genes, such as Gal/GalNAc lectin subunits, amoebapore C, and cysteine proteases. Upregulated transcripts included Hsps and some of their co-chaperones (24).

In eukaryotic pathogens, Hsps have been shown to play roles in virulence, differentiation, and parasite development, which makes them interesting vaccine candidates (23). BiP, a 70-kDa Hsp, and Hsp70 are conserved in the *Entamoebae,* and were shown to be upregulated during heat shock in *E. invadens*, along with encystation-specific genes, chitinase, and Jacob, suggesting that heat shock and encystation are related in this parasite (25). Additionally, expression of an atypical protein arginine methyltrasferase (EhPRMTA), found in *E. histolytica* is increased by 2.5-fold after incubation at 42℃ for 60 minutes. Similarly, expression of this gene was observed after incubating parasites with human red blood cells. Hsp 70 is known to aid in the refolding of denatured and misfolded proteins, and translocation of secretory proteins. *E. histolytica* Hsp70 (EhHsp70) is essential for the resistance of the parasite to oxidative stress, the formation of liver abscess, and its levels are also upregulated during heat shock (26). This is significant as the amoebic Hsp70 isoforms have key structural motifs that are different from those in the human homolog (27). These data suggest that the heat shock response and virulence are related in *E. histolytica* (28). Thus, exploring the mechanisms and proteins required to navigate this stress may represent novel drug targets.

Oxidative Stress

While reactive oxygen species (ROS) are byproducts of cellular respiration and are used as second messengers for several biological processes, ROS damages proteins, lipids, and nucleic acids, while leading to fragmentation of the endoplasmic reticulum; all of which can trigger cell death (26). Most organisms have complex antioxidant defenses to maintain a delicate balance (29). As *E. histolytica* trophozoites colonize the large intestine and invade colonic epithelium, they may face tissue oxygen concentrations between 4-14% pO_2 (27). Additionally, upon invasion of host tissues, neutrophils and macrophages are recruited to infection sites and release high levels ROS to combat parasites (23, 28). Hydrogen peroxide (H_2O_2) damages proteins by interacting with thiol groups, present in cysteine side chains and metal cofactors (26).

To survive this, *E. histolytica* possesses an effective O_2 reduction pathway, which functions through reductive intermediaries and is mediated by L-cysteine, a major thiol (26, 29). *E. histolytica* in a microaerophilic organism that breaks down glucose as is main energy source via glycosylation, which requires the Fe–S enzyme, pyruvate:ferredoxin oxidoreductase (PFOR). The reductive intermediaries used in this glycolytic pathway are essential for ATP production, as well as the parasites antioxidant defense. The amoebic PFOR is extremely susceptible to ROS and inhibition leads to decreased ATP production (30). Experiments show that when parasites are cultured in the absence of L-cysteine, intracellular levels of ROS increase by 3-fold, suggesting that this amino acid is also required for the parasite's antioxidant defense pathway (30).

Initial studies showed a general upregulation of genes relevant to oxidative stress responses, including thiol-dependent peroxidase, superoxide dismutase, cysteine proteinase 5, G protein, Hsp70, and peptidylprolyl isomerase. Furthermore, comparison of the transcriptomes of the virulent *E. histolytica* strain (HM1: IMSS) with the nonvirulent (Rahman) strain, showed that, upon exposure oxidative or nitrosative stress, the virulent strain upregulated genes encoding for heat shock proteins, ubiquitin-conjugating enzymes, protein kinases, and small GTPases.

7

Moreover, studies of virulent and nonvirulent trophozoites demonstrate that nonvirulent parasites are unable to establish amoebic liver abscesses and are more susceptible to oxidative stress (30). Analyses of the parasite's transcriptome in response to oxidative stress demonstrated *E. histolytica* copes by modulating a broad set of genes encoding proteins that are involved in protein folding Hsps), amino acid catabolism, signaling/regulatory pathways, and those involved in DNA damage repair and metabolism (26). Ultimately, these data suggest that virulence is highly dependent on the parasite's ability to respond to oxidative stress.

While this parasite relies on reductive intermediaries and gene expression modulation to combat oxidative stress, *E. histolytica* also acquires assistance from the host gut microbiota. Recently, researchers have demonstrated that microbiome metabolites affect pathogenicity of *E. histolytica* parasites (31,32). Exposure of parasites to live *Escherichia coli* increased the parasites ability to withstand oxidative stress imparted by hydrogen peroxide (H_2O_2). Upon further investigation, this effect was contributed to this bacteria's production of oxaloacetate, and this compound's ability to scavenge H_2O_2 (32). Additionally, queuosine, a naturally occurring modified ribonucleoside found in the first position of the anticodon of the transfer RNAs for certain amino acids, is produced by gut bacteria and leads to tRNA modifications at the anticodon loops of specific tRNAs. Exposure of *E. histolytica* parasites to queuine, the nucleobase precursor to queuosine, causes upregulation of gene expression involved in the oxidative stress response, while simultaneously, downregulating genes involved in virulence. (31). Since bacterially-derived products are critical in shaping the stress response and virulence of the parasite, further insight into these mechanisms may reveal new treatment strategies.

Nitrosative Stress

As trophozoites degrade the mucus layer of the large intestine, intestinal epithelial cells release proinflammatory factors including interleukin-1, interleukin-8, and tumor necrosis factor-α, which recruit macrophages, natural killer cells, and neutrophils to the site of invasion. The

primary response of these immune effector cells is to release reactive nitrogen species (RNS) in micromolar concentrations (10). The effect of RNS on target cells has been termed nitrosative stress. (26). RNS attack cell components, such as proteins, lipids, and nucleic acids, of invading organisms. RNS lead to the S-nitrosylation of proteinsl, which is the covalent attachment of an NO group to the thiol side chain of cysteine residues. This modification leads to aberrant protein activity by inducing conformation changes. Thus, S-nitrosylation of proteins can also lead to an accumulation of misfolded proteins, which may induce ER stress (26,33). S-nitrosylation of key glycosylation enzymes in this parasite results in inhibition of glycolysis (18) and fragmentation of the ER, triggering cell death (34). Furthermore, nitrosative stress inhibits protein synthesis by inducing cleavage of ribosomal proteins (35). Finally, S-nitrosylation of cysteine proteases results in decreased amoebic virulence because these enzymes are responsible for the parasite's destruction of the mucus layer of the colon (26).

E. histolytica possesses detoxification enzymes and repair systems that cope with nitrosative stress (36). One such mechanism involves a DNA methyltransferase, Dnmt2, which is part of the canonical methyltranserfase family of proteins that include Dnmt1 and Dnmt3. In support of this, when mutant cells overexpressing Dnmt2 were subjected to nitrosative stress, the transgenic cells exhibited higher viabilities than wildtype control parasites (35). In *E. histolytica*, Dnmt2 catalyzes tRNA[Asp] methylation, which maintains protein synthesis, by protecting the tRNAs from degradation during protein synthesis. The depletion of specific tRNAs may cause ribosomes to stall or fall off the mRNA during translation, leading to reduced protein synthesis. Additionally, tRNA cleavage that results from unmethylated tRNAs have been proposed to inhibit translation initiation, by displacing eukaryotic initiation factor 4F (eIF4F) from capped mRNAs (37) . Therefore, methylation of tRNAs maintains protein translation, which can aid in countering damage induced during nitrosative stress (35).

Another way in which *E. histolytica* circumvents host defense is by inhibiting macrophages from releasing RNS by producing prostaglandin E2 (PGE), a principle mediator of inflammation. PGE prevents RNS synthesis by triggering the protein kinase C pathway. The parasite also produces monocyte locomotion inhibitory factor (MLIF), an anti-inflammatory factor, that prevents immune effector cells from producing RNS. *E. histolytica* can also quickly destroy host immune cells by inducing apoptosis or simply by phagocytosis. In one *in vitro* study, one trophozoite was able to kill 3000 neutrophils in 22 hours (10).

There is also evidence to suggest that *E. histolytica* adapts to nanomolar levels of RNS because nitric oxide appears to be a homeostatic regulator of the gastrointestinal muscosa. Studies show that nitric oxide influences microvascular and epithelial permeability and maintains adequate perfusion in the cells of the large intestine. So, there are homeostatic concentrations of nitric oxide, which could prepare invading parasites to withstand a larger RNS released by immune effector cells (38).

While *E. histolytica* possesses mechanisms to counter nitrosative stress, and may also adapt to nanomolar levels of RNS, nitrosative stress still results in high parasite mortality. Therefore, there is much more to learn about how this parasite responds to this stressor. To further evaluate this mechanism, transcriptomic studies have been conducted with parasites that were exposed to nitrosative stress. Santi-Rocca, *et al.* (20) and Vicente, *et al.* (36) found that when this organism was exposed to RNS, several heat shock proteins (Hsp) were upregulated by 2 or 4-fold, respectively, compared to unstressed trophozoites. Hsp are molecular chaperones that aid in protein folding and degradation. Therefore, the protective function of these Hsp may be overwhelmed by the increase in misfolded proteins (34,36). Vicente, *et al.* (36) found that the largest group of genes upregulated were signaling proteins such as protein kinases, phosphatases, and acetyltransferases. Other genes that were upregulated in these studies encoded proteins involved in metabolism, and nucleic acid repair (36). The exact mechanisms of

how these upregulated genes counter nitrosative stress are currently unknown. More studies are needed to further illuminate this stress response pathway.

Endoplasmic Reticulum Stress

In mammalian cells, the endoplasmic reticulum (ER) is a membrane-bound organelle that is responsible for calcium storage and the synthesis, modification, and folding of secretory proteins (20,33). *E. histolytica* lacks many organelles that are found in mammalian cells, such as mitochondria and peroxisomes. Additionally, this amoeba has no recognizable Golgi apparatus or rough ER but possesses a simple endomembrane system. In 2008, Teixeira, *et al.* demonstrated the presence of a continuous ER in *E. histolytica* by using a green fluorescent protein (GFP) tagged N-terminal signal sequence, a FLAG epitope, and C-terminal ER retention peptide, KDEL. KDEL is a specific sequence of amino acids, lysine (K), aspartic acid (D), glutamic acid (E), and leucine (L), that retains a protein to the ER. By using immunofluorescence and confocal microscopy, this group showed that the GFP-tagged protein resided within a continuous compartment, that was responsible for N-linked glycosylation of membrane proteins that also contained the conserved KDEL signal. These data support the idea that the molecular mechanisms regulating basic vesicle trafficking are conserved in this parasite. Prior to this study, it was thought that these protein modifications occurred in cytoplasmic vesicles (33,39).

ER stress is caused by an accumulation of misfolded proteins in the ER, and is induced by various physiological and pathological stresses, including glucose deprivation, hypoxia, oxidative stress, inflammatory cytokines, and an increase in protein folding demand. In mammalian cells, ER stress can also be induced by mutant protein expression or by using pharmacological reagents, such as Brefeldin A, dithiothreitol, and tunicamycin. These reagents induce the buildup of proteins within the ER. For example, Brefeldin A inhibits transport of proteins from the ER to the Golgi Apparatus, while simultaneously inducing the retrograde transport of proteins from the Golgi to the ER. Dithiothrietol disrupts the formation of disulfide bonds and

11

tunicamycin inhibits N-linked glycosylation of proteins. (33,40). Since *E. histolytica* experiences harsh environments while invading the host, it is likely to encounter stressors that are known to induce ER stress. However, data supporting this hypothesis are limited. Several studies on *E. histolytica* show that stress (e.g., overexpression of mutant proteins, exposure to RNS) induces morphological changes in the ER, such as fragmentation and dispersal into vesicles. (20,41).

In higher eukaryotes, ER stress activates a mechanism known as the unfolded protein response (UPR), an evolutionary conserved adaptive response, which functions to alleviate stress and restore the ER to homeostasis. The UPR is a signaling cascade that consists of three main signaling proteins: Inositol Requiring Enzyme 1 (IRE1), PKR-like ER kinase (PERK), and Activating Transcription Factor 6 (ATF6). Under normal conditions, these ER-resident transmembrane proteins are rendered inactive by ER-bound Hsp, immunoglobin binding protein (BiP). BiP senses misfolded proteins and subsequently dissociates from each of these proteins. Once free, IRE1, ATF6, and PERK initiate complex signaling cascades that ultimately reduce ER stress by altering gene expression (33).

Microarray analysis of trophozoites exposed to RNS showed that there was a marked increase in Hsp, upregulation of DNA repair and redox gene expression, and an upregulation of glycosylation-related gene expression. While it has been shown that *E. histolytica* experiences ER stress, the exact mechanism by which this parasite is able to counter this stress, remains largely unknown. Therefore, more studies are needed to elucidate this mechanism.

Glucose Starvation

Once mature cysts are ingested via contaminated food and water, unknown cues trigger the excystation of trophozoites in the small intestine. As parasites traverse the small intestine and travel to the colon, they experience a large decrease in environmental glucose. Since *E. histolytica* relies solely on glycolysis to breakdown glucose as its primary energy source, the

parasite must be able to adapt to glucose starvation as it colonizes the large intestine (42). To do this, *E. histolytica* and *E. invadens* down-regulate expression of glycolysis related genes, while simultaneously upregulating genes needed to catabolize amino acids. Additionally, these pathogens use stored glycogen reserves when in a glucose-poor environment. Various transcriptomic studies show that during glucose starvation, virulence-related genes, such as the Gal/GalNAc lectins, cysteine proteases, and amoebapore-A are upregulated, which is expected since *E. histolytica* colonizes and subsequently may degrade the intestinal epithelium of the colon (42).

The parasite's response to glucose deprivation could also be regulated, in part, by epigenetic modifications, such as tRNA methylation, as seen in *Escherichia coli* (42) during iron deprivation and *Saccharomyces cerevisiae* (42) when exposed to chemical toxicants, where alterations in tRNA modifications lead to stress-specific protein translation. Ehmeth, a Dmnt2-type methyltransferase, catalyzes the cytosine-38 tRNAasp methylation in *E. histolytica*, and has been shown to interact with accumulated enolase in the nuclei of glucose-starved parasites. This interaction leads to an inhibition of Ehmeth and subsequent increased sensitivity of glucose-starved trophozoites to oxidative stress. Furthermore, overexpression of Ehmeth leads to resistance to oxidative and nitrosative stresses (42). The mechanism by which tRNA modifications and the stress response are related remain enigmatic and warrant further investigation. Gaining additional insight into the mechanism by which *E. histolytica* regulates its response to changes in environmental glucose concentration will inform future drug and virulence studies.

III.   Translation Regulation via eIF-2α Kinases and how they are found in other eukaryotic pathogens.

While many of the countermeasures described above aim to neutralize the stress that a cell is experiencing, eukaryotic cells have also developed methods of countering stress, by decreasing global protein translation. This mechanism involves the eukaryotic initiation factor 2 (eIF-2) pathway. Not only does the eIF-2 mechanism result in decreased protein translation, but it facilitates an increase in the expression of a subset of stress-specific genes (25).

eIF-2 is a multi-subunit protein complex, that initiates protein translation in a GTP-dependent manner, by delivering the Met-tRNA$_i$ to the ribosomal initiation complex. eIF-2 is composed of alpha, beta, and gamma subunits. Under normal conditions, eIF-2 is bound to GTP (active), and associates with Met-tRNA$_i$, delivering it to the 40S ribosomal subunit of the initiation complex. To release the Met-tRNA$_i$, eIF-2 must hydrolyze its bound GTP, resulting in an inactive eIF-2-GDP complex. To be reactivated, eIF-2 requires a guanine nucleotide exchange factor (GEF), eIF-2B, to exchange its bound GDP for GTP (43). Under stressful conditions, eIf-2α kinases are activated in a stress-specific manner and interact with eIF-2. This interaction induces a conformational change of eIF-2, exposing serine 51 of the alpha subunit (eIF-2α). Once exposed, eIF-2α is phosphorylated on serine 51 and becomes an inhibitor of its own GEF, eIF2B. Therefore, the eIF-2 complex becomes inactive, ultimately reducing general protein translation.

Simultaneous to a reduction in general protein synthesis, translation of select mRNAs is, paradoxically, initiated. The resulting proteins are needed for the stress response, and include activating transcription factor 4 (ATF4), activating transcription factor 3 (AFT3), and cationic amino acid transporter-1 (CAT-1) (44). During unstressed conditions, the translation of these stress-specific genes is inhibited by the presence of upstream short open reading frames (ORFs), which attract ribosomes to translate short peptides, preventing the flow of scanning ribosomes, to the genuine stress-specific gene sequence. Phosphorylated eIF-2α not only significantly decreases global translation, but also limits the number of ribosomal complexes, which promotes the translation of these genes (45).

Translation initiation is the rate limiting step of protein synthesis and is the central control point (46), and small increases in phosphorylated eIF-2α profoundly inhibits global protein translation (47). This reduction in protein synthesis allows the cell to direct gene expression to counter damage accrued during stress (23). This mechanism of translational control has been demonstrated extensively in yeast (48,49) and mammalian cells (43), and has also been demonstrated human pathogens: *Toxoplasma gondii* (50,51), *Plasmodium* (52), and *Leishmania* (53).

This system is also conserved in *E. histolytica* (21)*.* Genomic data revealed that *E. histolytica* possesses eIF2α (*Ehe*IF2α) with a conserved phosphorylatable serine at position 59 (Ser[59]). Hendrick *et al*. (21) exposed cells to different stress conditions and measured the level of total and phospho-*Ehe*IF2α. Long-term serum starvation, long-term heat shock, and oxidative stress increased the level of phospho-*Ehe*IF2α, while short-term serum starvation, short-term heat shock, or glucose deprivation did not. Long-term serum starvation also caused a decrease in polyribosome abundance, which is in accordance with the role of this protein complex in protein translation. Additionally, Walters *et al*. (54) exposed wildtype parasites to nitrosative stress and endoplasmic reticulum stress and measured levels of phospho-*Ehe*IF2α and general protein translation. These data demonstrate that ER stress induces phosphorylation of *Ehe*IF2α while nitrosative stress does not. Interestingly, both ER stress and nitrosative stress resulted in a general decrease in protein translation, suggesting that *E. histolytica* may possess an alternate stress response pathway, independent of the eIF2 mechanism (54).

Hendrick *et al*. (21) also generated transgenic cells that overexpress wildtype *Ehe*IF2α, a non-phosphorylatable variant of eIF2α in which Ser[59] was mutated to alanine (*Ehe*IF2α-S59A), and a phosphomimetic variant of eIF2α in which Ser[59] was mutated to aspartic acid (*Ehe*IF2α-S59D). Consistent with the known functions of eIF2α, cells expressing wildtype or *Ehe*IF2α-S59D exhibited increased or decreased translation, respectively. Surprisingly, cells expressing *Ehe*IF2α-S59A also exhibited reduced translation. Cells expressing *Ehe*IF2α-S59D were more

resistant to long-term serum starvation underscoring the significance of *Ehe*IF2α phosphorylation in managing stress. Finally, phospho-eIF2α accumulated during encystation in *E. invadens*, a model encystation system. Together, these data demonstrate that the eIF2α-dependent stress response system is operational in *Entamoeba* species. Phosphorylation of eIF-2α is facilitated by specific kinases. Four mammalian eIF-2α kinases have been identified (55) (See Figure 1.2).

Figure 2α

1.2: eIF-Kinases

There are kinases in
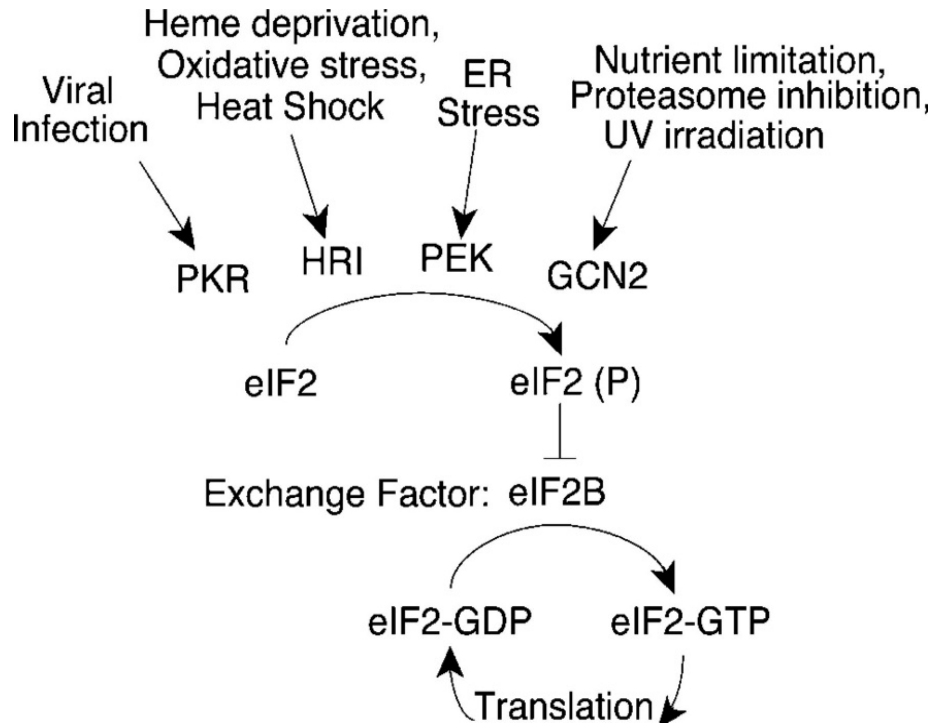
4 eIf-2α

mammalian cells. PKR, HRI, PEK/PERK, and GCN2. Each kinase is activated by a specific stress, but each kinase functions to phosphorylate the alpha subunit of eIF-2, eukaryotic translation initiation factor. This phosphorylation results in a general decrease in protein translation, which allows the cell time to correct any damage incurred from the stress. Figure taken from Wek, 2006 (36).

Heme regulated inhibitor (HRI)

HRI, also known as EIF2AK1, is an eIF-2α kinase expressed in erythrocytes, macrophages, and hepatocytes (56). This kinase has two roles during development: to couple the synthesis of globin genes to the amount of heme present and to promote survival of erythroid cells when intracellular iron levels are low. Additionally, HRI has been implicated in the stress response in proteasome inhibition and also during signaling for erythroid differentiation. When HRI is synthesized, the protein is bound by heme, which triggers autophosphorylation, stabilizing it against aggregation and generating an HRI dimer. The HRI dimer senses heme concentrations. When levels are high, heme binds to the kinase, where it inhibits any further autophosphorylation. When low levels of heme are detected, the kinase is activated by multiple autophosphorylations, and then it phosphorylates eIF-2α (56).

This decrease in global protein translation in erythrocytes coordinates globin mRNA translation with available iron, preventing accumulation of misfolded globin proteins in the absence of heme. Furthermore, in the liver, HRI activation negatively regulates enzymes involved in the metabolism of L-tryptophan, and in murine macrophages, HRI is required for maturation (56).

dsRNA-dependent Protein Kinase (PKR)

PKR, also known as EIF2AK2, is located within the nucleus and cytosol of various cell types. Its transcription is induced by interferon, an antiviral protein that is secreted in response to viral infections. When bound to dsRNA, PKR dimerizes, autophosphorylates, and becomes active. Once active, PKR is able to phosphorylate eIF-2α. This phosphorylation results in reduced translation of viral mRNAs and can lead to apoptosis if the viral infection cannot be controlled. Moreover, PKR is involved in several signaling pathways and can be activated independently of dsRNA, by oxidative stress, ER stress, and protein activator (PACT). Upon activation, PKR can

phosphorylate p53, facilitate activation of STAT transcription factors and MAPK, and mediate NF-κB activation (56,57).

Pancreatic eIF-2α Kinase/PKR like ER kinase (PEK/PERK)

PERK or EIF2K3 is a transmembrane ER protein and represents one major arm of the unfolded protein response. PERK's regulatory region is located within the ER lumen, and the kinase domains lies in the cytosol. The luminal domain senses misfolded proteins within the ER. During unstressed conditions, the luminal domain of PERK is bound by ER chaperone, BiP/GRP78, which renders the kinase inactive. Within minutes of sensing ER stress, BiP/GRP78 dissociates, and PERK is free to oligomerize and autophosphorylate. Once active, the cytosolic kinase domain phosphorylates eIF-2α, to reduce global protein translation. This decrease in protein synthesis slows the flow of newly synthesized proteins into the ER, ultimately allowing the cell time to refold proteins or degrade any critically misfolded proteins (43).

PERK can also be activated by calcium fluctuations in the ER, oxidative stress, and hypoxia. In some studies, PERK has been implicated in cancer. It is known that solid tumors tend to grow in hypoxic areas and are invasive and chemoresistant. Since PERK can be activated by hypoxia, its activation is correlated with increased tumor size, vascularization, and cell survival. Additionally, it was found that tumors deficient in PERK were smaller than their wildtype counterparts, and cancer cells that were PERK-deficient were stalled in the cell cycle because of ROS-induced damaged. Finally, PERK has also been implicated in Wolcott–Rallison syndrome in humans, which is a disease characterized by lifelong diabetes, as well as skeletal and pancreatic defects (56).

General Control non-inducible-2 (GCN2)

Also known as EIF2K4, GCN2 is an eIF-2α kinase that is activated by amino acid starvation, UV irradiation, and viral infections (43). In yeast and mammals, GCN2 is also activated by glucose starvation. During amino acid starvation, uncharged tRNAs accumulate and bind to

the histidyl-tRNA synthase-like domain on GCN2, which results in allosteric rearrangements and dimerization. Subsequent autophosphorylation allows GCN2 to phosphorylate eIF-2α. While phosphorylated eIF-2α results in decreased protein translation, it also prompts translation of specific mRNAs, such as ATF4, which is critical in the stress response, as it induces the expression of amino acid biosynthetic enzymes and amino acid transporters (45,58).

This kinase is present in most eukaryotes and is involved in major biological processes. In mammals, this kinase is crucial for long-term memory formation, feeding behavior and immune system regulation. Evidence for this comes from studies that showed that the accumulation of uncharged tRNAs lead mice to reject diets low in amino acids, while mutant mice lacking functional GCN2, did not discriminate between amino acid-rich and amino acid-deficient foods. It was also found that when wildtype mice were fed diets deficient in amino acids, lipid metabolism was affected, leading to decreased liver mass and adipose tissue (45,56,58).

Conservation of eIF-2α kinases in lower eukaryotes

Translation regulation via eIF-2α phosphorylation is necessary to counter various stresses and is an evolutionary conserved mechanism in eukaryotes. In *Plasmodium falciparum*, the causative agent of malaria in humans, *Pf*PK4 resembles mammalian HRI and is also inhibited by heme. Zhang, *et al*. (52) showed that *Pf*PK4 is required for development of *Plasmodium* blood stage development and regulates protein translation by phosphorylating eIF-2α in trophozoites, schizonts, and gametocytes(23,52). Another parasite, *Toxoplasma gondii* has four putative eIF-2α kinases, two of which most closely resemble GCN2. *Tg*IF2K-A, the most extensively characterized, appears to be a transmembrane ER protein, like PERK, and phosphorylates eIF-2α when exposed to ER stress. *Tg*IF2K-B has no orthologs but is a true eIF-2α kinase (50). Furthermore, *Trypanosoma brucei,* the causative agent of African sleeping sickness, has three putative kinases. *Tb*eIF2K2 is a confirmed eIF-2α kinase, *Tb*eIF2K1 is a GCN2 ortholog, while no clear homology has been determined for *Tb*eIF2k3 (23). Genome data demonstrate that there

20

are 2 putative eIF-2α kinases in *E. histolytica* (EHI_035950 and EHI_109700) and 2 putative eIF-2α kinases in *E. invadens* (EIN_052050 and EIN_096010). However, these have not been authenticated.

IV. Potential drug targets in the *Entamoebae*

Kinases

Kinases are responsible for cell signaling cascades that regulate many cellular processes, including vital gene expression programs, such as the eIF2α kinase family and their dysregulation have been implicated in many human pathologies including cancer (43), diabetes (59), and neurodegenerative disorders (60). Therefore, this kinase family has been the subject of intense study because they represent logical targets for the design of therapies. For instance, overactivation of PERK has been associated with neurological disorders such as Parkinson's Disease and Alzheimer's Disease (61). It has been found that the compound, LDN-0060609, significantly inhibits PERK-mediated phosphorylation of eIF2α in rat astrocytes, which suggests that it may be a suitable drug for the treatment of neurological diseases (61). Targeting the eIF2α-based regulation of translation in protozoan parasites is also underway. For example, pharmacological inhibition of PK4 in *P. falciparum* with the PERK inhibitor, GSK2606414, blocks parasite differentiation and reduces artemisinin-induced latency (62). Inhibition of PERK-like eIF2 kinase, TgIF2K-A, in *T. gondii*, with the same inhibitor, blocked multiple steps of the tachyzoite lytic cycle and lowered the rate of bradyzoite differentiation (63). Finally, GSK2606414 reduced *Leishmania amazonensis* infection of macrophages (64). Therefore, it is conceivable that if authentic, the *Entamoeba* eIF2α kinases may serve as novel targets for drug inhibition.

Hypothetical Proteins

Moreover, the genomes of the *Entamoebae* remain enigmatic as approximately 54% of *E. histolytica* genes and 66% of *E. invadens* genes are annotated as hypothetical proteins (HPs) (65) and one third of the *E. histolytica* genome is not conserved within the human host (66). Thus, HPs also represent potential drug targets for the treatment of amoebiasis.

Recently, investigation of HPs and proteins of unknown function have become the center of investigation as potential drug targets for the treatment of various human diseases, including tuberculosis (67), and infections with chlamydia (68), adenoviruses (69), and *E. coli* (70). For example, antibiotic-resistant *Mycobacterium tuberculosis* strains are increasingly prevalent and are a threat to public health. Studies suggested that overexpression of HPs may be responsible for drug-resistance and emerging proteomic and bioinformatic analyses can serve as major analytical tools for identification and characterization of such proteins (67). Using SSEalign, a novel algorithm employing structural information, Yang and colleagues (2019) annotated 823 out of 1051 HPs in *M. tuberculosis*, while also identifying 6 of them as favorable drug targets (71). Similarly, Naqvi et al. (2016) assigned functions to 89 HPs, in the bacterium, *Chlamydia trachomatis*, 24 of which are essential proteins for virulence and pathogenesis, suggesting that these HPs would serve as encouraging drug targets (68). Likewise, the function of 6 HPs of human adenovirus were predicted via various sequence and structure-based bioinformatics tools, with the goal of identifying novel drug targets (69). The proteome of hypervirulent *E. coli* strain, CFT073, contains 992 HPs, 6 of which were found to be therapeutically targetable proteins (70). Ultimately, these studies suggest that investigating hypothetical proteins in the *Entamoebae* may reveal novel drug targets for the treatment of amoebiasis.

V.   Summary

E. histolytica faces numerous stressors as it travels through the host digestive system and other tissues. These include changes in pH, glucose deprivation, osmotic shock, heat shock, and immune pressure, which could impart oxidative and nitrosative stresses (21,30). To be a successful pathogen, *E. histolytica* must employ mechanisms that counter these stresses. In many species, response to these types of stressors involves translational control by phosphorylating eIF-2α. It has been demonstrated that long-term serum deprivation, long-term heat shock, oxidative stress, and endoplasmic reticulum stress induce phosphorylation of *Ehe*IF2-α (21,54) . However, no eIF2α kinases have been identified in the *Entamoebae*. Additionally, over half of the *Entamoebae* genomes are annotated as hypothetical proteins and over one-third of the *E. histolytica* genome has no homologs in the human host. Further investigation of these stress response mechanisms and hypothetical proteins these parasites may reveal novel pathways for drug or vaccine development.

Therefore, the aims of this study are as follows:

Aim 1: To authenticate and characterize two putative eIF2α kinases in the reptilian protozoan parasite, *Entamoeba invadens*.

In Aim 1, we identified two eIF2α kinases in *E. invadens*, EiIF2K-A and EiIF2K-B. Their identity as eIF2α kinases was validated using a heterologous yeast system. We used an RNAi Trigger-mediated silencing system to reduce expression of EiIF2K-A, which also reduced expression of EiIF2K-B. Parasites with decreased kinase expression exhibited decreased phosphorylation of eIF2α and increased sensitivity to oxidative stress. Diminished kinase expression also correlates with an increased rate of encystation, a decreased the rate of

23

excystation, and an increase of several virulence functions, erythrophagocytosis and adhesion to host cells. Taken together, these data suggest that EiIF2K-A and EiIF2K-B are authentic eIF2α kinases that may regulate the *Entamoeba* stress response.

Aim 2: To characterize two hypothetical proteins in the *Entamoebae* and investigate their role in the *Entamoebae* stress response.

In Aim 2, we identified and characterized a hypothetical protein in *E. invadens*, EIN_059080, which has an ortholog in *E. histolytica* (EHI_056700), but no homolog in the human host. We used an RNAi-based silencing system to reduce expression of EIN_059080 in *E. invadens* and EHI_056700 in *E. histolytica*. We found that loss of EIN_059080 resulted in decreased rates of encystation and increased erythrophagocytosis, an important virulence function. Additionally, mutant parasites were less viable when exposed to oxidative Interestingly, loss of EHI_056700 in *E. histolytica* trophozoites resulted in decreased erythrophagocytosis and adhesion. Mutant *E. histolytica* parasites were also less viable when exposed to oxidative stress and glucose deprivation Taken together, these data suggest that these hypothetical proteins play a role in stage conversion, virulence, and the stress response in the *Entamoeba*.

VI. Literature Cited

1.   Bercu TE, Petri W a, Behm JW. Amebic colitis: new insights into pathogenesis and treatment. Current gastroenterology reports [Internet]. 2007;9(5):429–33. Available from: http://www.ncbi.nlm.nih.gov/pubmed/17991346

2.   WHO & UNICEF. Progress on Household Drinking Water, Sanitation and Hygiene 200-2020 [Internet]. UNICEF journal. 2021. Available from: https://www.eea.europa.eu/publications/industrial-waste-water-treatment-pressures%0Ahttp://files/558/Rapport EEA Industrial wastewater treatment – pressures on Europe's environment.pdf

3.   Grebmer K, Bernstein J, de Waal A, Prasai N, Yin S, Yohannes Y. UNICEF and WHO, 2015 Update and MDG Assessment - Progress on Sanitation and Drinking Water. 2015;

4.   Kasper MR, Lescano AG, Lucas C, Gilles D, Biese BJ, Stolovitz G, et al. Diarrhea outbreak during U.S. military training in El Salvador. PLoS ONE. 2012;7(7):1–8.

5.   Shirley DAT, Farr L, Watanabe K, Moonah S. A review of the global burden, new diagnostics, and current Therapeutics for amebiasis. Open Forum Infectious Diseases. 2018;5(7):1–9.

6.   Michaels J. Fighting Terrorism: These are the most dangerous places U.S. troops are deployed. USA Today [Internet]. 2018 Mar 5; Available from: https://www.usatoday.com/story/news/world/2018/03/05/look-most-dangerous-places-u-s-troops-deployed/396737002/

7.   Eichinger D. Encystation in parasitic protozoa. Current Opinion in Microbiology. 2001;4(4):421–6.

8.   Petri W a, Singh U. Diagnosis and Management of Amebiasis. Clinical Infectious Diseases. 1990;29:1117–25.

9.   Tanyuksel, M. Petri W. Laboratory Diagnosis of Amebiasis. Clinical Microbiolody Reviews. 2003;16(4):713–29.

10.   Begum S, Quach J, Chadee K. Immune evasion mechanisms of Entamoeba histolytica: Progression to disease. Frontiers in Microbiology. 2015;6(DEC):1–8.

11.   Wesel J, Shuman J, Bastuzel I, Dickerson J, Ingram-Smith C. Encystation of entamoeba histolytica in axenic culture. Microorganisms. 2021;9(4).

12.   Wang Z, Samuelson J, Clark CG, Eichinger D, Paul J, Van Dellen K, et al. Gene discovery in the Entamoeba invadens genome. Molecular and Biochemical Parasitology. 2003;129(1):23–31.

13.   Löfmark S, Edlund C, Nord CE. Metronidazole Is Still the Drug of Choice for Treatment of Anaerobic Infections. Clinical Infectious Diseases [Internet]. 2010;50(s1):S16–23. Available from: https://academic.oup.com/cid/article-lookup/doi/10.1086/647939

14.   Ralston K, Petri WA. Tissue Destruction and invasion by Entamoeba histolytica. Trends in Parasitology. 2011;27(6):254–63.

15. Cherian PT, Wu X, Yang L, Scarborough JS, Singh AP, Alam ZA, et al. Gastrointestinal localization of metronidazole by a lactobacilli-inspired tetramic acid motif improves treatment outcomes in the hamster model of Clostridium difficile infection. Journal of Antimicrobial Chemotherapy. 2015;70(11):3061–9.

16. Seifert K, Duchêne M, Wernsdorfer WH, Kollaritsch H, Scheiner O, Wiedermann G, et al. A New Approach for Chemotherapy Against Entamoeba histolytica. 2000;31:6–7.

17. Knight R. The chemotherapy of amoebiasis. 1980;577–93.

18. Samarawickrema NA, Brown DM, Upcroft JA, Thammapalerd N, Upcroft P. Involvement of superoxide dismutase and pyruvate:ferredoxin oxidoreductase in mechanisms of metronidazole resistance in Entamoeba histolytica. 1997;833–40.

19. Bendesky A, Menéndez D, Ostrosky-wegman P. Is metronidazole carcinogenic？ 2002;511:133–44.

20. Santi-Rocca J, Smith S, Weber C, Pineda E, Hon CC, Saavedra E, et al. Endoplasmic reticulum stress-sensing mechanism is activated in entamoeba histolytica upon treatment with nitric oxide. PLoS ONE. 2012;7(2):1–14.

21. Hendrick HM, Welter BH, Hapstack MA, Sykes SE, Sullivan WJ, Temesvari LA. Phosphorylation of Eukaryotic Initiation Factor-2α during Stress and Encystation in Entamoeba Species. PLoS Pathogens. 2016;12(12):1–14.

22. Richter K, Haslbeck M, Buchner J. The Heat Shock Response: Life on the Verge of Death. Molecular Cell [Internet]. 2010;40(2):253–66. Available from: http://dx.doi.org/10.1016/j.molcel.2010.10.006

23. Vonlaufen N, Kanzok SM, Wek RC, Sullivan WJ. Stress response pathways in protozoan parasites. Cellular Microbiology. 2008;10(12):2387–99.

24. Weber C, Guigon G, Bouchier C, Frangeul L, Moreira S, Sismeiro O, et al. Stress by heat shock induces massive down regulation of genes and allows differential allelic expression of the Gal/GalNAc lectin in Entamoeba histolytica. Eukaryotic Cell. 2006;5(5):871–5.

25. Field J, Dellen KVAN, Ghosh SK, Samuelson J. Responses of Entamoeba invadens to Heat Shock and Encystation are Related. Journal of Eukaryotic Microbiology. 2000;47(5):511–4.

26. Nagaraja S, Ankri S. Utilization of Different Omic Approaches to Unravel Stress Response Mechanisms in the Parasite Entamoeba histolytica. Frontiers in Cellular and Infection Microbiology [Internet]. 2018;8(February):1–12. Available from: http://journal.frontiersin.org/article/10.3389/fcimb.2018.00019/full

27. Santos F, Marcial-Quino J, Gómez-Manzo S, Enríquez-Flores S, Nequiz-Avendaño M, Cortes A, et al. Functional characterization and subcellular distribution of two recombinant cytosolic HSP70 isoforms from Entamoeba histolytica under normal and stress conditions. Parasitology Research. 2020;119(4):1337–51.

28. Medina-Gómez C, Bolaños J, Borbolla-Vázquez J, Munguía-Robledo S, Orozco E, Rodríguez MA. The atypical protein arginine methyltrasferase of Entamoeba histolytica

(EhPRMTA) is involved in cell proliferation, heat shock response and in vitro virulence. Experimental Parasitology. 2021;222(June 2020).

29. Auten RL, Davis JM. Oxygen toxicity and reactive oxygen species: The devil is in the details. Pediatric Research. 2009;66(2):121–7.

30. Pineda E, Perdomo D. Entamoeba histolytica under Oxidative Stress: What Countermeasure Mechanisms Are in Place? Cells [Internet]. 2017;6(4):44. Available from: http://www.mdpi.com/2073-4409/6/4/44

31. Nagaraja S, Cai MW, Sun J, Varet H, Sarid L, Trebicz-Geffen M, et al. Queuine is a nutritional regulator of entamoeba histolytica response to oxidative stress and a virulence attenuator. mBio. 2021;12(2):1–28.

32. Shaulov Y, Shimokawa C, Trebicz-Geffen M, Nagaraja S, Methling K, Lalk M, et al. Escherichia coli mediated resistance of Entamoeba histolytica to oxidative stress is triggered by oxaloacetate. PLoS Pathogens. 2018;14(10):1–29.

33. Oslowski CM, Urano F. Measuring ER stress and the unfolded protein response using mammalian tissue culture system. Methods in Enzymology [Internet]. 2013;490(508):71–92. Available from: http://www.sciencedirect.com/science/article/pii/B9780123851147000040

34. Santi-Rocca J, Smith S, Weber C, Pineda E, Hon CC, Saavedra E, et al. Endoplasmic reticulum stress-sensing mechanism is activated in entamoeba histolytica upon treatment with nitric oxide. PLoS ONE. 2012;7(2):1–14.

35. Hertz R, Tovy A, Kirschenbaum M, Geffen M, Nozaki T, Adir N, et al. The Entamoeba histolytica Dnmt2 homolog (Ehmeth) confers resistance to nitrosative stress. Eukaryotic Cell. 2014;13(4):494–503.

36. Vicente JB, Ehrenkaufer GM, Saraiva LM, Teixeira M, Singh U. Entamoeba histolytica modulates a complex repertoire of novel genes in response to oxidative and nitrosative stresses: Implications for amebic pathogenesis. Cellular Microbiology. 2009;11(1):51–69.

37. Tuorto F, Liebers R, Musch T, Schaefer M, Hofmann S, Kellner S, et al. RNA cytosine methylation by Dnmt2 and NSun2 promotes tRNA stability and protein synthesis. Nature Publishing Group. 2012;19(9):900–5.

38. Kolios G, Valatas V, Ward SG. Nitric oxide in inflammatory bowel disease: A universal messenger in an unsolved puzzle. Immunology. 2004;113(4):427–37.

39. Teixeira JE, Huston CD. Evidence of a continuous endoplasmic reticulum in the protozoan parasite Entamoeba histolytica. Eukaryotic Cell. 2008;7(7):1222–6.

40. Galluzzi L, Diotallevi A, Magnani M. Endoplasmic reticulum stress and unfolded protein response in infection by intracellular parasites. Future Science Open Access [Internet]. 2017;00(3):FSO198. Available from: http://www.ncbi.nlm.nih.gov/pubmed/28883998%0Ahttp://www.pubmedcentral.nih.gov/articlerender.fcgi?artid=PMC5583660

41. Welter BH, Temesvari LA. Overexpression of a mutant form of EhRabA, a unique rab GTPase of entamoeba histolytica, alters endoplasmic reticulum morphology and localization of the Gal/GalNAc adherence lectin. Eukaryotic Cell. 2009;8(7):1014–26.

42. Baumel-Alterzon S, Ankri S. Entamoeba histolytica adaptation to glucose starvation: A matter of life and death. Current Opinion in Microbiology [Internet]. 2014;20:139–45. Available from: http://dx.doi.org/10.1016/j.mib.2014.06.005

43. Wek RC, Cavener DR. Translational Control and the Unfolded Protein Response. Antioxidants & Redox Signaling [Internet]. 2007;9(12):2357–72. Available from: http://www.liebertonline.com/doi/abs/10.1089/ars.2007.1764

44. Cao SS, Kaufman RJ. Unfolded protein response. Current Biology [Internet]. 2012;22(16):R622–6. Available from: http://dx.doi.org/10.1016/j.cub.2012.07.004

45. Castilho BA, Shanmugam R, Silva RC, Ramesh R, Himme BM, Sattlegger E. Keeping the eIF2 alpha kinase Gcn2 in check. Biochimica et Biophysica Acta - Molecular Cell Research [Internet]. 2014;1843(9):1948–68. Available from: http://dx.doi.org/10.1016/j.bbamcr.2014.04.006

46. Ventoso I, Kochetov A, Montaner D, Dopazo J, Santoyo J. Extensive translatome remodeling during ER stress response in mammalian cells. PLoS ONE. 2012;7(5):1–12.

47. McEwen E, Kedersha N, Song B, Scheuner D, Gilks N, Han A, et al. Heme-regulated inhibitor kinase-mediated phosphorylation of eukaryotic translation initiation factor 2 inhibits translation, induces stress granule formation, and mediates survival upon arsenite exposure. Journal of Biological Chemistry. 2005;280(17):16925–33.

48. Wek RC, Cannon JF, Dever TE, Hinnebusch a G. Truncated protein phosphatase GLC7 restores translational activation of GCN4 expression in yeast mutants defective for the eIF-2 alpha kinase GCN2. Molecular and cellular biology. 1992;12(12):5700–10.

49. Zhan K, Vattem KM, Bauer BN, Thomas E, Chen J, Wek RC, et al. Phosphorylation of Eukaryotic Initiation Factor 2 by Heme-Regulated Inhibitor Kinase-Related Protein Kinases in Schizosaccharomyces pombe Is Important for Resistance to Environmental Stresses Phosphorylation of Eukaryotic Initiation Factor 2 by Heme-Regul. 2002;22(20):7134–46.

50. Sullivan WJ, Narasimhan J, Bhatti MM, Wek RC. Parasite-specific eIF2 (eukaryotic initiation factor-2) kinase required for stress-induced translation control. The Biochemical journal [Internet]. 2004;380(Pt 2):523–31. Available from: http://www.pubmedcentral.nih.gov/articlerender.fcgi?artid=1224182&tool=pmcentrez&rendertype=abstract

51. Joyce BR, Tampaki Z, Kim K, Wek RC, Sullivan WJ. The unfolded protein response in the protozoan parasite Toxoplasma gondii features translational and transcriptional control. Eukaryotic Cell. 2013;12(7):979–89.

52. Zhang M, Mishra S, Sakthivel R, Rojas M, Ranjan R, Sullivan WJ. PK4, a eukaryotic initiation factor 2a(eIF2a) kinase, is essential for the development of the erythrocytic cycle of Plasmodium. Proceedings of the National Academy of Sciences. 2012;109(10):3956–61.

53. Cloutier S, Laverdière M, Chou MN, Boilard N, Chow C, Papadopoulou B. Translational control through eIF2alpha phosphorylation during the Leishmania differentiation process. PLoS ONE. 2012;7(5).

54. Walters HA, Welter BH, Sullivan WJ, Temesvari LA. Phosphorylation of eukaryotic initiation factor-2α in response to endoplasmic reticulum and nitrosative stress in the human protozoan parasite, Entamoeba histolytica. Vol. 234, Molecular and Biochemical Parasitology. 2019.

55. Wek RC, Jiang H-Y, Anthony TG. Coping with stress: eIF2 kinases and translational control. Biochemical Society Transactions [Internet]. 2006;34(1):7–11. Available from: http://biochemsoctrans.org/lookup/doi/10.1042/BST0340007

56. Donnelly N, Gorman AM, Gupta S, Samali A. The eIF2α kinases: Their structures and functions. Cellular and Molecular Life Sciences. 2013;70(19):3493–511.

57. Garcia MA, Gil J, Ventoso I, Guerra S, Domingo E, Rivas C, et al. Impact of Protein Kinase PKR in Cell Biology: from Antiviral to Antiproliferative Action. Microbiology and Molecular Biology Reviews [Internet]. 2006;70(4):1032–60. Available from: http://mmbr.asm.org/cgi/doi/10.1128/MMBR.00027-06

58. Anda S, Zach R, Grallert B. Activation of Gcn2 in response to different stresses. PLoS ONE. 2017;12(8):1–13.

59. Kim MJ, Kim MN, Min SH, Ham DS, Kim JW, Yoon KH, et al. Specific PERK inhibitors enhanced glucose-stimulated insulin secretion in a mouse model of type 2 diabetes. Metabolism: Clinical and Experimental [Internet]. 2019;97:87–91. Available from: https://doi.org/10.1016/j.metabol.2018.12.007

60. Axten JM, Romeril SP, Shu A, Ralph J, Medina JR, Feng Y, et al. Discovery of GSK2656157: An optimized PERK inhibitor selected for preclinical development. ACS Medicinal Chemistry Letters. 2013;4(10):964–8.

61. Rozpedek, Wioletta; Pytel, Dariusz; Poplawski, Tomasz; Walczak, Anna; Gradzik, Kinga; Wawrzynkiewicz, Adam; Wojtczak, Radoslaw; Mucha, Bartosz; Diehl, John Alan; Majsterek I. Inhibition of the PERK-Dependent Unfolded Protein Response Signaling Pathway Involved in the Pathogenesis of Alzheimer's Disease. CURRENT ALZHEIMER RESEARCH [Internet]. 2019;16(3):209–18. Available from: https://pubmed.ncbi.nlm.nih.gov/30819079/

62. Zhang M, Gallego-Delgado J, Fernandez-Arias C, Waters NC, Rodriguez A, Tsuji M, et al. Inhibiting the Plasmodium eIF2α Kinase PK4 Prevents Artemisinin-Induced Latency. Cell Host and Microbe [Internet]. 2017;22(6):766-776.e4. Available from: https://doi.org/10.1016/j.chom.2017.11.005

63. Augusto L, Martynowicz J, Staschke K, Wek RC, Sullivan WJ. Effects of PERK eIF2α Kinase Inhibitor against Toxoplasma gondii. Antimicrobial Agents and Chemotherapy. 2018;62(11):1–10.

64. Dias-Teixeira KL, Calegari-Silva TC, Medina JM, Vivarini ÁC, Cavalcanti Á, Teteo N, et al. Emerging Role for the PERK/eIF2α/ATF4 in Human Cutaneous Leishmaniasis. Scientific Reports. 2017;7(1):1–11.

65. VEuPathDB: the eukaryotic pathogen vector and host bioinformatics resource center, J ABaCbMbAbEbWbRbAbUbJbBcMcDcLcMcGcKdKdJdRdYdMfDfSfPfBgBg-CGhO. VEuPathDB: the eukaryotic pathogen, vector and host bioinformatics resource center. Nucleic Acids Research. 2021;2021.

66. Marchat LA, Hernández-de la Cruz ON, Ramírez-Moreno E, Silva-Cázares MB, López-Camarillo C. Proteomics approaches to understand cell biology and virulence of Entamoeba histolytica protozoan parasite. Journal of Proteomics [Internet]. 2020;226(July):103897. Available from: https://doi.org/10.1016/j.jprot.2020.103897

67. Sharma D, Bisht D. M. tuberculosis hypothetical proteins and proteins of unknown function: Hope for exploring novel resistance mechanisms as well as future target of drug resistance. Frontiers in Microbiology. 2017;8(MAR):1–5.

68. Turab Naqvi AA, Rahman S, Rubi, Zeya F, Kumar K, Choudhary H, et al. Genome analysis of Chlamydia trachomatis for functional characterization of hypothetical proteins to discover novel drug targets. International Journal of Biological Macromolecules [Internet]. 2017;96:234–40. Available from: http://dx.doi.org/10.1016/j.ijbiomac.2016.12.045

69. Naveed M, Tehreem S, Usman M, Chaudhry Z, Abbas G. Structural and functional annotation of hypothetical proteins of human adenovirus: prioritizing the novel drug targets. BMC research notes [Internet]. 2017;10(1):706. Available from: https://doi.org/10.1186/s13104-017-2992-z

70. Kaur H, Singh V, Kalia M, Mohan B, Taneja N. Identification and functional annotation of hypothetical proteins of uropathogenic Escherichia coli strain CFT073 towards designing antimicrobial drug targets. Journal of Biomolecular Structure and Dynamics [Internet]. 2021;0(0):1–12. Available from: https://doi.org/10.1080/07391102.2021.2000499

71. Yang Z, Zeng X, Tsui SKW. Investigating function roles of hypothetical proteins encoded by the Mycobacterium tuberculosis H37Rv genome. BMC Genomics. 2019;20(1):1–10.

CHAPTER TWO

EUKARYOTIC INITIATION FACTOR 2α KINASES REGULATE VIRULENCE
FUNCTIONS, STAGE CONVERSION, AND THE STRESS RESPONSE IN
ENTAMOEBA INVADENS

Heather A. Walters [1,2], Brenda H. Welter [1,2], Ronny Orobio-Hurtado [1,2], Harrison C.
Moss [1,2], Martha A. Villano [1,2], William J. Sullivan, Jr. [3,4], Lesly A. Temesvari [1,2]

[1] Department of Biological Sciences

[2] Eukaryotic Pathogens Innovations Center (EPIC)

Clemson University

Clemson, South Carolina United States of America 29634

[3] Department of Pharmacology and Toxicology

[4] Department of Microbiology and Immunology

Indiana University School of Medicine

Indianapolis, IN United States of America 46202

*Corresponding author

Lesly A. Temesvari (LAT)

Email: LTEMESV@clemson.edu

I.   Abstract

Entamoeba histolytica is a protozoan parasite that causes amebic dysentery and amoebic liver abscess. This pathogen possesses a two-stage life cycle consisting of an environmentally stable latent cyst and a pathogenic amoeboid trophozoite. Since infection is acquired by ingestion of cysts from contaminated food and water, this parasite is prevalent in underdeveloped countries. A reptilian pathogen, *Entamoeba invadens*, which can encyst in culture, has long-served as a surrogate to study stage conversion. In the host, the *Entamoebae* must manage stress including nutrient deprivation and stress imposed by the host immune response. In many systems, the stress response is characterized by down-regulation of translation, which is initiated by the phosphorylation of eukaryotic initiation factor-2 alpha (eIF2α). In mammalian cells, this phosphorylation is carried out by a family of eIF2α kinases. A canonical eIF2α translational control system exists in the *Entamoebae*; however, no eIF2α kinases have been characterized. In this study, we identified two eIF2α kinases in *E. invadens*, EiIF2K-A and EiIF2K-B. Their identity as eIF2α kinases was validated using a heterologous yeast system. We used an RNAi Trigger-mediated silencing system to reduce expression of EiIF2K-A, which also reduced expression of EiIF2K-B. Parasites with decreased kinase expression exhibited decreased phosphorylation of eIF2α and increased sensitivity to oxidative stress. Diminished kinase expression also correlated with an increased rate of encystation, a decreased the rate of excystation, and an increase in several virulence functions, erythrophagocytosis and adhesion to host cells. Taken together, these data suggest that EiIF2K-A and EiIF2K-B are authentic eIF2α kinases that may regulate the *Entamoeba* stress response.

II.   Introduction

Entamoeba histolytica is a human pathogen that causes amoebiasis and amoebic liver abscess, affecting millions of people worldwide and causing an estimated 55,000 deaths annually (1). *E. histolytica* has a two-stage life cycle: the infectious cyst and the pathogenic amoeboid trophozoite. Latent cysts are ingested from fecally-contaminated food or water; thus, this parasite is prevalent in underdeveloped countries, where sanitation and other infrastructure is substandard. In 2015, 663 million people lacked access to clean drinking water and almost 1 billion people still practiced open defecation (2). Additionally, amoebiasis is the leading cause of diarrheal disease in travelers returning to the US (1). Considered together, these characteristics demonstrate that *E. histolytica* constitutes a significant global health problem.

After ingestion, cysts traverse the stomach and enter the small intestine, where unknown cues trigger the excystation of mature trophozoites. The amoebae travel to the colon where infection can progress along several non-mutually exclusive routes. The trophozoites may establish a noninvasive infection, feeding on natural gut flora or host cells by phagocytosis. The parasites may also adhere to and degrade the gut epithelial lining, causing a diarrheal disease known as amoebic dysentery. Occasionally, the parasites breach the intestinal wall, enter the bloodstream, and establish extraintestinal infection in the liver (amoebic liver abscess), or more rarely, in the lungs and brain. In the large intestine, unknown signals trigger aggregation and encystation of trophozoites, which generate environmentally-stable mature cysts that are shed into the environment to facilitate host-to-host spread (3). While navigating the human host, *E. histolytica* faces numerous stresses, such as nutrient deprivation, oxidative stress, nitrosative stress, and heat shock (4,5). To survive, the parasite must surmount these damaging conditions.

E. invadens, a reptilian parasite, has been a long-standing model to study stage conversion in this genus, because it readily encysts and excysts in culture (6,7,8). Stage conversion is thought to be a response to stress encountered in the colon, and many of the features of the stress response overlap with those of stage conversion. For example, both heat shock proteins and cyst wall proteins are upregulated during heat shock in *E. invadens* (9). Additionally, a eukaryotic type IIA topoisomerase II is upregulated during oxidative stress, heat shock, and encystation (10). Given the importance of stress management during the parasite's life cycle, stress response pathways may represent a novel targetable vulnerability. Thus, it is crucial to understand the molecular mechanisms that regulate the parasite stress response. Such information would provide significant insight into *Entamoeba* pathogenicity and would inform future studies focused on anti-parasitic drug design.

In most organisms, one branch of the stress response is characterized by the phosphorylation of a conserved serine residue in the alpha subunit of eukaryotic initiation factor-2 (eIF2α). eIF2α is a component of a ternary complex with GTP and the initiator methionyl transfer RNA (Met-tRNAi). This ternary complex binds the 40S ribosomal subunit, delivering Met-tRNAi for translation initiation. Phosphorylation of eIF2α during stress inhibits this activity, causing a sharp decline in global protein synthesis and preferential translation of a subset of mRNAs that encode stress-related factors. This process of translational control allows cells to conserve resources and reconfigure gene expression to effectively counter stress. In mammalian cells, phosphorylation of eIF2α is regulated by a family of four eIF2α kinases (GCN2, PKR, PERK, HRI) that are activated in a stress-specific manner. GCN2 is activated by nutrient starvation, PKR is activated in response to viral infections, PERK is activated by misfolded proteins, and HRI is activated by heme starvation (11). Although translational control, via eIF2α phosphorylation, was shown to exists in *E. histolytica* (4,5), no eIF2α kinases have been characterized in the *Entamoebae.*

In this study, we identified two putative eIF2α kinases, EiIF2K-A and EiIF2K-B in *E. invadens*. We used a heterologous yeast system (12,13) to confirm that EiIF2K-A and EiIF2K-B are *bona fide* eIF2α kinases. We used a Trigger-mediated silencing approach (14) to knock down expression of EiIF2K-A, which simultaneously reduced expression of EiIF2K-B. Parasites with reduced expression of both kinases exhibited decreased levels of phosphorylated eIF2α, a diminished ability to surmount oxidative stress, and altered rates of stage conversion. Furthermore, decreased kinase expression was correlated with an increase of two virulence functions, erythrophagocytosis and adhesion. Taken together, these data show that EiIF2K-A and EiIF2K-B are authentic eIF2α kinases that may be involved in the parasite stress response, stage conversion, and virulence.

III.   Material and Methods

Protein Alignment and phylogenetic analysis

The kinase domain sequences of the four putative *Entamoebae* kinases were obtained from UniProt (38). Sequences were also analyzed using ScanProsite (39) to identify the kinase domains and to search for other possible domains and motifs. The catalytic domains of the four putative kinases were aligned with the kinase domains of previously characterized eIF2a kinases, using the Clustal W algorithm with the standard parameters with SnapGene (Version 5.2.1; GSL Biotech, LLC., San Diego, CA, USA). The software, Jalview (40), was used to remove the inserts with high length variability for clearer visualization. A phylogenetic analysis was performed using the unedited alignment and the website Méthodes et Algorithmes pour la Bio-informatique LIRMM (http://www.phylogeny.fr/index.cgi) (41). The Newick format of the phylogeny was imported into the Interactive Tree of Life (iTOL) (itol.embl.de) (42) to generate the visual tree. All webpages and applications were used with the standard settings for each step. The tree was rooted to the more distantly related sequence of the pool (CDK1).

Strains and Culture conditions

Entamoeba invadens (strain IP-1) was cultured axenically in TYI-S-33 medium in 15 mL glass screw cap tubes or 25 cm^2 culture flasks at 25°C (44). Parasites were passaged into fresh media every 7 days. Chinese hamster ovary (CHO) cells were cultured in DMEM supplemented with 10% (v/v) fetal bovine serum (FBS), PenStrep, and HEPES in 25 cm^2 culture flasks at 37°C. To generate a plasmid to reduce expression of EiIF2K-A, PCR was employed to amplify the kinase domain of EiIF2K-A using genomic DNA as a template and gene-specific primers (Table 2.1). The primers also added AvrII restriction sites to the 3' and 5' ends, which facilitated subcloning into the Trigger plasmid (4) (kind gift of Dr. Upinder Singh, Stanford University). Successful subcloning was confirmed by sequencing.

E. invadens was transfected by electroporation as described (43), with minor modifications. Briefly, two 25 cm^2 flasks containing 100% confluent log-phase trophozoites were iced for 15 min to release adherent parasites. The parasites were collected by centrifugation at 500 x *g* for 5 min and washed with 20 mL ZM phosphate buffered saline (PBS) buffer (132 mM NaCl, 8 mM KCl, 8 mM NaPO$_4$, 1.5 mM KH$_2$PO$_4$). Parasites were pelleted by centrifugation at 500 x *g* for 5 mins and resuspended in 1.6 mL complete ZM PBS buffer (ZM PBS with 0.5 mM Mg(CH$_3$COO)$_2$ • 4H$_2$O and 0.09 mM CaCl$_2$). Eight hundred µL of parasite suspension was combined with 150 µg plasmid DNA and electroporated in a 0.4 cm cuvette with two pulses at 1.2 kV and 25 µF using a BioRad Gene Pulser II. Parasites were transferred to 15 mL culture tubes containing 13 mL TYI-S-33 and allowed to recover for 48 h. Neomycin selection was added initially at 5 µg/ml and gradually increased by 5 µg/mL each week until a concentration of 50 µg/mL was reached.

To assess expression of EiIF2K-A and EiIF2K-B, RNA was extracted from trophozoites or cysts using TRIZOL (ThermoFisher; Waltham, MA). Two µg of total RNA was treated with RQ1 DNase enzyme (Promega; Madison, WI) per manufacturer's instructions. Treated RNA was used to synthesize cDNA using the Invitrogen Superscript III First Stand Synthesis kit per the

manufacturer's instruction. (ThermoFisher). One µL of cDNA was used as template and PCR was carried out using EiIF2K-A specific primers or EiIF2K-B gene specific primers (Table 2.1). We confirmed that these primers do not cross-react to amplify both genes. EIN_327460 was used as an internal load control for analysis of gene expression in trophozoites and EIN_162500 was used as an internal load control for analysis of gene expression in cysts (see Table 2.1).

Analysis of eIF2 kinase function in yeast

The coding sequence of the kinase domain of EiIF2K-A (1313 bp) and EiIF2K-B (1397 bp) was synthesized and ligated into the pYES-NT/C plasmid (ThermoFisher, kind gift of Dr. William Marcotte, Clemson University) by Genscript (Piscataway, NJ USA), using the restriction enzyme sites BamHI and NotI. The resulting construct contained the kinase domains in-frame with a N-terminal poly-histidine tag, which was confirmed by sequencing. To generate an inactive kinase, the conserved lysine in kinase subdomain II (EiIF2K-A, position 43 and EiIF2K-B, position 45), was mutated to arginine using the Phusion Site Directed mutagenesis kit (Thermo-Fisher) and mutagenic primers (Table 2.1). Successful mutagenesis was confirmed by sequencing. Live and dead human PKR kinase domains in yeast expression plasmid pYES2 were kind gifts from Dr. Ronald Wek (Indiana University School of Medicine).

The pYES-NT/C or pYES2 plasmids encoding the active or dead kinase domain, or no gene product (empty pYES-NT/C), were introduced into *Saccharyomyces cerevisiae* strain H1894 (*MATa ura3-52 leu2-3 leu2-112 gnc2Δ trp1 Δ-63*), which lacks the sole yeast eIF2α kinase, GNC2 (12,16). Yeast was cultured at 30°C on YPAD agar plates containing 2% (w/v) glucose prior to transformation. Yeast transformation was carried out as described (17). Since pYES-NT/C confers uracil prototrophy to transformants, selection was carried out by plating transformed yeast cells on agar plates containing synthetic dropout medium (SD) (Sigma-Aldrich St. Louis, MO, USA) (without uracil), and 2% (w/v) glucose, and growing them overnight at 30°C.

To induce expression of exogenous protein, cells from each transformed yeast strain were inoculated into liquid SD medium containing 2% (w/v) raffinose and 10% (w/v) galactose (13) and grown overnight at 30˚C prior to western blotting.

Western blotting

Western blotting of whole cell lysates was used to assess the expression of kinases in yeast or the level of total and phosphorylated eIF2α in yeast or in *E. invadens*. For yeast, cell lysates were prepared as described (44). Briefly, 1.89×10^7 yeast cells were pelleted by centrifugation at 3,000 x *g* for 5 min. To prepare yeast for lysis, cells were resuspended in 0.5 mL 2 M lithium acetate (Sigma-Aldrich) and incubated on ice for 5 min. Cells were pelleted by centrifugation at 500 x *g*, 5 min, resuspended in 0.5 mL 0.4 M NaOH, and incubated on ice 5 min. For *E. invadens*, trophozoites or encysting parasites (3×10^5) were pelleted by centrifugation at 500 x *g* for 5 min. Both yeast cells and *E. invadens* parasites were resuspended in NuPAGE LDS sample buffer (Life Technologies; Carlsbad, CA, USA). An additional step was required to lyse *E. invadens* cysts. Cysts (in NuPAGE LDS buffer) were also exposed to three cycles of freeze/thaw in liquid nitrogen. All samples were heated for 5 min at 100˚C and loaded onto a precast NuPAGE 12% Bis-Tris Gel (Life Technologies; Carlsbad, CA). The gels were electrophoresed at 180V for 60 min and proteins were transferred to PVDF membranes (Life Technologies) at 12V for 1.5 h in Towbin transfer buffer (25 mM Tris, 192 mM glycine, 20% (v/v) methanol). Prior to blocking, membranes were stained with Ponceau S reagent (Sigma-Aldrich) to record protein load. The membranes were blocked with 5% (w/v) Blotting Grade powdered milk blocker (Bio-Rad Laboratories, Hercules, CA) and 0.5% (w/v) bovine gelatin (Sigma-Aldrich) in TBST (50 mM Tris,

Table 2.1: Primers used in this study

Primer Name	Sequence
Cloning Primers	
EiIF2K-A-AvrII-F (EIN_052052)	5'-CCCCTAGGATGTCCGTCAC-3'
EiIF2K-A-AvrII-R (EIN_052052)	5'-CCCCTAGGTTAGTCGGACGGAG-3'
RT PCR primers	
EiIF2K-A-F (EIN_052050)	5'-CGAAGACGAGATGGGTTCTTT-3'
EiIF2K-A-R (EIN_052050)	5'-CGAAGTGGAGTTCACGATTCT-3'
EiIF2K-B-F (EIN_096010)	5'-GAAGGCCAACGAGTGAGGAA-3'
EiIF2K-B-R (EIN_096010)	5'-CTCACTTCTCCGCCACACAT-3'
Trophozoite Internal control-F (EIN_327460)	5'-CCGACAGCAGAAGAACAAGA-3'
Trophozoite Internal control-R (EIN_327460)	5'-GGAGATGAGTAAGCGAAGAACA-3'
Cyst Internal Control-F (EIN_162500)	5'-ACCAGCCGAGGTCAAGAAAG-3'
Cyst Internal Control-R (EIN_162500)	5'-TCTTCGGGTGTGGCTTTACC-3'
Mutagenic Primers	
Dead-EiIF2K-A-F (EIN_052050)	5'- AGAAGTACGCAATCA**g**GGTATTAATTGTGTC-3'
Dead-EiIF2K-A-R (EIN_052050)	5'- TCTTATCGTCTTTTCTAATACCACTGTAGAC-3"

150mM NaCl, 0.5% (v/v) Tween 20) for 35 min at 37°C. Membranes were incubated overnight at 4°C in primary antibodies (diluted 1:1000 in TBST). For yeast, the primary antibodies were horse radish peroxidase-conjugated α-poly-histidine tag antibody (Sigma Aldrich; St. Louis, MO; kind gift of Dr. Michael Sehorn, Clemson University), yeast-specific α-phosphorylated eIF2α antibody (Thermo-Fisher), or yeast-specific α-total eIF2α antibody (gift of Dr. Thomas Dever, NIH). For *E. invadens*, the primary antibodies were *Entamoeba*-specific α-phosphorylated eIF2α antibody (4) or α-total eIF2α antibody (4). The membranes were washed in TBST for 45 min with 6 buffer changes. Membranes were incubated in commercially available horseradish peroxidase-conjugated goat anti-rabbit antibody (Thermo-Fisher, diluted 1:5000 in TBST) for 1 h at room temperature and extensively washed as described above. All blots were developed using a commercially available Enhanced ChemiLuminescence Western Blotting Detection system (ThermoScientific) according to the manufacturer's instructions. Protein bands were quantified using scanning densitometry and Image J software (Version 1.51, NIH).

Induction of Stage Conversion

To induce encystation, control and mutant trophozoites (6.5×10^6) were pelleted by centrifugation at 500 x *g* for 5 min and resuspended in 47% (w/v) low glucose/serum free/high osmolarity encystation medium (4,7), supplemented with 50 mg/mL neomycin. Parasites were incubated at 25°C for either 48 h or 72 h and encystation was tracked by staining with Congo Red (Amresco; Solon, OH) and flow cytometry (19).

Excystation was induced as described (8) Briefly, Trig Luc and EiIF2K-KD trophozoites were induced to encyst for 72 h. Parasites were then incubated in 13 mL ddH$_2$O at 4°C overnight to lyse unencysted trophozoites. Cysts were enumerated using a Luna Automated Hemocytometer (Logos Biosystems), pelleted by centrifugation at 500 x *g* for 5 min, and resuspended in 13 mL TYI-S-33 medium, 1 mg/mL bile salts (Sigma-Aldrich), and 40 mM

NaHCO$_3$, and incubated at 25°C for 2 h or 8 h. After incubation, cultures were iced for 8 min to detach any trophozoites from the glass culture tubes, pelleted by centrifugation at 500 x g for 5 min, resuspended in 1 mL of 1% (v/v) sarkosyl in PBS and incubated on ice for 30 min to lyse any trophozoites or immature cysts. The remaining detergent-resistant cysts were enumerated and the percent excystation was calculated by comparing total cysts remaining to the starting number of cysts.

Phagocytosis Assays

Phagocytosis assays were carried as previously described (20) with minor changes. Briefly, control or mutant trophozoites were rinsed once in PBS (GE Life Sciences) and twice in serum free TYI-S-33 medium (SFM). Trophozoites (2x10^5) were resuspended in 150 μL SFM. Freshly isolated human red blood cells (hRBCS) were pelleted by centrifugation (2000 x g for 1 min) and rinsed once with PBS and twice with SFM and were resuspended at a concentration of 4x10^5 cells/μL in SFM. hRBCs (2x10^7) were added to the trophozoites and incubated at 25°C for 10 min. Samples were pelleted by centrifugation (2000 x g for 1 min), and undigested hRBCs were hypotonically lysed by washing twice with 1 mL of ice-cold ddH$_2$O. Parasites were washed with 1mL ice-cold PBS, collected by centrifugation (2000 x g for 1 min) and lysed with 200 μL concentrated formic acid (Fisher). Phagocytosis was measured as the absorbance of heme in the lysate at 405 nm. Sample values were corrected for the formic acid blank.

Adhesion Assays

Adhesion assays were carried as previously described (21) with minor changes. Briefly, Chinese hamster ovary (CHO) cells (1.5x10^5) were seeded into a 96-well plate and grown at 37°C for 24 h. CHO monolayers were fixed by incubating with 4% (v/v) paraformaldehyde in PBS for 10 min at 37°C. To inactivate paraformaldehyde, the CHO monolayer was incubated with 200 μL of 250 mM glycine for 15 min. Glycine was removed by rinsing with PBS. Control and mutant

parasites were incubated with calcein-AM (Invitrogen) (5 µg/mL) for 30 min at 25°C. Calcein-AM labeled parasites were washed once with room temperature SFM and 5×10^4 parasites were seeded onto the fixed monolayer of CHO cells. Parasites were incubated with fixed CHO cells in SFM for 30 min at 25°C. The media was carefully aspirated, and the cell layer was gently rinsed twice with room temperature PBS. The number adherent parasites was determined by measuring fluorescence at excitation and emission wavelengths of 495 and 525 nm, respectively, with a fluorimeter/plate reader (Model FLX800, BioTek Instruments, Winooski, VT).

Induction of Oxidative stress

Control or mutant parasites were incubated with 4 mM or 1M H_2O_2 for 1 h at 25°C. Viability was assessed using trypan blue exclusion and quantified by a Luna Automated Hemocytometer (Logos Biosystems).

Statistical Analysis

All values are presented as means ± standard error of at least 3 separate trials. Means of treated groups were compared against the appropriate control and statistical analyses were performed using Graph Pad prism 9 (v9.0.0, San Diego, CA, US) with a one-way analysis of variance (ANOVA). *P* values of less than 0.05 were considered statistically significant. *P* values less than 0.01 or 0.001 were considered highly statistically significant.

Ethics Statement

Whole blood was donated by a healthy adult volunteer, who provided oral consent, at Clemson University. The collection was approved by Clemson's Institutional Biosafety Committee under safety protocol #IBC2018-12.

IV.   Results

The *E. invadens* and *E. histolytica* genomes each encode two putative eIF2α kinases

Using the amino acid sequences of the four human eIF2α kinases, we searched the *E. invadens* genome (Amoebadb.org) for candidate sequences that contained hallmarks of eIF2α kinases (15). We found two presumptive *E. invadens* eIF2α kinases, which we named EiIF2K-A (EIN_052050, formerly labeled EIN_033330) and EiIF2K-B (EIN_096010, formerly labeled EIN_059080), which share ~33.5% identity and ~48.1% similarity with each other within their kinase domains (Table 2.2). According to RNA sequencing data, reported as transcript abundance in transcripts per million (TPM) (Amoebadb.org), these kinases exhibit stage-specific expression. EiIF2K-A is predominantly expressed in trophozoites and at 48 h into encystation, while EiIF2K-B is only expressed during stage conversion, at low levels during encystation, and at higher levels during excystation (8) Like the genome of *E. invadens*, the genome of the human pathogen, *E. histolytica*, also possessed two putative eIF2α kinases, which we named EhIF2K-A (EHI_035950) and EhIF2K-B (EHI_109700). The kinase domain of EiIF2K-A shares ~49.9% identity (~64.6% similarity) and ~28.1% identity (~43.9% similarity) with the kinase domains of EhIF2K-A and EhIF2K-B, respectively (Table 2.2). The kinase domain of EiIF2K-B shares ~31.1% identity (~45% similarity) and ~48.4% identity (~64.9% similarity) with the kinase domains EhIF2K-A and EhIF2K-B, respectively (Table 2.2). The kinase domains of EiIF2K-A and EiIF2K-B also share at least 16.57% identify and at least 28.57% similarity with the human eIF2α kinases (Table 2.2).

We aligned the putative *Entamoeba* kinases with other known eIF2α kinases, as well as with a control kinase, human CDK1, which does not belong to the family of eIF2α kinases. For clarity, only kinase subdomain II is shown (Fig 2.1). The *Entamoeba* kinases possess all eleven subdomains characteristic of the eIF2α kinase family, with highly conserved residues making

them more closely related to eIF2α kinases than to the control kinase, CDK1 (Fig 2.1). The *Entamoeba* kinases share little homology with other members of this kinase family beyond the kinase domains. A phylogenetic analysis of eIF2α kinases showed that both EiIF2K-A and EiIF2K-B were more closely related to each other and to their *E. histolytica* counterparts (EhIF2K-A and EhIF2K-B) than to any of the other kinases. Additionally, the *Entamoeba* kinases were more closely related to PKR- and PERK-related kinases than to GCN2- or HRI-related kinases (Fig 2.2).

EiIF2K-A and EiIF2K-B regulate phosphorylation of eIF2α in a heterologous system

To validate EiIF2K-A and EiIF2K-B as eIF2α kinases, we utilized a yeast model system that uses the *Saccharomyces cerevisiae* strain, H1894, in which the sole endogenous eIF2α kinase is deleted. Exogenous expression of authentic eIF2α kinases in this yeast strain results in phosphorylation of endogenous eIF2α. (12,13,16). A truncated cDNA encoding the catalytic domain of EiIF2K-A or EiIF2K-B, was inserted into the yeast expression vector, pYES-NT/C, which confers uracil prototrophy and allows for galactose-inducible expression of exogenous genes (13). The pYES-NT/C plasmid also adds a polyhistidine tag to the N-terminus of the expressed protein. A pYES-NT/C vector lacking an insert (empty pYES) was used as a control plasmid and pYES2 plasmid harboring the active kinase domain of human PKR was used as a positive control (13) A standard transformation protocol (17) was used to introduce the expression vectors into the H1894 strain and transformants were selected by growth on media that lacked uracil.

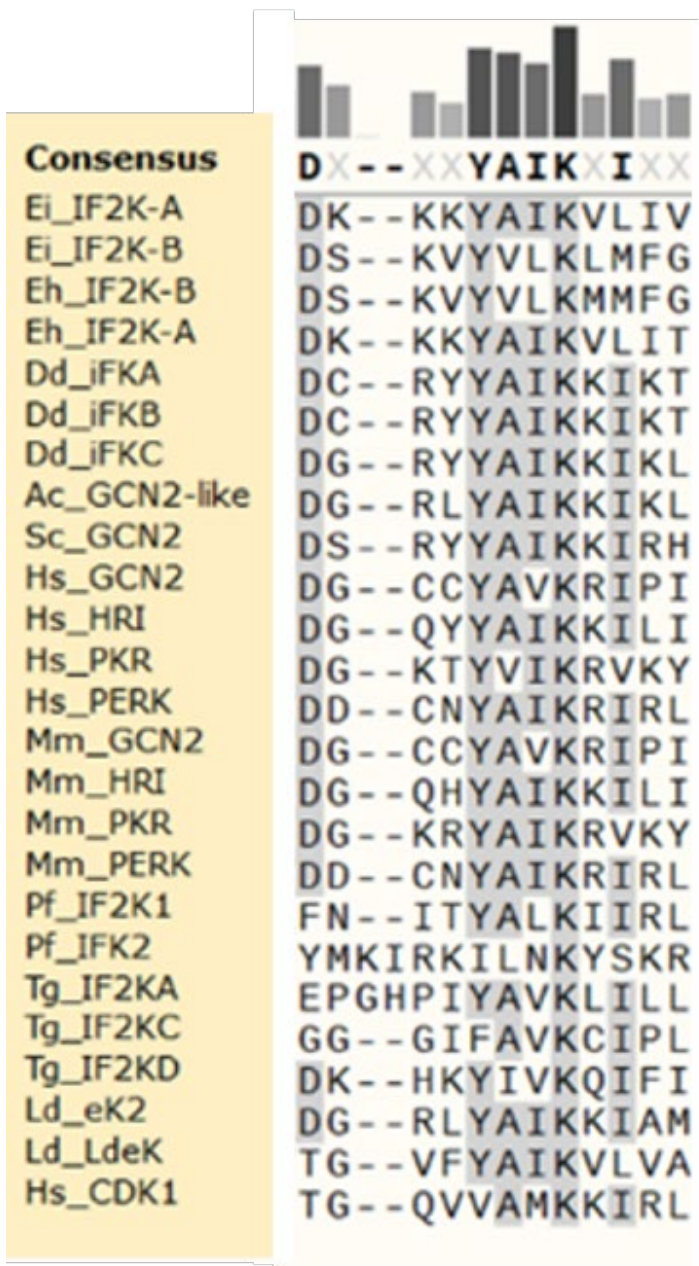Table 2.2: Percent Identity and Similarity Shared eIF2α kinases

Upper-right triangle = **% SIMILARITY**; lower-left triangle = **% IDENTITY**. Orange borders highlight values shared by *Entamoebae* species.

KINASE DOMAIN*	Ei_IF2K-A	Ei_IF2K-B	Eh_IF2K-A	Eh_IF2K-B	Ac_GCN2-like	Dd_iFKA	Dd_iFKB	Dd_iFKC	Hs_GCN2	Hs_HRI	Hs_PERK	Hs_PKR	Ld_eK2	Ld_LdeK	Mm_GCN2	Mm_HRI	Mm_PERK	Mm_PKR	Pf_IFK1	Pf_IFK2	Sc_GCN2	Tg_IF2K A	Tg_IF2K B	Tg_IF2K C	Tg_IF2K D	Hs_CDK1
Ei_IF2K-A	■	48.12	64.57	43.97	29.51	25.83	25.36	27.72	31.31	28.82	29.18	29.86	32.24	17.72	30.42	29.45	30.06	31.19	28.6	13.01	32.49	17.73	7.65	17.72	27.37	13.64
Ei_IF2K-B	33.48	■	44.96	64.88	29.81	28.96	28.41	28.62	30.02	29.33	30.63	28.57	30.69	17.86	29.41	30.15	30.76	28.83	26.77	12.18	29.09	17.82	7.12	17.12	26.09	13.36
Eh_IF2K-A	49.88	31.14	■	48.15	27.81	24.61	24.06	24.61	28.37	29.29	25.54	32.01	31.58	15.47	28.37	26.3	25.45	31.74	26.53	13.91	31.08	16.08	7.02	16.52	26.79	13.2
Eh_IF2K-B	28.12	48.39	32.46	■	28.34	27.66	27.12	28.74	27.82	29.29	29.35	28.08	29.22	16.17	27.46	29.91	30.02	28.1	25.98	12.94	29.32	18.13	7.36	17.74	25.2	13.31
Ac_GCN2-like	19.61	18.87	17.9	17.37	■	44.76	43.92	42.14	43.86	35.67	34.41	33.18	36.69	20.33	42.71	35.05	34.54	32.25	34.97	14.12	39.15	17.3	8.19	24.89	29.85	15.43
Dd_iFKA	17.27	17.6	17.03	17.6	44.76	■	98.3	42.19	36.47	29.1	34.74	34.41	29.71	19.18	34.53	28.62	35.17	23.32	26.09	11.97	36.06	20.93	9.14	22.77	22.7	12.17
Dd_iFKB	16.64	17.5	17.08	17.08	43.92	98.3	■	41.69	35.31	28.55	33.93	23.78	29.48	18.72	33.39	28.06	34.36	22.56	25.6	12.08	35.51	20.73	9.09	22.1	22.13	11.75
Dd_iFKC	17.35	16.5	15.79	18.6	42.14	42.19	41.69	■	40.04	31.16	33.22	25.6	30	21.31	39.43	31.16	33.67	24.58	26.44	13.37	40.81	17.86	8.51	23.01	24.35	13.64
Hs_GCN2	18.99	16.57	16.86	16.6	43.86	36.47	35.31	40.04	■	36.11	33.22	25.6	31.62	21.06	90.48	33.33	36.23	34.52	30.59	15.99	35.33	17.55	7.93	22.76	30.07	16.81
Hs_HRI	17.56	17.53	16.86	17.75	35.67	29.1	28.55	31.16	36.11	■	37.98	24.03	21.41	21.37	31.31	88.49	40.12	91.79	33.79	13.76	30.38	20.59	8.09	21.95	34.19	15.87
Hs_PERK	17.47	18.75	15.94	15.94	34.41	34.74	33.93	33.22	34.41	37.98	■	23.3	21.06	22.16	33.89	40.12	91.79	22.79	35.71	15.9	30.27	20.06	8.5	22.07	30.02	13.97
Hs_PKR	21.09	17.07	19.01	15.69	33.18	34.41	23.78	25.6	33.41	24.03	23.3	■	22.16	11.23	32.16	22.3	22.16	65.94	24.02	11.51	35.71	16.97	5.47	16.97	34.19	18.91
Ld_eK2	18.07	17.07	17.89	15.69	36.69	29.71	29.48	30	31.62	21.41	21.06	22.16	■	10.88	32.66	25.87	21.22	24.02	18.57	8.14	22.54	13.43	6.72	18.97	30.02	14.7
Ld_LdeK	9.67	9.24	8.4	7.9	20.33	19.18	18.72	21.31	20.79	21.37	17.12	11.23	10.88	■	21	20.66	21.22	17	18.04	9.6	20.5	16.7	10.91	16.7	15.16	10.25
Mm_GCN2	18.89	18.24	17.66	18	42.71	34.53	33.39	39.43	90.48	31.15	33.89	31.95	32.66	21	■	32.27	33.83	34.37	30.59	16.22	35.62	18.83	10.91	22.98	31.15	16.81
Mm_HRI	17.59	16.98	16.31	16.31	35.05	28.62	28.06	31.16	33.33	88.49	40.12	22.3	25.87	20.66	32.27	■	40.35	34.37	33.14	14.2	35.71	20.5	7.74	22.98	28.42	16.18
Mm_PERK	17.81	17.86	15.52	17.57	34.54	35.17	34.36	33.67	36.23	40.12	91.79	22.16	21.22	21.22	33.83	40.35	■	21.06	30.27	14.2	35.62	20.06	8.5	18.93	23.52	14.1
Mm_PKR	22.38	19.37	22.42	18.52	32.25	23.32	22.56	24.58	34.52	74.28	22.79	65.94	25.87	17	34.37	34.37	21.06	■	22.02	15.21	34.95	15.33	7.11	21.56	34.88	21.53
Pf_IFK1	17.8	15.21	15.37	15.82	34.97	26.09	25.6	26.44	30.59	33.79	35.71	24.02	18.57	18.04	30.59	33.14	30.27	22.02	■	14.82	35.71	12.87	6.83	16.36	31.6	15.63
Pf_IFK2	8.61	7.63	8.8	8.31	14.12	11.97	12.08	13.37	15.99	13.76	15.9	11.51	8.14	9.6	16.22	14.2	14.2	15.21	14.82	■	10.73	8.84	7.11	10.72	14.26	8.06
Sc_GCN2	22.43	18.38	22.42	19.22	39.15	36.06	35.51	40.81	35.33	30.38	30.27	35.71	22.54	20.5	35.62	35.71	35.62	34.95	35.71	10.73	■	16.67	8.5	20.24	33.79	17.16
Tg_IF2KA	10.19	10.5	9.39	10.38	17.3	20.93	20.73	17.86	17.55	20.59	20.06	20.5	13.43	11.93	18.83	20.5	20.06	15.33	12.87	8.84	16.67	■	8.98	15.52	12.36	6.94
Tg_IF2KB	4.09	3.82	3.35	3.97	8.19	9.14	9.09	8.51	7.93	8.09	5.47	10.91	6.72	10.91	10.91	7.74	8.5	7.11	6.83	7.11	15.18	8.98	■	6.1	5.37	3.87
Tg_IF2KC	10.54	10.41	10.38	9.92	24.89	22.77	22.1	23.01	22.76	21.95	22.07	22.98	18.97	16.7	22.98	22.98	18.93	21.56	16.36	10.72	15.52	10.5	6.1	■	11.69	9.05
Tg_IF2KD	13.58	14.29	14.06	13	29.85	22.7	22.13	24.35	30.07	34.19	30.02	34.19	30.02	15.16	31.15	28.42	23.52	34.88	31.6	14.26	33.79	12.36	5.37	19.32	■	18.32
Hs_CDK1	8.47	7.66	8.01	7.22	8.85	7.7	7.42	8.42	10.21	10.23	8.64	12.61	8.91	5.45	9.87	10.71	8.61	14.16	9.89	4.34	9.93	4.02	2.3	5.71	8.65	■

Identity and similarity shared by *Entamoebae* species are highlighted by orange borders.

*NCBI Accession numbers: *Entamoebae*; EiIF2K-A (XP_004259781.1), EiIF2K-B (XP_004254115.1), EhIF2K-A (XP_648932.2), EhIF2K-B (XP_652189.2). *Dictyostelium discoideum*; Dd_iFKA (Q558U1.1), Dd_iFKB (Q550L8), Dd_iFKC (Q75JN1). *Acanthamoeba castellani*; Ac_GCN2-like (L8HJ53). *Saccharomyces cerevisiae*; Sc_GCN2 (P15442). Human; Hs_GCN2 (Q9P2K8.3), Hs_HRI (Q9BQI3), Hs_PKR (P19525), Hs_PERK (Q9NZJ5). Mouse; Mm_GCN2 (NP_001171277.1), Mm_HRI (Q9Z2R9), Mm_PKR (Q03963), Mm_PERK (Q9Z2B5). *Plasmodium falciparum*; Pf_IF2K1 (XP_001348597.1), Pf_IFK2 (Q8I265). *Toxoplasma gondii*; Tg_IF2KA (S8F350), TgIF2K-B (ACA62938), Tg_IF2KC (AHM92904), Tg_IF2KD (AED01979.1). *Leishmania donovani*; Ld_eK2 (A0A0F7CYG9), Ld_LdeK (A9YF35). Human; Hs_CDK1 (NP_203698).

48

Kinase subdomain II

Consensus

Name	Sequence
Ei_IF2K-A	DK--KKYAIKVLIV
Ei_IF2K-B	DS--KVYVLKLMFG
Eh_IF2K-B	DS--KVYVLKMMFG
Eh_IF2K-A	DK--KKYAIKVLIT
Dd_iFKA	DC--RYYAIKKIKT
Dd_iFKB	DC--RYYAIKKIKT
Dd_iFKC	DG--RYYAIKKIKL
Ac_GCN2-like	DG--RLYAIKKIKL
Sc_GCN2	DS--RYYAIKKIRH
Hs_GCN2	DG--CCYAVKRIPI
Hs_HRI	DG--QYYAIKKILI
Hs_PKR	DG--KTYVIKRVKY
Hs_PERK	DD--CNYAIKRIRL
Mm_GCN2	DG--CCYAVKRIPI
Mm_HRI	DG--QHYAIKKILI
Mm_PKR	DG--KRYAIKRVKY
Mm_PERK	DD--CNYAIKRIRL
Pf_IF2K1	FN--ITYALKIIRL
Pf_IFK2	YMKIRKILNKYSKR
Tg_IF2KA	EPGHPIYAVKLILL
Tg_IF2KC	GG--GIFAVKCIPL
Tg_IF2KD	DK--HKYIVKQIFI
Ld_eK2	DG--RLYAIKKIAM
Ld_LdeK	TG--VFYAIKVLVA
Hs_CDK1	TG--QVVAMKKIRL

Consensus: D X - - X X Y A I K X I X X

Figure 2.1: Alignment of kinase domains. Clustal W alignment of the kinase subdomain II of different eIF2α kinases. The grey scale bars represent level of residue conservation. Dashes represent gaps in the sequences that were used to maximize the alignment. The numbers between the dashes indicate the size of each insert removed. NCBI Accession numbers: *Entamoebae*; EiIF2K-A (XP_004259781.1), EiIF2K-B (XP_004254115.1), EhIF2K-A (XP_648932.2), EhIF2K-B (XP_652189.2). *Dictiostelium discoideum*; Dd iFKA (Q558U1.1), Dd_iFKB (Q550L8), Dd_iFKC (Q75JN1). *Acanthamoeba castellani*; Ac_GCN2-like (L8HJ53). *Saccharomyces cerevisiae*; Sc_GCN2 (P15442). Human; Hs_GCN2 (Q9P2K8.3), Hs_HRI (Q9BQI3), Hs_PKR (P19525), Hs_PERK (Q9NZJ5), Hs_CDK1 (NP_203698). Mouse; Mm_GCN2 (NP_001171277.1), Mm_HRI (Q9Z2R9), Mm_PKR (Q03963), Mm_PERK (Q9Z2B5). *Plasmodium falciparum*; Pf_IF2K1 (XP_001348597.1), Pf_IFK2 (Q8I265). *Toxoplasma gondii*; Tg_IF2KA (S8F350), TgIF2K-B(ACA62938), Tg_IF2KC (AHM92904), Tg_IF2KD (AED01979.1). *Leishmania donovani*; Ld_eK2 (A0A0F7CYG9), Ld_LdeK (A9YF35); Mouse; Mm GCN2 (NP_001171277.1), Mm HRI (Q9Z2R9), Mm PKR (Q03963), Mm_PERK (Q9Z2B5). *Plasmodium falciparum*; Pf IF2K1 (XP_001348597.1), Pf IFK2 (Q8I265). *Toxoplasma gondii*; Tg IF2KA (S8F350), Tg IF2K-B (ACA62938) Tg IF2KC (AHM92904), Tg IF2KD (AED01979.1). *Leishmania donovani*; Ld eK2 (A0A0F7CYG9), Ld LdeK (A9YF35).
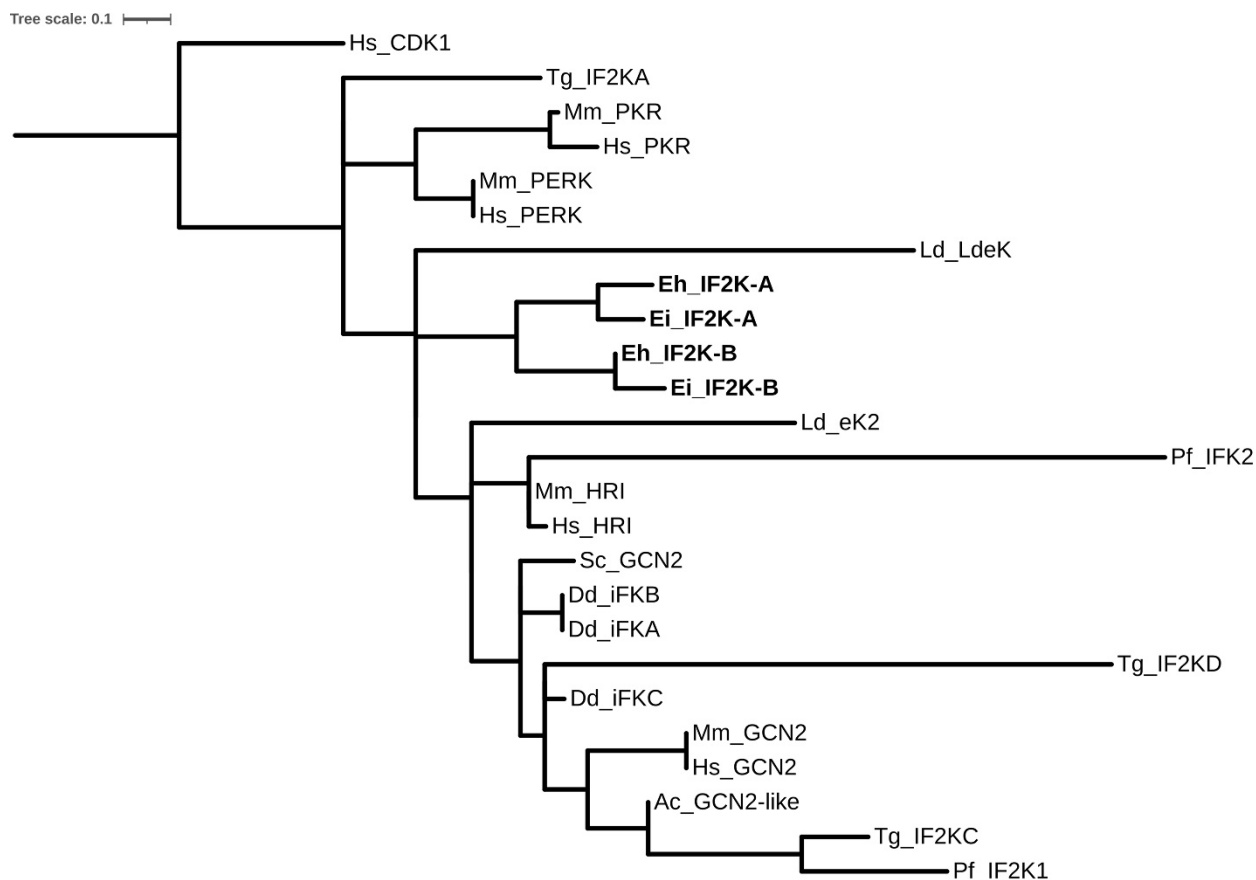
Figure 2.2: Phylogenetic tree of eIF2a kinases. The alignment of the catalytic domains of known eIF2a kinases and putative *Entamoebae* kinases was used to propose phylogenetic relationships by generating a tree. NCBI Accession numbers: *Entamoebae*; EiIF2K-A (XP_004259781.1), EiIF2K-B (XP_004254115.1), EhIF2K-A (XP_648932.2), EhIF2K-B (XP_652189.2). *Dictiostelium discoideum*; Dd iFKA (Q558U1.1), Dd iFKB (Q550L8), Dd iFKC (Q75JN1). *Acanthamoeba castellani*; Ac GCN2-like (L8HJ53). *Saccharomyces cerevisiae*; Sc GCN2 (P15442). Human; Hs GCN2 (Q9P2K8.3), Hs HRI (Q9BQI3), Hs PKR (P19525), Hs PERK (Q9NZJ5), Hs CDK1 (NP_203698). Mouse; Mm GCN2 (NP_001171277.1), Mm HRI (Q9Z2R9), Mm PKR (Q03963), Mm_PERK (Q9Z2B5). *Plasmodium falciparum*; Pf IF2K1 (XP_001348597.1), Pf IFK2 (Q8I265). *Toxoplasma gondii*; Tg IF2KA (S8F350), Tg IF2K-B (ACA62938) Tg IF2KC (AHM92904), Tg IF2KD (AED01979.1). *Leishmania donovani*; Ld eK2 (A0A0F7CYG9), Ld LdeK (A9YF35).

Expression of exogenous protein was induced by plating yeast cells on galactose-containing medium. Western blot analysis using an α-polyhistidine antibody demonstrated successful induction of exogenous protein expression with little to no expression prior to exposure to galactose (Fig 2.3A). We used western blot to assess the level of phosphorylated and total eIF2α in the transgenic yeast strains expressing EiIF2K-A, EiIF2K-B, empty pYES, or human PKR. All 3 kinases could phosphorylate endogenous yeast eIF2α (Fig 2.3B) demonstrating that EiIF2K-A and EiIF2K-B have eIF2α kinase activity. EiIF2K-A and EiIF2K-B possess the conserved lysine in kinase subdomain II (Fig 2.1) that is critical for catalytic activity (18). As a control, we mutated this key lysine residue to arginine and expressed these "dead" kinase domains in the H1894 yeast strain. Western blotting confirmed that dead kinases were incapable of phosphorylating yeast eIF2α (Fig 2.3B). These findings further support the notion that EiIF2K-A and EiIF2K-B are authentic eIF2α kinases.

Generation of *E. invadens* parasites with reduced expression of EiIF2K-A and EiIF2K-B

We used a RNAi Trigger-mediated gene silencing approach to reduce the expression of EiIF2K-A (14). Since the coding sequence of EiIF2K-A is large (2727 nucleotides), we subcloned a partial cDNA encoding amino acids 1-267, which contains the kinase domain, into the gene silencing Trigger plasmid (14). Complete cDNAs are not required for efficient knockdown using this system (14). Stable transfectants (EiIF2K-KD) were selected for and maintained by growth in the presence of neomycin. Parasites harboring the Trigger plasmid, with an insert encoding luciferase, an irrelevant protein, was used as a control (Trig Luc). Using this approach, we obtained substantial knockdown of EiIF2K-A mRNA levels in trophozoites as assessed by RT-PCR analysis (Fig 2.4). Additionally, we measured EiIF2K-A expression during stage conversion in control and knockdown parasites.
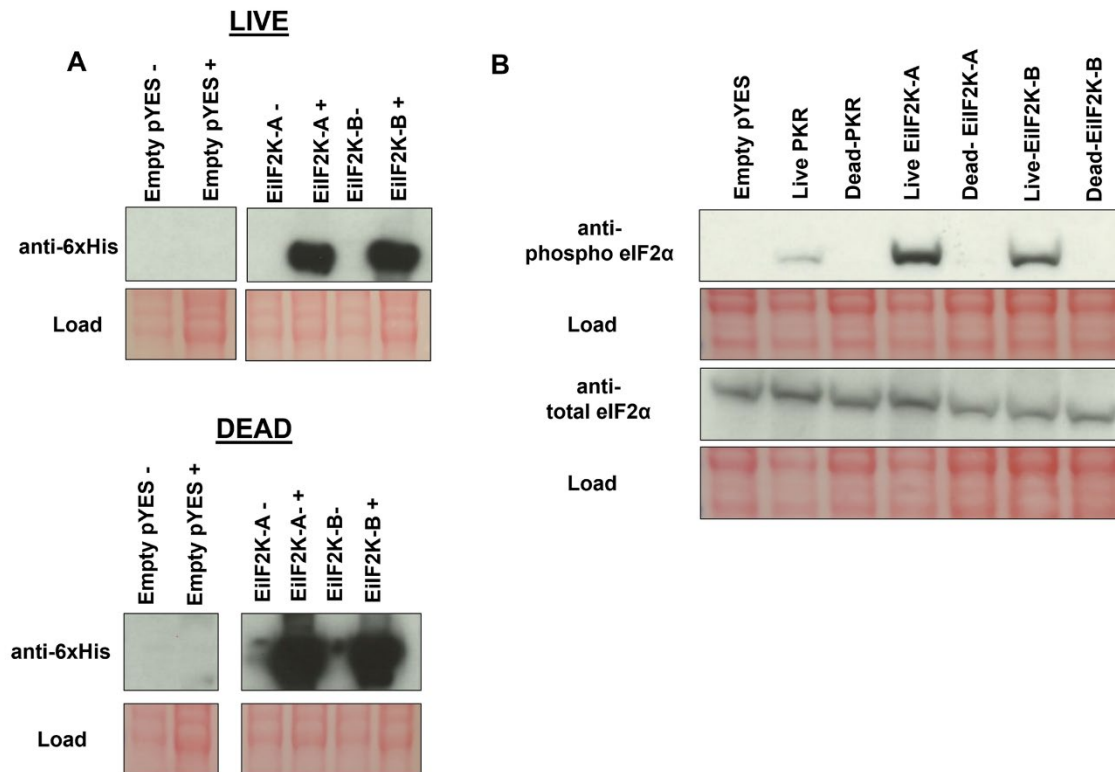
Figure 2.3: Expression of EiIF2K-A and EiIF2K-B kinase domains in a heterologous yeast system demonstrates kinase activity.

Yeast strain H1894, which contains a genetic deletion of its sole eIF2α kinase, was transformed with the galactose-inducible pYES expression vector (empty pYES) or the same vector harboring wildtype (live) or mutated (dead) coding sequences for EiIF2K-A or EiIF2K-B kinase domains. For the dead kinases, a conserved lysine in each kinase subdomain II was mutated to arginine to create an inactive kinase. (A) Western blot, using anti-polyhistidine tag antibody, confirmed galactose-inducible protein expression. "-" symbol represents strains grown on glucose as a carbon source, while "+" symbol represents strains grown on galactose as a carbon source. Expression of the EiIF2K-A or EiIF2K-B kinase domains (live or dead) was only evident when cells were grown on galactose. (B) Western blot showing the level of phosphorylated eIF2α and total eIF2α in H1894 yeast strain harboring empty pYES, a control eIF2α kinase, human PKR (pYES-PKR (live or dead) [13]), pYES-EiIF2K-A (live or dead), or pYES-EiIF2K-B (live or dead). Hyperphosphorylation of eIF2α was only observed in the yeast expressing live kinase domains. Ponceau red staining of membranes (red) indicate load.

We found EiIF2K-A mRNA is undetectable in control and knockdown parasites at 24 h (Fig 2.4) and 48 h (Fig 2.4C) into encystation. EiIF2K-A mRNA was expressed at low levels in the control Trig Luc parasites at 2 h into excystation but was undetectable in the EiIF2K-KD parasites (Fig 2.4D). Since closely related genes may simultaneously be silenced by RNAi approaches (14), it was necessary to also measure expression of EiIF2K-B during growth and stage conversion. EiIF2K-A and EiIF2K-B share 32.64% identity within the kinase domain (Table 2.2). Consistent with published transcriptomic data (8), expression of EiIF2K-B was undetectable in control or mutant trophozoites growing in nutrient-rich medium (Fig 2.4A). On the other hand, the level of EiIF2K-B mRNA was reduced during both encystation (Fig 2.4B) and excystation (Fig 2.4D) in the EiIF2K-KD parasites compared to the Trig Luc control parasites, suggesting that reducing expression of EiIF2K-A caused simultaneous reduced expression of EiIF2K-B during stage conversion.

Since the trigger plasmid containing the kinase domain of EiIF2K-A (5' segment), was sufficient to reduce expression of both kinases, simultaneously, we assembled two new trigger constructs, containing the 3' end of EiIF2K-A (last 909 bp) or EiIF2K-B (last 861 bp), to attempt to knock down genes individually. Electroporation of parasites with the new trigger-EiIF2K-A plasmid failed and as we never obtained neomycin-resistant parasites. On the other hand, we successfully transformed parasites harboring the Trigger-EiIF2K-B-3' plasmid and obtained neomycin-resistant parasites. RT-PCR with EiIF2K-B or EiIF2K-A specific primers (Table 1) demonstrated that EiIF2K-B expression was reduced in EiIF2K-B-KD trophozoites, at 24 hr encystation, and at 2 hr excystation, compared to Trig Luc control parasites. Surprisingly, the Trigger-EiIF2K-B-3' plasmid was also sufficient to reduce expression of EiIF2K-A in EiIF2K-B-KD trophozoites and 2 hr excysting parasites, compared to Trigger Luc parasites (Fig 2.5). Therefore, we only characterized our original EiIF2K-KD cell line.
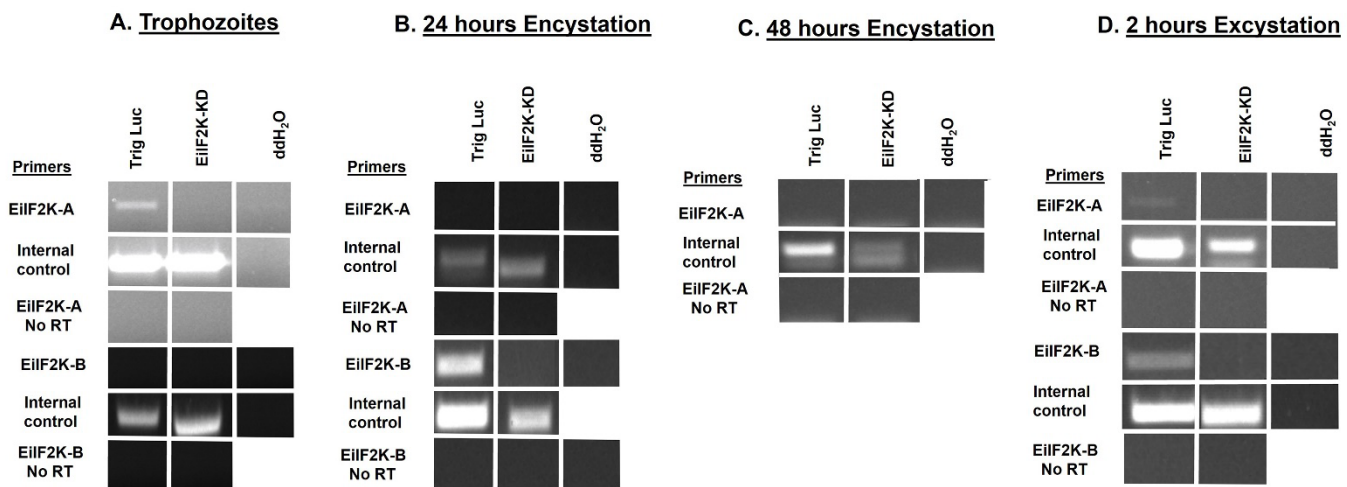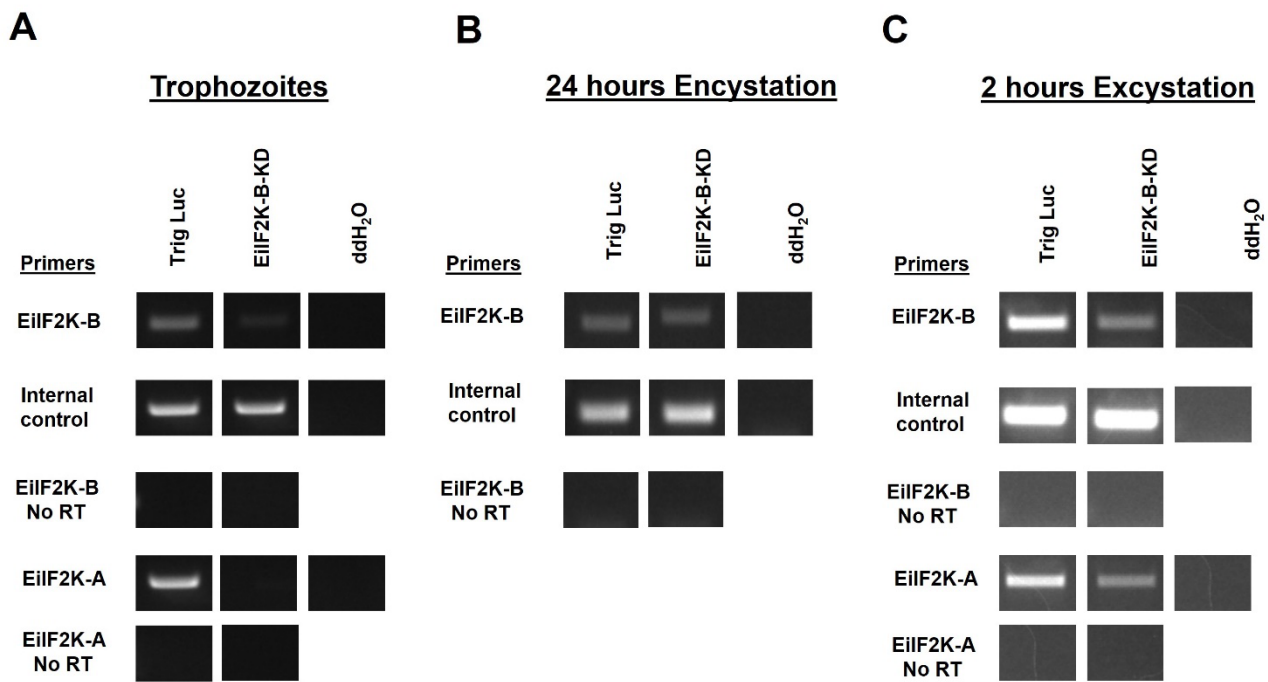
Figure 2.4: Trigger-mediated knockdown of EiIF2K-A and EiIF2K-B expression during growth and stage conversion

RT-PCR was used to measure the level of EiIF2K-A or EiIF2K-B mRNA in transfected parasites harboring the Trigger-EiIF2K-A plasmid (EiIF2K-KD) or the Trigger-Luc control plasmid (Trig Luc). (A) EiIF2K-A mRNA is undetectable in trophozoites harboring Trigger-EiIF2K-A plasmid. EiIF2K-B mRNA is undetectable in Trig Luc and EiIF2K-KD trophozoites. (B) EiIF2K-A mRNA is undetectable in Trig Luc or EiIF2K-KD parasites at 24 h encystation, while there is a decrease in EiIF2K-B mRNA in the EiIF2K-KD parasites line compared to the Trig Luc control at 24 h into encystation. (C) EiIF2K-A mRNA is undetectable at 48 h into encystation. (D) Low levels of EiIF2K-A and EiIF2K-B mRNA are detectable at 2 h into excystation in Trig Luc parasites, but not in EiIF2K-KD parasites. EIN_192230 and EIN_162500 served as load controls for trophozoites or encysting cells, respectively. No RT reactions eliminated reverse transcriptase to confirm that there was no genomic (gDNA) contamination in cDNA samples. Panels labeled "ddH$_2$O" represent reactions in which ddH$_2$O was used as template. A lack of product confirms no gDNA contamination in the reagents.

Figure 2.5: Trigger-mediated knockdown of EiIF2K-A and EiIF2K-B expression during growth and stage conversion in EiIF2K-B-KD parasites

RT-PCR was used to measure the level of EiIF2K-A or EiIF2K-B mRNA in transfected parasites harboring the Trigger-EiIF2K-B-3' plasmid (EiIF2KB-KD) or the Trigger-Luc control plasmid (Trig Luc). (A) EiIF2K-B mRNA is slightly detectable in trophozoites harboring Trigger-EiIF2K-B-3' plasmid. EiIF2K-A mRNA is undetectable in EiIF2KB-KD trophozoites. (B) EiIF2K-B mRNA expression is reduced in EiIF2K-B-KD parasites at 24 h encystation compared to Trig Luc parasites. (C) EiIF2K-A and EiIF2K-B mRNA expression are both reduced at 2 h into excystation in EiIF2K-B-KD parasites compared to Trig Luc parasites. EIN_192230 and EIN_162500 served as load controls for trophozoites or encysting cells, respectively. No RT reactions eliminated reverse transcriptase to confirm that there was no genomic (gDNA) contamination in cDNA samples. Panels labeled "ddH$_2$O" represent reactions in which ddH$_2$O was used as template. A lack of product confirms no gDNA contamination in the reagents.

EiIF2K-KD parasites exhibit lower phospho-eIF2α levels and altered growth in nutrient-rich media than control parasites

Previously, we showed that *E. histolytica* parasites possess a basal level of phosphorylated eIF2α, which increases after exposure to a subset of stressful conditions (4,5) and during encystation (4). Therefore, we measured the level of phosphorylated eIF2α relative to total eIF2α in both trophozoites and encysting control and EiIF2K-KD parasites (Fig 2.6). In agreement with previously published data (4) Trig Luc control parasites exhibited a basal level of phosphorylated eIF2α, which increased at 48 and 72 h into encystation (Fig 2.6A, B). In contrast, parasites with diminished kinase expression displayed decreased, albeit slightly variable, levels of phosphorylated eIF2α in trophozoites and in encysting parasites. The most dramatic decrease in phosphorylation of eIF2α was observed in the mutant at 48 h into the stage conversion program. While mRNA levels of EiIF2K-A and EiIF2K-B are undetectable by RT-PCR in our knockdown cell line (Fig 2.4), there must be some remaining level of kinase mRNA expression as we see some phosphorylation of eIF2α in EiIF2K-KD parasites (Fig 2.6A, B). Overall, these data demonstrate that EiIF2K-KD parasites have a reduced capacity for phosphorylating eIF2α, supporting the identity of EiIF2K-A and EiIF2K-B as eIF2α kinases.

We also measured the growth rate of Trig Luc and EiIF2K-KD parasites in both standard nutrient-rich medium and nutrient-poor/low osmolarity encystation medium for up to 72 h post-inoculation (Fig 2.6). EiIF2K-KD parasites exhibited a lag in growth when seeded into nutrient-rich medium, but eventually exhibited a higher rate of growth than control parasites (Fig 2.6C). This growth phenotype, exhibited by EiIF2K-KD parasites in nutrient-rich medium, is likely the result of reduced EiIF2K-A expression as it is the only kinase expressed in trophozoites.
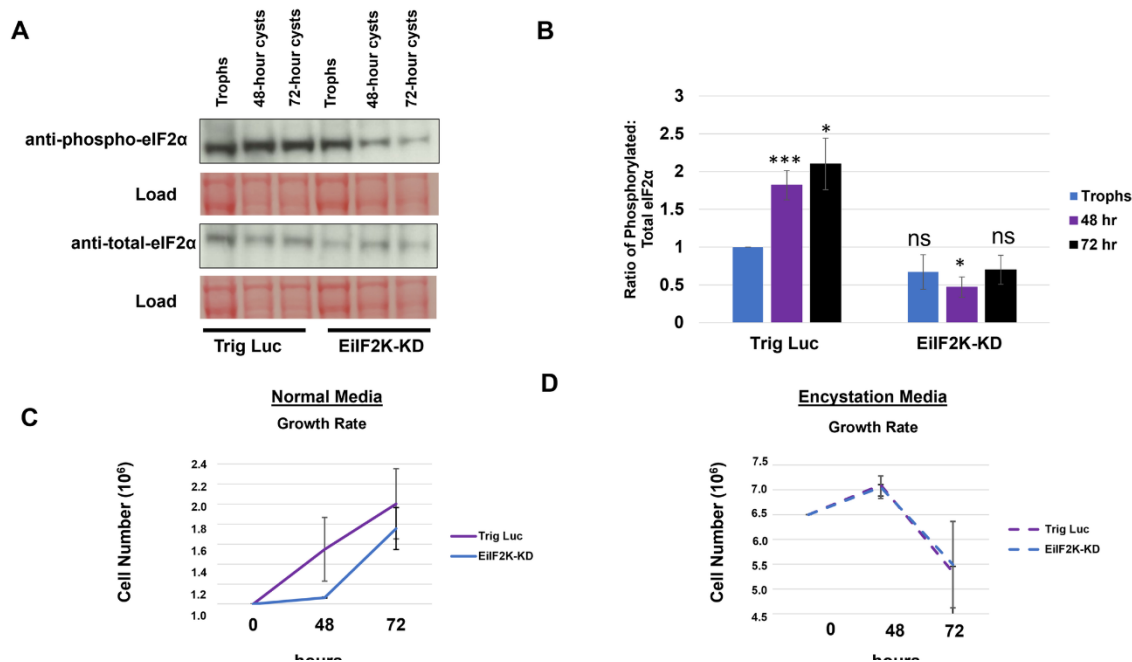
Figure 2.6: EiIF2K-KD parasites exhibit reduced phosphorylation of eIF2α and reduced growth in nutrient-rich medium.

The level of phosphorylated and total eIF2α in Trig Luc and EiIF2K-KD parasites was measured during growth and encystation by western blotting using antibodies specific for phosphorylated or total or eIF2α. Levels of protein were quantified using scanning densitometry of bands on the same blot (Image J) and the ratio of phosphorylated eIF2α to total eIF2α was calculated after correcting for load. (A) Representative western blots for control (Trig Luc) or knockdown (EiIF2K-KD) trophozoites and encysting parasites. (B) Ratio of phosphorylated eIF2α to total eIF2α for Trig Luc or EiIF2K-KD trophozoites (blue), or 48-h cysts (purple), and 72-h cysts (black). The ratio for Trig Luc trophozoites was arbitrarily set to 1.0 and was used as the basis for comparison. During encystation, the ratio of phosphorylated eIF2α to total eIF2α increases in Trig Luc parasites ($P<0.05$). In all stages of the life cycle, the ratio of phosphorylated eIF2α to total eIF2α was generally decreased in EiIF2K-KD parasites compared to Trig Luc parasites. The most dramatic decrease in the ratio of phosphorylated:total eIF2α in was observed in the mutant at 48 h into the encystation program ($P<0.05$). (ns, not statistically significant). Data represent the mean ± standard error of at least 5 separate trials. Trophozoites were seeded into standard nutrient-rich culture media (1×10^6 initial inoculum) (C) or into encystation media (6.5×10^6 initial inoculum) (D) for 48 or 72 h. At each time point, parasites were enumerated using trypan blue exclusion and light microscopy. (C) EiIF2K-KD parasites exhibit an initial lag in growth when seeded into nutrient-rich medium, but eventually show an increased growth rate between

On the other hand, there was no difference in the growth kinetics of the mutant in encystation medium when compared to that of the control parasites (Fig 2.6D). The decrease in parasite number during incubation in encystation medium (Fig 2.6C, D) is typical as a fraction of the population loses viability instead of encysting.

EiIF2K-KD parasites have altered rates of stage conversion

To elucidate the role of the kinases in stage conversion, we measured the rate of encystation and excystation in both Trig Luc and EiIF2K-KD parasites. Encystation was induced by inoculating parasites into nutrient-poor/low osmolarity encystation media. Hallmarks of encystation include the accumulation of a chitin-rich cell wall and a reduction in cell size (19). To assess encystation, we used flow cytometry (19) and Congo Red staining to track the accrual of chitin as well as changes in cell size. In the EiIF2K-KD parasites, the percent of parasites that had encysted was significantly higher at 48 h post inoculation, but not at 72 h post inoculation, when compared to control parasites (Fig 2.7A). This suggests that the rate, but not the overall efficiency, of encystation is higher in parasites with diminished kinase expression. Since both kinases are expressed during encystation, we cannot discern if the encystation phenotype is due to loss of one or both kinases. To induce excystation, cysts were incubated in excystation media, which restores nutrients and osmolarity and contains bile salts to mimic passage through the host digestive system (8). EiIF2K-KD parasites exhibited a significantly lower rate of excystation compared to control parasites at 2 h and 8 h into the excystation program (Fig 2.7B). Since EiIF2K-B is the only kinase expressed during excystation, we posit that reduced EiIF2K-B expression may be solely responsible for the excystation phenotype.
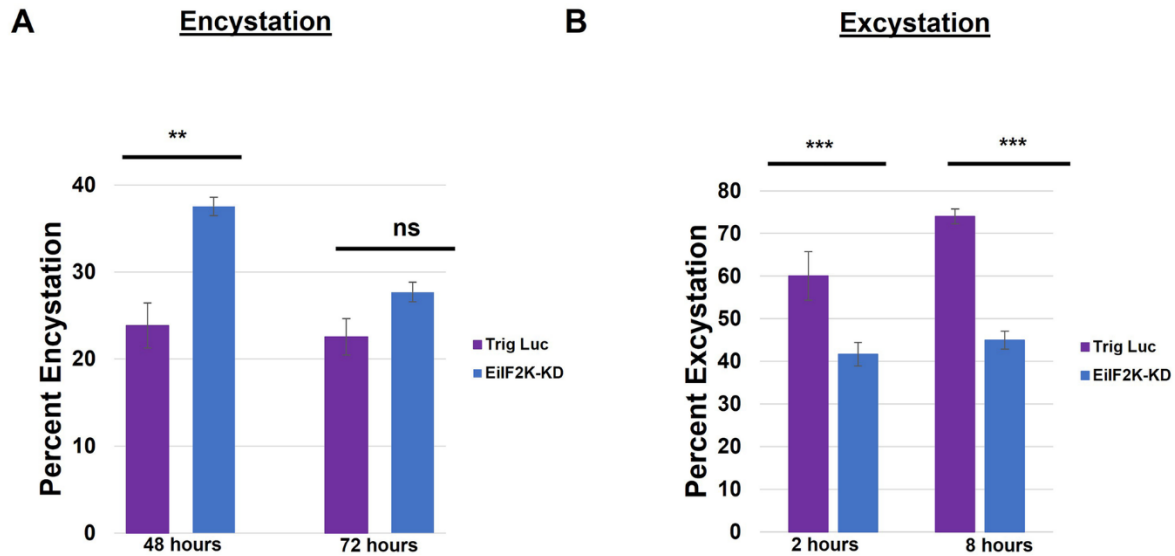
Figure 2.7: The rate of encystation is increased and the rate of excystation is decreased in EiIF2K-KD parasites

(A) Trig Luc and EiIF2K-KD parasites were induced to encyst for either 48 or 72 h. Mature cysts were stained with Congo Red and quantified using flow cytometry. A higher percent of EiIF2K-KD parasites encysted by 48 h and at 72 h compared to Trig Luc parasites. However, the increase was only statistically significant at 48 h (P<0.01), suggesting that the mutants have a higher initial rate of encystation but not a higher efficiency of encystation. (B) Trig Luc cells and EiIF2K-KD cysts were induced to excyst by incubation in excystation media for 2 or 8 h. The number of mature cysts was quantified before and after excystation and the decrease in the number of cysts represented the fraction (percent) of parasites that had excysted. The excystation rate of EiIF2K-KD was significantly (P<0.001) lower than that of Trig Luc parasites at both 2 and 8 h. Data represent the mean ± standard error of at least 3 separate trials.

EiIF2K-KD trophozoites are more susceptible to oxidative stress

Previously, we demonstrated that *E. histolytica* phosphorylates eIF2α in response to several different stressful conditions including oxidative stress (4) As such, EiIF2K-A, the sole kinase expressed in trophozoites, may be responsible for countering oxidative stress. Suresh et al., (2016) demonstrated that exposing *E. invadens* parasites to 4 mM H_2O_2 for 1 h induced oxidative stress, as evidenced by detachment and rounding of parasites, while maintaining ≥90% viability (14). However, the level of phospho-eIF2α in H_2O_2-treated *E. invadens* trophozoites has not been examined. Therefore, we exposed wildtype (WT) *E. invadens* trophozoites to ddH_2O (diluent) or 4 mM H_2O_2 for 1 h at 25°C and measured levels of total and phosphorylated eIF2α by western blotting (Fig 2.8A?). Phosphorylation increased in parasites treated with 4 mM H_2O_2 compared to the unstressed control. To ascertain if EiIF2K-A regulates the response to oxidative stress in trophozoites, we measured the viability of WT, Trig Luc, and EiIF2K-KD parasites exposed to 4 mM H_2O_2; however, we observed no difference in viability (Fig 2.8B?). Therefore, we used a higher concentration of H_2O_2 that could reduce viability of WT *E. invadens* parasites. WT, Trig Luc, and EiIF2K-KD parasites were exposed to 1 M H_2O_2 for 1 h at 37°C. This treatment caused approximately 30% parasite death in WT parasites, 40% parasite death in Trig Luc parasites (Fig 2.9A?) and approximately 65% parasite death in EiIF2K-KD parasites. The statistically significant reduction in viability in EiIF2K-KD parasites supports the notion that EiIF2K-A may regulate the response to oxidative stress in *E. invadens* trophozoites.

EiIF2K-KD parasites may be more susceptible to oxidative stress because of their reduced capacity to phosphorylate eIF2α. Thus, we used western blotting to measure the levels of phosphorylated and total eIF2α in control and EiIF2K-KD parasites exposed to H_2O_2. The ratio of phosphorylated eIF2α to total eIF2α increased significantly in stressed Trig Luc parasites, but not in EiIF2K-KD parasites (Fig 2.9B, C). There is a slight increase in phosphorylation of eIF2α in

Figure 2.8: Phosphorylation of eIF2α and viability of parasites in response to 4 mM H₂O₂

(A) Wildtype (WT) parasites were exposed to ddH₂O (diluent) or 4 mM H₂O₂ for 1 h at 25°C and the levels of total and phosphorylated eIF2α were measured by western blotting. There is a basal level of phosphorylated eIF2α, which increased after treatment with H₂O₂. Coomassie stained gel bands demonstrate equal load. (B) We exposed WT, Trig Luc, and EiIF2K-KD parasites to 4 mM H₂O₂ for 1 h at 25°C and measured viability using trypan blue exclusion and an Automated Luna Hemocytometer. There is no difference in viability among cell lines. Data represent the mean ± standard error of at least 3 separate trials.
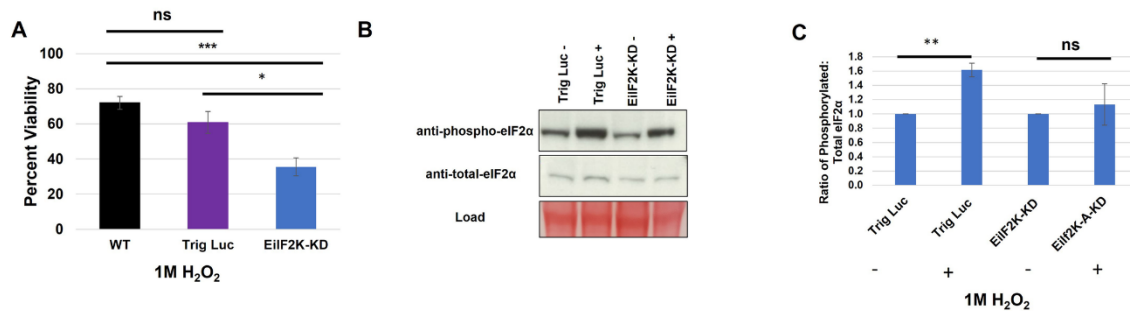
Figure 2.9: EiIF2K-KD trophozoites are more susceptible to oxidative stress

Wildtype (WT), Trig Luc, or EiIF2K-KD trophozoites were exposed to 1M H_2O_2 for 1 h at 25°C.

(A) Viability was assessed using trypan blue exclusion and a Luna Automated Hemocytometer. EiIF2K-KD parasites were significantly less viable when exposed to oxidative stress compared to WT and Trig Luc parasites ($P<0.05$). (B) Representative western blot showing the level of phosphorylated and total eIF2α in Trig Luc or EiIF2-KD cells before (-) and after (+) H_2O_2-treatment. (C) Western blotting was used to measure levels of total and phosphorylated eIF2α in parasites exposed to ddH_2O or 1 M H_2O_2 for 1 h at 25°C. Levels of protein were quantified using scanning densitometry of bands on the same blot (Image J) and the ratio of phosphorylated eIF2α to total eIF2α was calculated after correcting for load. Trig Luc parasites exposed to 1 M H_2O_2 exhibited significantly higher ($P<0.01$) levels of phosphorylated eIF2α compared to controls, while EiIF2K-KD parasites exposed to the same conditions did not exhibit significantly increased levels of phosphorylated eIF2α. Data represent the mean ± standard error of at least 3 separate trials.

EiIF2K-KD parasites treated with 1M H_2O_2 compared to those parasites treated with ddH_2O. Currently, there are no methods to knockout genes in the *Entamoebae*. Therefore, there remains some level of kinase expression in our EiIF2K-KD parasites, which may respond to stress. Overall, these data support the identity of EiIF2K-A as an authentic kinase and emphasize the importance of the eIF2α mechanism in parasite stress management.

EiIF2K-KD trophozoites exhibit increased virulence functions

To discern the effect of decreased EiIF2K-A expression on parasite virulence, we measured two key virulence functions: erythrophagocytosis and adhesion to host cells. Trig Luc and EiIF2K-KD trophozoites were exposed to human red blood cells (hRBCs) for 10 min, after which uptake of heme was quantified spectrophotometrically (20). Adhesion was measured by quantifying the degree to which fluorescently-labeled parasites could adhere to a fixed monolayer of Chinese hamster ovary (CHO) cells (21). EiIF2K-KD parasites exhibited significantly increased phagocytosis (Fig 2.10A) and adhesion (Fig 2.10B), which suggests that EiIF2K-A may directly or indirectly modulates virulence functions because EiIF2K-A is the only eIF2α kinase expressed in trophozoites.

V.   Discussion

This is the first study to characterize eIF2α kinases in the *Entamoebae.* We used a heterologous yeast system to show that EiIF2K-A and EiIF2K-B are authentic eIF2α kinases. Using an established RNAi silencing approach (14), we knocked down both kinases using a single Trigger-EiIF2K-A plasmid. We found that EiIF2K-KD parasites were more susceptible to oxidative stress and exhibited increased virulence functions (erythrophagocytosis and parasite-host cell adhesion). We also observed an increased rate of encystation and decreased rate of excystation in EiIF2K-KD parasites. Due to the stage-specific expression patterns of these kinases, we posit that EiIF2K-A may regulate phenotypes observed in trophozoites, while the
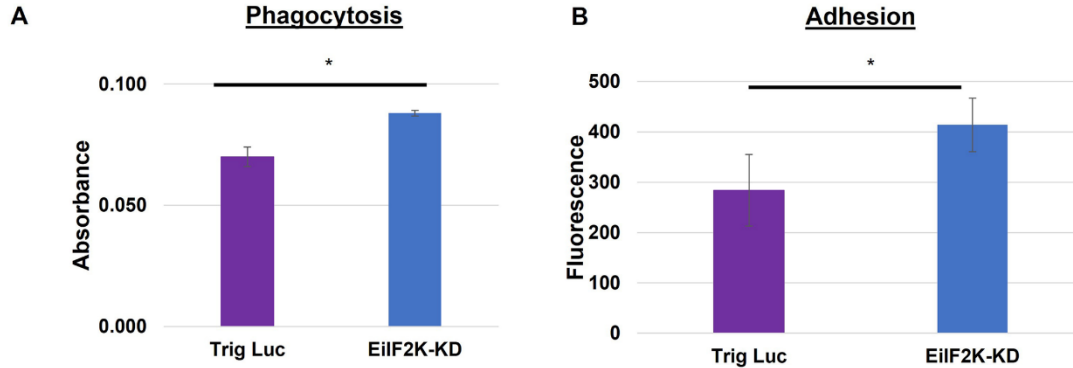
Figure 2.10: Erythrophagocytosis and adhesion are increased in EiIF2K-KD parasites

(A) Trig Luc or EiIF2K-KD parasites were incubated with human red blood cells (hRBCs: amoeba ratio; 100:1) for 10 min, lysed, and spectrophotometrically analyzed for internalized heme at 405 nm. Amoebae with reduced expression of EiIF2K-A exhibited increased phagocytosis of hRBCs. The data represent the mean ± standard error. of at least 3 separate trials ($P<0.05$). (B) Calcein AM-stained control or mutant parasites were incubated with fixed monolayers of Chinese Hamster Ovary (CHO) cells for 30 min. Unadhered parasites were rinsed off the monolayer of CHO cells and the level of adhesion (calcein-AM fluorescence) was measured by spectrofluorimetry using an excitation wavelength of 485 nm and an emission wavelength of 528 nm. EiIF2K-KD trophozoites exhibited significantly higher adhesion to host cells than Trig Luc trophozoites ($P<0.05$). Data represent the mean ± standard error of at least 3 separate trials.

excystation phenotype may be due to the loss of EiIF2K-B. Furthermore, we attempted to obtain individual knockdown of each eIF2α kinase using trigger plasmids containing the 3' end of the kinase genes and found that Trigger-EiIF2K-B-3' plasmid is also sufficient to reduce expression of both kinases. Overall, this study advances our knowledge about the stress response and stage conversion in *Entamoeba* species, as well as highlights the urgent need for more sophisticated gene modifying tools in the *Entamoebae.*

In mammalian cells, phosphorylation of eIF2α is regulated by a family of four eIF2α kinases that are activated in a stress-specific manner. The ability of the kinases to respond to various stresses rely on regulatory domains. Interestingly, in several protozoan parasites (13, 22, 23, 24), the eIF2α kinases possess divergent regulatory domains, suggesting that protozoan eIF2α kinases may respond differently to environmental stress than their mammalian counterparts (11). Currently, it is not possible to predict, by sequence-analysis, the types of stresses to which the *Entamoeba* kinases will respond.

Nevertheless, we demonstrate that trophozoites with reduced EiIF2K-A expression are more susceptible to at least one stressful condition, oxidative stress. EiIF2K-KD parasites were less viable in the presence of high concentrations of H_2O_2 and possessed decreased levels of phosphorylated eIF2α when compared to control parasites (Fig 2.9A). This is not surprising since Hendrick et al. (4) demonstrated that oxidative stress induces the phosphorylation of eIF2α in *E. histolytica*. Likewise, Augusto et al. (25) knocked out an eIF2α kinase, TgIF2K-B, in *T. gondii*, and found that null parasites had an impaired response to oxidative stress. To further illuminate the stress-specific response of this kinase, it will be necessary to assess the ability of the EiIF2K-KD cells to survive other stressful conditions. Additionally, examining the transcriptome and translatome of EiIF2K-KD and control parasites under oxidative stress would help determine if these eIF2α kinases directly regulate the stress response of *E. histolytica*.

EiIF2K-KD parasites exhibited no growth phenotype in encystation medium and a transient lag in growth in nutrient-rich medium (Fig 2.6C,D). This is unlike *Trypanosoma cruzi* parasites lacking the eIF2α kinase, TcK2, which exhibit a growth deficiency (26). However, the *E. invadens* phenotype is similar that of *Leishmania donovani* parasites expressing a dominant negative version of a GCN2-like kinase, which do not exhibit a growth defect (22). It is possible that in *L. donovani,* multiple eIF2α kinases share redundant functions and the loss of one kinase is compensated by other related kinases. However, in *E. invadens,* EiIF2K-A is the only eIF2α kinase expressed in trophozoites ((8) and the current study). Thus, compensation by related kinases may not be possible in the trophozoite stage of this parasite.

EiIF2K-A is expressed in trophozoites and decreases during initial encystation (8). Since decreased EiIF2K-A expression correlates with initiation of encystation, it is conceivable that EiIF2K-KD parasites are primed to encyst. In support of this, the encystation rate of the EiIF2K-KD parasites was significantly higher than that of control parasites at 48 h (Fig 2.7A). If EiIF2K-KD parasites are primed to encyst, they may exhibit early expression of encystation-specific genes, which, in turn, could lead to an increased rate of encystation, but not necessarily an increased efficiency. To gain further insight into the relationship between eIF2α kinase expression and encystation, it will be necessary to define the cyst-specific translatome, perhaps by ribosome-profiling (Ribo-seq) (27), in EiIF2K-KD trophozoites.

The excystation rate of EiIF2K-KD parasites was significantly decreased (Fig 2.7B). EiIF2K-B is expressed at low levels during encystation, and at high levels during excystation (8). Therefore, we hypothesize that the excystation phenotype may be due to the loss of EiIF2K-B, as it is the only eIF2α kinase expressed during excystation. At present, we cannot determine if the encystation phenotype is due to loss of EiIF2K-A, EiIF2K-B, or both. To understand the exact

roles of EiIF2K-A and EiIF2K-B in stage conversion, it will be essential to knock down each gene individually and evaluate stage conversion.

Previously, we demonstrated that the level of phosphorylated eIF2α increases significantly during encystation (4). Thus, it was not surprising that EiIF2K-A and/or EiIF2K-B may play a role in stage conversion in *E. invadens*. Likewise, eIF2α kinases play roles in stage conversion in other protozoa. For instance, phosphorylation of eIF2α increases during stage conversion or differentiation of *T. cruzi* (26, 28), *T. gondii* (29), and *Plasmodium falciparum* (23). It was unanticipated that reduced phosphorylation of eIF2α would correlate with an *increased* rate of encystation in *E. invadens*. Perhaps in the *Entamoebae*, precise timing of translation is necessary to control the rate of encystation in such a way as to guarantee the accurate conversion of trophozoites into environmentally-stable cysts. Without the kinases that control phosphorylation of eIF2α, the rate of translation becomes unbridled, and the rate of encystation becomes unregulated. Defining the transcriptome and translatome, perhaps by Ribo-seq (27), during stage conversion in EiIF2K-KD parasites will provide additional insight into the roles of these kinases during stage conversion.

EiIF2K-KD parasites exhibited increased erythrophagocytosis and adhesion to host cells, which are two important virulence functions (Fig 2.10). These data suggest that EiIF2K-A, the only eIF2α kinase expressed in trophozoites (8), may directly or indirectly regulate erythrophagocytosis and adhesion. Similarly, *T. gondii* parasites lacking one eIF2α kinase, TgIF2K-B, were more virulent *in vivo* (25). Given the role of eIF2α kinases in the management of translation, one explanation for increased parasite virulence functions is dysregulated translation of genes that control virulence. To establish a causal relationship between decreased kinase expression and increased virulence phenotypes, we must define the translatome and transcriptome of EiIF2K-KD and control parasites.

It may be argued that an increase in virulence functions or the rate of encystation in the EiIF2K-KD parasites implies that this kinase is not a suitable target for anti-parasitic drug design. However, increased sensitivity to oxidative stress in the EiIF2K-KD parasites supports its potential as a drug target. The *Entamoebae* are microaerophilic. Therefore, to survive in the host, these parasites must preserve intracellular hypoxia within oxygenated host tissues, such as the liver, and surmount attacks on cellular homeostasis by reactive oxygen species originating from the host immune response (30). Thus, it is conceivable that disabling EiIF2K-A would simultaneously restrict the ability of the pathogen to endure in the host. In support of this, genetic loss of the eIF2α kinases, PERK and GCN2, in immortalized mouse fibroblasts and human tumor cells increases their susceptibility to oxidative stress (31).

The eIF2α kinases are also implicated in human pathologies including cancer (32), diabetes (33), and neurodegenerative disorders (34) and are the subject of intense study because they represent logical targets for the design of therapies. For instance, overactivation of PERK has been associated with neurological disorders such as Parkinson's Disease and Alzheimer's Disease (34). It has been found that the compound, LDN-0060609, significantly inhibits PERK-mediated phosphorylation of eIF2α in rat astrocytes, which suggests that it may be a suitable drug for the treatment of neurological diseases (35). Targeting the eIF2α-based regulation of translation in protozoan parasites is also underway. For example, pharmacological inhibition of PK4 in *P. falciparum* with the PERK inhibitor, GSK2606414, blocks parasite differentiation and reduces artemisinin-induced latency (36). Inhibition of PERK-like eIF2 kinase, TgIF2K-A, in *T. gondii*, with the same inhibitor, blocked multiple steps of the tachyzoite lytic cycle and lowered the rate of bradyzoite differentiation (37). Finally, GSK2606414 reduced *Leishmania amazonensis* infection of macrophages (38). Together, with the data presented in this study, these encouraging results in other pathogens support the potential for the *Entamoeba* eIF2α kinases to serve as targets for drug inhibition.

VI. Acknowledgements

VII.   Literature Cited

[1] Shirley DT, Farr L, Watanabe K, Moonah S. A review of the global burden, new diagnostics, and current therapeutics for amebiasis. Open Forum Infect Dis. 2018;*5*(7): 1–9.

[2] Grebmer K, Bernstein J, de Waal A, Prasai N, Yin S, Yohannes, Y. Progress on sanitation and drinking water. UNICEF and WHO 2015 Update and MDG Assessment.

[3] Bercu T, Petri W, Behm JW. Amebic colitis: new insights into pathogenesis and treatment. Current Gastroenterol Rep. 2007;9(5): 429–433.

[4] Hendrick H., Welter BH, Hapstack MA, Sykes SE, Sullivan WJ, Temesvari LA. Phosphorylation of eukaryotic initiation factor-2 alpha during stress and encystation in *Entamoeba* Species. PLoS Pathog. 2016;12(12): 1–14.

[5] Walters HA, Welter BH, Sullivan WJ, Temesvari LA. Phosphorylation of eukaryotic initiation factor-2α in response to endoplasmic reticulum and nitrosative stress in the human protozoan parasite, *Entamoeba histolytica*. Mol Biochem Parasitol. 2019;234(2019): 1-9.

[6] Avron B, Stolarsky T, Chayen A, Mirelman D. Encystation of *Entamoeba invadens* IP-1 is induced by lowering the osmotic pressure and depletion of nutrients from the medium. J Protozool. 1986;33:522– 525.

[7] Coppi A., Eichinger D. Regulation of *Entamoeba invadens* encystation and gene expression with galactose and N -acetylglucosamine. Mol. Biochem. Parasitol. 1999;102(1999): 67–77.

[8] Ehrenkaufer GM, Weedall GD, Williams D, Lorenzi HA, Caler E, Hall N, Singh U. The genome and transcriptome of the enteric parasite *Entamoeba invadens*, a model for encystation. Genome Biol. 2013;14(7): 1-29.

[9] Field J, Dellen KV, Ghosh SK, Samuelson J. Responses of *Entamoeba invadens* to Heat Shock and Encystation are Related. J. Eukaryot. Microbiol. 2000;47(5): 511–514.

[10] Varghese SS, Ghosh SK. Stress-responsive *Entamoeba* topoisomerase II: a potential antiamoebic target. FEBS Lett. 2020;594: 1005–1020.

[11] Vonlaufen N, Kanzok SM, Wek RC, Sullivan WJ. Stress response pathways in protozoan parasites. Cellular Microbiol. 2008;10(12): 2387–2399.

[12] Dever TE. Using GCN4 as a reporter of eIF2 α phosphorylation and translational regulation in yeast. Methods. 1997;11(4): 403–417.

[13] Sullivan WJ, Narasimhan J, Bhatti MM, Wek RC. Parasite-specific eIF2 (eukaryotic initiation factor-2) kinase required for stress-induced translation control. Biochem J. 2004;380(Pt 2): 523–531.

[14] Suresh S, Ehrenkaufer G, Zhang H, Singh U. Development of RNA interference trigger-mediated gene silencing in *Entamoeba invadens*. Infect Immun. 2016;84(4), 964–975.

[15] Donnelly N, Gorman AM, Gupta S, Samali A. The eIF2α kinases: Their structures and functions. Cell Mol Life Sci. 2013;70(19): 3493–3511.

[16] Vattem K, Staschke KA, Wek RC. Mechanism of activation of the double-stranded-RNA-dependent kinase, PKR: role of dimerization and cellular localization in the stimulation of PKR phosphorylation of eukaryotic initiation factor-2α (eIF2α). Eur. J. Biochem. 2001;268: 3674–3684

[17] Gietz R, Schiestl RH. High-efficiency yeast transformation using the LiAc / SS carrier DNA / PEG method. Nat. Protoc. 2007;2: 31–35.

[18] Hanks SK, Hunter T. The eukaryotic protein kinase superfamily: kinase (catalytic) domain structure and classification. The FASEB J. 1995;9(8): 576–596.

[19] Welter BH, Sehorn MG, Temesvari LA. Flow cytometric characterization of encystation in *Entamoeba invadens*. Mol Biochem Parasitol. 2017;218(October): 23–27.

[20] King AV, Welter BH, Koushik AB, Gordon LN, Temesvari LA. A Genome-Wide Over-Expression Screen Identifies Genes Involved in Phagocytosis in the Human Protozoan Parasite, *Entamoeba histolytica*. PLoS ONE. 2012;7(8): e43025.

[21] Powell RR, Welter BH, Hwu R, Bowersox B. Attaway C, Temesvari LA. *Entamoeba histolytica*: FYVE-finger domains, phosphatidylinositol 3-phosphate biosensors, associate with phagosomes but not fluid filled endosomes. Exp Parasitol. 2006;112(4): 221–231.

[22] Rao SJ, Meleppattu S, Pal JK. A GCN2-like eIF2α kinase (LdeK1) of *Leishmania donovani* and its possible role in stress response. PLoS ONE. 2016;11(6). e0156032

[23] Zhang M, Mishra S, Sakthivel R, Rojas M, Ranjan R, Sullivan WJ. PK4, a eukaryotic initiation factor 2α (eIF2α) kinase, is essential for the development of the erythrocytic cycle of *Plasmodium*. Proc Natl Acad Sci. U.S.A. 2012;109(10): 3956–61.

[24] Moraes MC, Jesus TC, Hashimoto NN, Dey M, Schwartz KJ, Alves VS, Avila CC, Bangs JD, Dever TE, Schenkman S, Castilho BA. Novel membrane-bound eIF2α kinase in the flagellar pocket of *Trypanosoma brucei*. Eukaryot. Cell. 2007;6(11): 1979–1991.

[25] Augusto L, Martynowicz J, Amin PH, Carlson KR, Wek, RC, Sullivan WJ. Tgif2k-b is an eif2a kinase in *Toxoplasma gondii* that responds to oxidative stress and optimizes pathogenicity. MBio. 2021;12(1): 1–14.

[26] da Silva Augusto L, Moretti NS, Ramos TCP, de Jesus TCL, Zhang M, Castilho BA, Schenkman S. A Membrane-bound eIF2 Alpha Kinase Located in Endosomes Is Regulated by Heme and Controls Differentiation and ROS Levels in *Trypanosoma cruzi*. PLoS Pathog. 2015;11(2), 1–27

[27] Holmes MJ, Shah P, Wek RC, Sullivan WJ Jr. Simultaneous Ribosome Profiling of Human Host Cells Infected with *Toxoplasma gondii*. mSphere. 2019;4(3):e00292-19.

[28] Tonelli RR, da Silva Augusto L, Castilho BA, Schenkman S. Protein synthesis attenuation by phosphorylation of eIF2α is required for the differentiation of *Trypanosoma cruzi* into infective forms. PLoS ONE. 2011;6(11), 1–10.

[29] Narasimhan J, Joyce BR, Naguleswaran A, Smith AT, Livingston MR, Dixon SE, Coppens I, Wek RC, Sullivan WJ. Translation regulation by eukaryotic initiation factor-2 kinases in the development of latent cysts in *Toxoplasma gondii*. J Biol Chem. 2008;283(24), 16591–16601.

[30] Pineda E, Perdomo D. *Entamoeba histolytica* under Oxidative Stress: What Countermeasure Mechanisms Are in Place? Cells. 2017;6(4), 44.

[31] Rajesh K, Krishnamoorthy J, Kazimierczak U, Tenkerian C, Papadakis AI, Wang S, Huang S, Koromilas AE. Phosphorylation of the translation initiation factor eIf2α at serine 51 determines the cell fate decisions of Akt in response to oxidative stress. Cell Death Dis. 2015;6(1).

[32] Wek RC, Cavener DR. Translational Control and the Unfolded Protein Response. Antioxid Redox Signal. 2007;9(12), 2357–2372.

[33] Kim MJ, Kim MN, Min SH, Ham DS, Kim JW, Yoon KH, Park KS, Jung HS. Specific PERK inhibitors enhanced glucose-stimulated insulin secretion in a mouse model of type 2 diabetes. Metabolism. 2019;97: 87-91.

[34] Axten JM, Romeril SP, Shu A, Ralph J, Medina JR, Feng Y, Li WH, Grant SW, Heerding DA, Minthorn E, et al. Discovery of GSK2656157: An optimized PERK inhibitor selected for preclinical development. ACS Med Chem Lett. 2013;4:964-968

[35] Rozpędek W, Pytel D, Popławski T, Walczak A., Gradzik K, Wawrzynkiewicz A, Wojtczak, R, Mucha B, Diehl JA, Majsterek I. Inhibition of the PERK-Dependent Unfolded Protein Response Signaling Pathway Involved in the Pathogenesis of Alzheimer's Disease. Curr Alzheimer Res. 2019;16(209): 1875-5828

[36] Zhang M, Gallego-Delgado J, Fernandez-Arias C, Waters NC, Rodriguez A, Tsuji M, Wek RC, Nussenzweig V, Sullivan WJ. Inhibiting the *Plasmodium* eIF2α Kinase PK4 Prevents Artemisinin-Induced Latency. Cell Host and Microbe. 2017;22(6): 766-776

[37] Augusto L, Martynowic J, Staschk K, Wek RC, Sullivan WJ. Effects of PERK eIF2α Kinase Inhibitor against *Toxoplasma gondii*. Antimicrob Agents Chemother. 2018;62(11), 1–10.

[38] Dias-Teixeira KL, Calegari-Silva TC, Medina JM, Vivarini ÁC, Cavalcanti Á, Teteo N, Santana AKM, Real F, Gomes CM, Pereira RMS, Fasel N, Silva JS, Aktas BH, Lopes UG. Emerging Role for the PERK/eIF2α/ATF4 in Human Cutaneous Leishmaniasis. Sci Rep. 2017;7(1): 1–11.

[39] Bateman A, Martin MJ, Orchard S, Magrane M, Agivetova R, Ahmad S, Alpi E, Bowler-Barnett EH, Britto R, Bursteinas B, Bye-A-Jee H, Coetzee R, Cukura A, Silva AD, Denny P, Dogan T, Ebenezer TG, Fan J, Castro LG. Zhang, J. UniProt: The universal protein knowledgebase in 2021. Nucleic Acids Res. 2021;49(D1): D480–D489.

[40] Hulo N, Bairoch A, Bulliard V, Cerutti L, De Castro E, Langendijk-Genevaux PS, Pagni M, Sigrist CJA.The PROSITE database. Nucleic Acids Res. 2006;34: D227-D230.

[41] Waterhouse AM, Procter JB, Martin DMA, Clamp M, Barton GJ. Jalview Version 2-a multiple sequence alignment editor and analysis workbench. Bioinform. 2009;25: 1189-1191.

[42] Dereeper A*, Guignon V*, Blanc G, Audic S, Buffet S, Chevenet F, Dufayard JF, Guindon S, Lefort V, Lescot M, Claverie JM, Gascuel O. Phylogeny.fr: robust phylogenetic analysis for the non-specialist. Nucleic Acids Res. 2008;36(Web Server issue): W465-9.

[43] Letunic I, Bork P. Interactive Tree of Life (iTOL) v4: Recent updates and new developments. Nucleic Acids Res. 2019;47(W1): 256–259.

[44] Singh N, Ojha S, Bhattacharya A, Bhattacharya S. Stable transfection and continuous expression of heterologous genes in *Entamoeba invadens*. Mol Biochem Parasitol. 2012;184: 9–12.

[45] Zhang T, Lei J, Yang H, Xu K, Wang R, Zhang Z. An improved method for whole protein extraction from yeast Saccharomyces cerevisiae. Yeast. 2011;28(11): 795–798.

CHAPTER THREE

HYPOTHETICAL PROTEINS PLAY A ROLE IN STAGE CONVERSION, VIRULENCE,
AND THE STRESS RESPONSE IN THE *ENTAMOEBA* SPECIES

Heather A. Walters [1,2], Brenda H. Welter [1,2], Lesly A. Temesvari [1,2]

[1] Department of Biological Sciences

[2]Eukaryotic Pathogens Innovations Center (EPIC)

Clemson University

Clemson, South Carolina United States of America 29634

*Corresponding author

Lesly A. Temesvari (LAT)

Email: LTEMESV@clemson.edu

I.   ABSTRACT

Entamoeba histolytica is a protozoan parasite that causes amebic dysentery and amoebic liver abscess in humans, affecting millions of people worldwide. This pathogen possesses a two-stage life cycle consisting of an environmentally stable cyst and a pathogenic amoeboid trophozoite. As cysts can be ingested from contaminated food and water, this parasite is prevalent in underdeveloped countries and poses a significant health burden. Until recently there was no reliable method for inducing synchronous stage conversion in *E. histolytica in vitro*. As such, the reptilian pathogen, *Entamoeba invadens*, has often served as a surrogate. Much remains unclear about stage conversion in these parasites and current treatments for amoebiasis are lacking, as they cause severe side effects. Therefore, new therapeutic strategies are needed. The genomes of these parasites remain enigmatic as approximately 54% of *E. histolytica* genes and 66% of *E. invadens* genes are annotated as hypothetical proteins. In this study, we characterized two hypothetical proteins in the *Entamoeba* species, EIN_059080, in *E. invadens*, and its homolog, EHI_056700, in the human pathogen, *E. histolytica*. EHI-056700 has no homolog in the human host. We used an RNAi-based silencing system to reduce expression of these genes in *E. invadens* and *E. histolytica* trophozoites. Loss of EIN_059080 resulted in a decreased rate of encystation and an increased rate of erythrophagocytosis, an important virulence function. Additionally, mutant parasites were more susceptible to oxidative stress. Similarly, loss of EHI_056700 in *E. histolytica* trophozoites resulted in increased susceptibility to oxidative stress and glucose deprivation, but not to nitrosative stress. Interestingly, parasites with decreased expression of EHI_056700 exhibited a decreased rate of erythrophagocytosis of and adhesion to host cells. Taken together, these data suggest that these hypothetical proteins play a role in stage conversion, virulence, and the response to stress in the *Entamoebae*. This supports the idea that hypothetical proteins may be promising therapeutic targets for the treatment of amoebiasis.

75

II.   Introduction

Entamoeba histolytica is an enteric parasite which causes amoebic dysentery and amoebic liver abscess in humans and nonhuman primates. This parasite has a two-stage life cycle, consisting of the infective, environmentally-stable cyst form and the pathogenic trophozoite form. *E. histolytica* cysts are transmitted via fecally-contaminated food and water, making this disease prevalent in sub-Saharan Africa and southern Asia, where sanitation is substandard (Shirley et al., 2018). As of 2020, 489 million people worldwide utilized unprotected drinking water sources, including wells, springs, and surface water. Additionally, 494 million people continue to practice open defecation (WHO & UNICEF, 2021). Thus, there is considerable risk for the spread of this disease. Globally, more than 50 million people become infected with the parasite, with over 100,000 deaths annually (Shirley et al., 2018).

E. histolytica is ingested as a latent cyst and travels through the digestive system until unknown cues trigger the excystation of trophozoites in the small intestine. Trophozoites colonize the large intestine where they feed on the natural gut flora and mucosal cells that compose the endothelial lining. In some cases, trophozoites will degrade the mucosal layer and enter the blood stream where they cause extra-intestinal infections in the liver, lungs, or, rarely, the brain (König et al., 2021). In the large intestine, unknown signals trigger aggregation and encystation of trophozoites, which generate environmentally stable cysts that are shed into the environment to facilitate host-to-host spread (Bercu et al., 2007). Until recently (Wesel et al., 2021)., there was no method for inducing efficient and synchronous stage conversion of *E. histolytica in vitro* (Wesel et al., 2021)However, *in vitro* stage conversion is easily achievable for *Entamoeba invadens*; therefore, this reptilian parasite is routinely used as a model organism (Avron et al., 1986; Coppi and Eichinger, 1999).

The molecular mechanisms governing stage conversion and virulence in the *Entamoeba* species remains unclear. Furthermore, metronidazole, the current treatment for amoebiasis, is

76

associated with high toxicity and severe side effects (Cherian et al., 2015; Ralston and Petri, 2011). Thus, there is a need to further characterize the cellular processes underlying the lifecycle of *E. histolytica* so that novel therapeutic targets can be identified. Hypothetical proteins are proteins that are predicted to be expressed, but for which there is no experimental evidence of translation (Ijaq et al., 2015). Hypothetical proteins have been explored as drug targets for several communicable diseases including, chlamydia (Turab Naqvi et al., 2017), tuberculosis (Yang et al., 2019), and shigellosis (Sen and Verma, 2020).

Unique hypothetical proteins may also present a promising source of potential new targets for the treatment of *E. histolytica* infection. According to AmoebaDB (amoebadba.org) the genomes of *E. invadens* and *E. histolytica* are predominately comprised of hypothetical proteins, (*i.e.,* proteins with unknown functions). In a study of the proteomic profiles of *E. histolytica* trophozoites, cysts, and cyst-like structures, Luna-Nacar et al., (2016) found that the cyst proteome was different from that of trophozoites, where almost 40% of the cyst proteome was annotated as hypothetical proteins (Luna-Nácar et al., 2016). Similarly, a quantitative proteomics analysis of membrane proteins between avirulent and virulent strains of *E. histolytica,* strain HM-1:IMSS, found that 19 hypothetical proteins were upregulated, while 18 hypothetical proteins were downregulated in the virulent strain (Ng et al., 2018). Furthermore, König and colleagues compared the genomes of pathogenic amoebae, *E. histolytica* and *E. nuttali* (the macaque pathogen) to the nonpathogenic amoeba, *E. dispar,* to elucidate virulence mechanisms (König et al., 2021). One hundred seventy-five proteins were found to be unique to *E. histolytica*, most of which were annotated as hypothetical proteins. *E. histolytica* trophozoites possessed 67 unique genes that had homologs in *E. nuttalli* but not in *E. dispar,* many of which were also hypothetical proteins (König et al., 2021). Furthermore, Matthiesen et al., (2019) silenced hypothetical protein, EHI_127670 in *E. histolytica* trophozoites and found that parasites with reduced expression of EHI_127670 were less able to form amoebic liver abscesses (ALAs) in mice. Alternatively,

overexpression of EHI_127670 in nonpathogenic amoebae lead to restoration of ALA formation ability (Matthiesen et al., 2019).

Luna-Nácar and colleagues (2016) identified 4 hypothetical cyst-specific proteins that could represent promising drug or vaccine targets as they were highly antigenic (Luna-Nácar et al., 2016). According to a review by Marchat and colleagues (2020), a third of the *E. histolytica* genome is not found within the human host, further indicating that many of these hypothetical proteins may be worthy drug targets (Marchat et al., 2020). Ultimately, the genomes of *E. histolytica* and *E. invadens* remain highly enigmatic and this represents a vast gap in knowledge. Therefore, the goal of this study was to characterize two hypothetical proteins in the *Entamoeba* species.

Using an RNAi silencing approach, we reduced expression of two such proteins, EIN_059080 in *E. invadens*, and EHI_056700 in *E. histolytica*. *E. invadens* parasites with reduced expression of EIN_059080 (EIN_059080-KD) possessed a significantly decreased rate of encystation, an increased rate of phagocytosis. These mutants were also significantly less viable than control parasites when exposed to oxidative stress. *E. histolytica* parasites with reduced expression of EHI_056700 (EHI_056700-KD) exhibited significantly lower rates of adhesion and erythrophagocytosis and were significantly less viable when exposed to oxidative stress and glucose deprivation. This study suggests that hypothetical proteins play important roles in stage conversion, virulence, and the stress response in the *Entamoeba* species.

III.　　MATERIALS AND METHODS

Strains and Culture conditions

Entamoeba invadens trophozoites (strain IP-1) were cultured axenically in TYI-S-33 medium in 15 mL glass screw cap tubes or 25 cm^2 culture flasks at 25°C (Singh et al., 2012). Parasites were passaged into fresh media every 7 days. *E. histolytica* trophozoites (strain HM-

1:1MSS) were cultured axenically in TYI-S33 medium at 37°C. Cells were passaged into fresh media every 72 to 96 h and were grown in 15 mL glass screw cap culture tubes (Diamond et al., 1978). Chinese hamster ovary (CHO) cells were cultured in DMEM supplemented with 10% FBS, PenStrep, and HEPES in 25 cm^2 treated tissue culture flasks at 37°C in 5% CO_2 and passaged into new flasks every 5 days.

To generate a plasmid to reduce expression of EIN_059080, PCR was employed to amplify a gene fragment using genomic DNA as a template and gene-specific primers (Table 3.1). The primers also added AvrII restriction sites to the 3' and 5' ends, which facilitated subcloning into the Trigger plasmid (Ehrenkaufer and Singh, 2012) (kind gift of Dr. Upinder Singh; Stanford University). Successful subcloning was confirmed by sequencing. To generate a plasmid to reduce expression of EHI_056700, PCR was used to amplify a gene fragment using genomic DNA as template and gene-specific primers (Table 3.1). The primers also added BglII and XhoI cutsites to the 3' and 5' ends, to facilitate subcloning into the pEhEx-04-trigger vector containing a 142-bp trigger region (EHI_048660) silencing plasmid (kind gift of Dr. Nozaki; University of Tokyo) (Nagaraja et al., 2021).

E. invadens was transfected by electroporation as described (Singh et al., 2012), with minor modifications. Briefly, two 25 cm^2 flasks containing log-phase trophozoites were iced for 15 min to release adherent parasites. The parasites were collected by centrifugation at 500 x *g* for 5 min and washed with 20 mL ZM phosphate buffered saline (PBS) buffer (132 mM NaCl, 8 mM KCl, 8 mM $NaPO_4$, 1.5 mM KH_2PO_4). Parasites were pelleted by centrifugation at 500 x *g* for 5 mins and resuspended in 1.6 mL complete ZM PBS buffer (ZM PBS with 0.5 mM $Mg(CH_3COO)_2$ • $4H_2O$ and 0.09 mM $CaCl_2$). Eight hundred μL of parasite suspension was combined with 150 μg plasmid DNA and electroporated in a 0.4 cm cuvette with two pulses at 1.2 kV and 25 μF using a BioRad Gene Pulser II. Parasites were transferred to 15 mL culture tubes containing 13 mL TYI-

Table 3.1: Primers used in this study

Primer Name	Sequence	Anneal Temperature
Cloning Primers		
EIN_059080-AvrII-F	5'- CCCCTAGGATGTCCGTCAC -3'	52°C
EIN_059080-AvrII-R	5'- CCGCTAGCATGTCCGTCAC -3'	52°C
EHI_056700-BglII-F	5'-CCAGATCTGCCTGAACATACTAGT-3'	60°C
EHI_056700-XhoI-R	5'-CCCTCGAGCTGGTCGTGTTAC-3'	60°C
RT PCR primers		
EIN_059080-RT-F	5'- CCCAACACTCCCAGAGTTAAA -3'	59°C
EIN_059080-RT-R	5'- GGAGGTAAACTGCCAACTGAA -3'	59°C
EHI_056700-RT-F	5'-GCACCTCAACCTCGTAGACC -3'	54°C
EHI_056700-RT-R	5'- ACTGGTGGTGGAGAAGCAAC -3'	54°C
E. invadens Internal control-F (EIN_327460)	5'-CCGACAGCAGAAGAACAAGA-3'	59°C
E. invadens Internal control-R (EIN_327460)	5'-GGAGATGAGTAAGCGAAGAACA-3'	59°C
E. histolytica Internal Control-F (X61116)	5'-AGGCGCGTAAATTACCCACTTTCG-3'	59°C
E. histolytica Internal Control-R (X61116)	5'- AGACGCATGCACCACTACCCAATA-3'	59°C

S-33 and allowed to recover for 48 h. Neomycin selection was added gradually at 5 µg/mL each week until a concentration of 50 µg/mL was reached.

Lipofectamine 3000 (ThermoFisher) was used to transfect *E. histolytica* trophozoites as described by (Manich et al., 2018). Briefly, $2x10^5$ trophozoites were seeded into a 6-well plate in 12 mL complete media and grown overnight until 80% confluency was reached. Fresh plasmid DNA (4 µg) was diluted in sterile transfection media (final volume 30 µL) (10 mL Opti-mem (ThermoFisher) containing 10 mg ascorbic acid and 50 mg L-cysteine, pH to 6.8), mixed with 15 µL Lipofectamine 3000 reagent (ThermoFisher) and incubated at room temperature for 15 min. After incubation, 960 µL of warm transfection media (37°C) was added to DNA/lipofectamine 3000 mixture. Media was removed by pipetting from the *E. histolytica* monolayer and the monolayer was washed twice with warm transfection media. One mL transfection mixture or control mixture (no DNA) was added to the parasite monolayer and incubated under anaerobic conditions for 3 h at 37°C. Trophozoites were removed by scraping and transferred to 15 mL glass screw cap tubes containing 12 mL prewarmed complete media and incubated overnight at 37°C. Control or transfected parasites were harvested by centrifugation at 500 x *g* for 5 min and resuspended in 13 mL fresh complete media and incubated at 37°C for 24 h. Parasites harboring the plasmid were selected for by adding 3 µg/mL neomycin. Once confluent, neomycin was increased to 6 µg/mL. Transfected parasites were cultured in 6 µg/mL neomycin for 6 weeks. Selection was then removed, and parasites were cultured in complete medium for all experiments.

To assess expression of EIN_059080 and EHI_056700, RNA was extracted from *E. invadens* or *E. histolytica* trophozoites using TRIZOL (ThermoFisher; Waltham, MA). Two µg of total RNA was treated with RQ1 DNase enzyme (Promega; Madison, WI) per manufacturer's instructions. Treated RNA was used to synthesize cDNA using the Invitrogen Superscript III First Stand Synthesis kit per the manufacturer's instruction. (ThermoFisher). One µL of cDNA was

used as template and PCR was carried out using EIN_059080 gene-specific primers or EHI_056700 gene-specific primers (Table 3.1). In all cases, 35 cycles were used to amplify PCR products, which were resolved and visualized by electrophoresis on 1% (w/v) agarose gels. We also confirmed that these primers do not cross-react to amplify both genes. EIN_327460 was used as an internal load control for analysis of gene expression in *E. invadens* trophozoites and X61116 was used as internal load control for analysis of gene expression in *E. histolytica* (see Table 3.1). In all experiments, EIN_059080-KD parasites were compared to Trig Luc parasites as a control and EHI_056700-KD parasites were compared to WT *E. histolytica* parasites.

Induction of Stage Conversion

To induce encystation of *E. invadens* parasites, control and mutant trophozoites (6.5×10^6) were pelleted by centrifugation at 500 x *g* for 5 min and resuspended in 13 mL 47% (w/v) low glucose/serum free/high osmolarity encystation medium (Coppi and Eichinger, 1999; Hendrick et al., 2016), supplemented with 50 mg/mL neomycin. Parasites were incubated at 25˚C for either 48 h or 72 h and encystation was tracked by staining with Congo Red (Amresco, Solon, OH). Briefly, encysting *E. invadens* cells were collected over time, stained with the fluorescent chitin stain, Congo Red, fixed with 4% (v/v) paraformaldehyde, and analyzed by collecting 10,000 individual events using a BD Accuri C6 flow cytometer (BD Biosciences, San Jose, CA). To evaluate information about cell size/shape and chitin simultaneously, all data were analyzed using forward scatter (FSC) data versus fluorescence density plots.

Excystation of *E. invadens* parasites was induced as described (Ehrenkaufer et al., 2013). Briefly, Trig Luc and EiIF2K-KD trophozoites were induced to encyst for 72 h. Parasites were then incubated in 13 mL ddH$_2$O at 4˚C overnight to lyse unencysted trophozoites. Cysts were enumerated using a Luna Automated Cell Counter (Logos Biosystems, Annandale, VA), pelleted by centrifugation at 500 x *g* for 5 min, and resuspended in 13 mL TYI-S-33 medium, 1 mg/mL bile

salts (Sigma-Aldrich), and 40 mM NaHCO$_3$, and incubated at 25°C for 2 h or 8 h. After incubation,

cultures were iced for 8 min to detach any trophozoites from the glass culture tubes, pelleted by

centrifugation at 500 x g for 5 min, resuspended in 1 mL of 1% (v/v) sarkosyl in PBS and incubated

on ice for 30 min to lyse any trophozoites or immature cysts. The remaining detergent-resistant

cysts were enumerated and the percent excystation was calculated by comparing total cysts

remaining to the starting number of cells.

Phagocytosis Assays

Phagocytosis assays were carried as previously described (King et al., 2012) with minor

changes. Briefly, control or mutant trophozoites were rinsed once in PBS (GE Life Sciences) and

twice in serum free TYI-S-33 medium (SFM). Trophozoites (2x10^5) were resuspended in 150 μL

SFM. Freshly isolated human red blood cells (hRBCS) were pelleted by centrifugation (2000 x g

for 1 min) and rinsed once with PBS and twice with SFM and were resuspended at a concentration

of 4x10^5 cells/μL in SFM. hRBCs (2x10^7) were added to the trophozoites and incubated at 25°C

for 10 min. Samples were pelleted by centrifugation (2000 x g for 1 min), and undigested hRBCs

were hypotonically lysed by washing twice with 1 mL of ice-cold ddH$_2$O. Parasites were washed

with 1 mL ice-cold PBS, collected by centrifugation (2000 x g for 1 min) and lysed with 1 mL

concentrated formic acid (Fisher). Phagocytosis was measured as the absorbance of heme in the

lysate at 405 nm, with a fluorimeter/plate reader (Synergy HTX, BioTek Instruments, Winooski,

VT). Sample values were corrected using a formic acid blank.

Adhesion Assays

Adhesion assays were carried as previously described (Powell et al., 2006) with minor

changes. Briefly, control and mutant parasites were incubated with calcein-AM (Invitrogen) (5

μL/mL) for 30 min at 25°C. CHO cells (1.5x10^5) were seeded into a 96-well plate and grown at

37°C for 24 h. CHO monolayers were fixed by incubating with 4% (v/v) paraformaldehyde in PBS

for 10 min at 37°C. To inactivate paraformaldehyde, the CHO monolayer was incubated with 200 µL of 250 mM glycine for 15 min. Glycine was removed by rinsing with PBS. Calcein-AM labeled parasites were washed once with room temperature SFM and 5×10^4 parasites were seeded onto the fixed monolayer of CHO cells. Parasites were incubated with fixed CHO cells in SFM for 30 min at 25°C. The media was carefully aspirated, and the cell layer was gently rinsed twice with room temperature PBS. The number adherent parasites was determined by measuring fluorescence at excitation and emission wavelengths of 495 and 525 nm, respectively, with a fluorimeter/plate reader (Synergy HTX, BioTek Instruments, Winooski, VT).

Statistical Analysis

All values are presented as means ± standard error of at least 3 separate trials. Means of treated groups were compared against the appropriate control and statistical analyses were performed using Graph Pad prism 9 (v9.0.0, San Diego, CA, US) with students T-Test. *P* values of less than 0.05 were considered statistically significant. *P* values less than 0.01 or 0.001 were considered highly statistically significant.

Ethics Statement

Whole blood was donated by a healthy adult volunteer, who provided oral consent, at Clemson University. The collection was approved by Clemson's Institutional Biosafety Committee under safety protocol #IBC2018-12.

IV.   RESULTS

Identification of hypothetical proteins EHI_056700 and EIN_059080

According to AmoebaDB (amoebadba.org), over half of the *Entamoeba* genomes are annotated as hypothetical proteins. *E. histolytica* possesses 8,308 genes with 53% (4,483/8,308) annotated as hypothetical proteins. Similarly, *E. invadens* possesses 11,997 protein coding genes

with 66% (7,876/11,997) annotated as hypothetical proteins (Fig 3.1A). To identify a candidate hypothetical protein for study, we looked for such proteins that were differentially expressed between virulent and aviurlent strains.   Hypothetical protein EHI_056700 is upregulated in pathogenic *E. histolytica* strain, HM-1:IMSS, when compared to nonpathogenic, Rahman, strain. A homolog in *E. invadens* (EIN_059080) was identified by protein blast (NCBI). Protein alignment using the Clustal Omega tool from Uniprot (uniport.org) shows that the amino acid sequences of EHI_056700 and EIN_059080 share 23% identity (Fig 3.1B). According to Predict Protein (predictprotein.org), both proteins are predicted to have several DNA binding sites and be localized the nucleus.

Generation of *E. invadens* and *E. histolytica* parasites with reduced expression of EIN_059080 or EHI_0567000

We used a RNAi Trigger-mediated gene silencing approach to reduce the expression of EHI_056700 in *E. histolytica* trophozoites or EIN_059080 in *E. invadens* trophozoites. We subcloned partial cDNAs of EIN_059080 or EHI_056700 into an *E. invadens* specific (Suresh et al., 2016) or *E. histolytica* specific gene silencing Trigger plasmids (Nagarajaet al., 2021). The Trigger plasmids facilitate the production of small interfering RNAs to the fused gene fragment, which binds to and targets the endogenous mRNA leading to mRNA degradation via the dicer pathway (Morf et al., 2013; Suresh et al., 2016). EIN_059080-Trigger plasmid DNA was transfected into wildtype *E. invadens* parasites via electroporation and stable transfectants (EIN_059080-KD) were selected for and maintained by growth in the presence of neomycin. *E. invadens* parasites harboring the Trigger plasmid, with an insert encoding luciferase, an irrelevant protein, was used as a control (Trig Luc). Using this approach, we obtained substantial knockdown of EIN_059080 mRNA levels in trophozoites as assessed by RT-PCR analysis (Fig 3.2A). The EHI_056700-Trigger plasmid DNA was transfected into *E. histolytica* parasites using Lipofectamine 3000 and stable transfectants were selected for using neomycin. After confirming
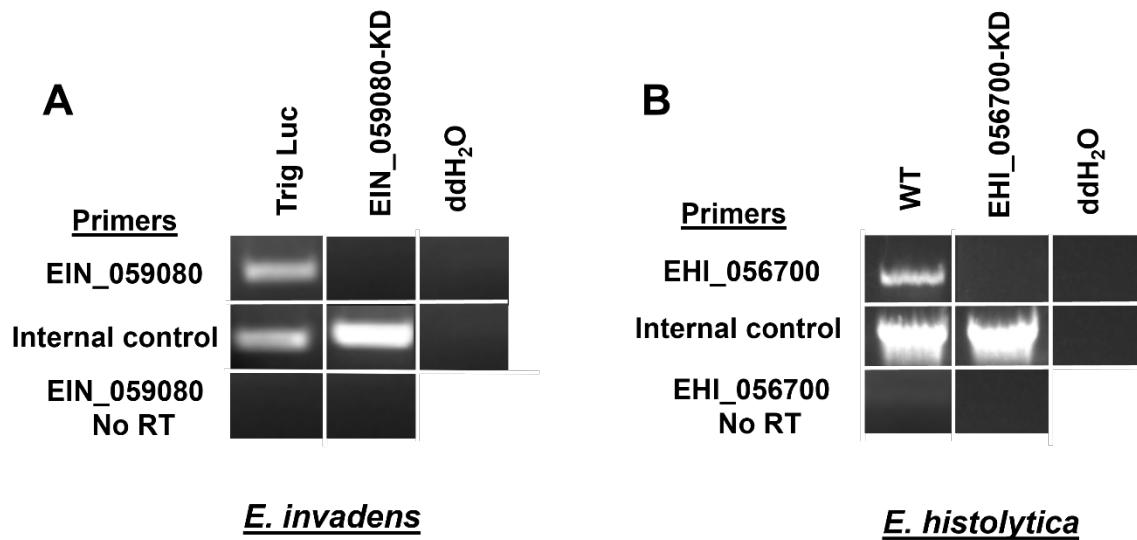
Fig 3.1: Large portions of the *Entamoeba* genomes are annotated as hypothetical proteins

Annotated genes for *Entamoeba histolytica* and *Entamoeba invadens* were downloaded from AmoebaDB (amoebadba.org). A) 66% of annotated *E. invadens* genes (7,876/11,998) and 54% of annotated *E. histolytica* genes (4,483/8,308) are annotated as hypothetical proteins. B) Uniprot Clustal Omega alignment of EHI_056700 and EIN_059080. Asterisks (*) represent identical residues, colons (:) represent conserved substitutions and periods (.) represent semi-conserved substitutions.

Fig 3.2: Knockdown of hypothetical proteins in *Entamoeba* species

RT-PCR was used to measure the level of EIN_059080 or EHI_056700 mRNA in transfected parasites. A) EIN_059080 mRNA is undetectable in *E. invadens* trophozoites harboring the Trigger-EIN_059080 plasmid (EIN_059080-KD), compared to control trophozoites harboring Trigger-Luciferase plasmid (Trig Luc). B) EHI_056700 mRNA is undetectable in *E. histolytica* trophozoites harboring Trigger-EHI_056700 plasmid (EHI_056700-KD) compared to control wildtype (WT) trophozoites. After confirmation of gene knockdown, antibiotic selection was removed from EHI_056700-KD parasites to directly compare mutant parasites to WT parasites. EIN_327460, (previously identified as EIN_192230) and X61116 served as load controls for *E. invadens* or *E. histolytica* trophozoites, respectively. "No RT" represents reactions without reverse transcriptase to confirm that there was no genomic (gDNA) contamination in cDNA samples. Panels labeled "ddH$_2$O" represent reactions in which ddH$_2$O was used as template. A lack of product confirms no gDNA contamination in the reagents.

knockdown of EHI_056700 in EHI_056700-KD parasites (Fig 3.2B), neomycin selection was removed. Knockdown (as compared to expression in WT cells) was monitored every 4 weeks (Nagaraja et al., 2021).

We measured growth rates of mutant and control parasites over the course of 96 h to ensure differences observed between control and mutant parasites were authentic phenotypes, and not due to differences in growth. No significant difference in growth was observed between knockdown and control parasites (Fig 3.3).

E. invadens parasites with reduced expression of EIN_059080 exhibit an altered rate of stage conversion compared to control parasites

To determine if EIN_059080 plays a role in stage conversion, we measured encystation and excystation in EIN_059080-KD and control parasites. Encystation of *E. invadens* parasites was induced by inoculating parasites at high density into low glucose/high osmolality media and incubated for 48 or 72 h. Hallmarks of encystation include the accumulation of a chitin-rich cell wall and a reduction in cell size (Welter et al., 2017). To assess encystation, we used flow cytometry (Welter et al., 2017) and Congo Red staining to track the accrual of chitin as well as changes in cell size. In the EIN_059080-KD parasites, the percent of parasites that had encysted was significantly lower at 48 h and 72 h post inoculation, when compared to control parasites (Fig 3.4A). To induce excystation, cysts were incubated in excystation media, which restores nutrients and osmolarity and contains bile salts to mimic passage through the host digestive system (Ehrenkaufer et al., 2013). EIN_059080-KD parasites exhibited a slightly higher rate of excystation compared to control parasites at 2 h and 8 h into the excystation program (Fig 3.4B).

Virulence functions are significantly altered in mutant parasites

To further elucidate the function of these hypothetical proteins, we measured two key virulence functions, erythrophagocytosis and adhesion to host cells. Parasites were incubated
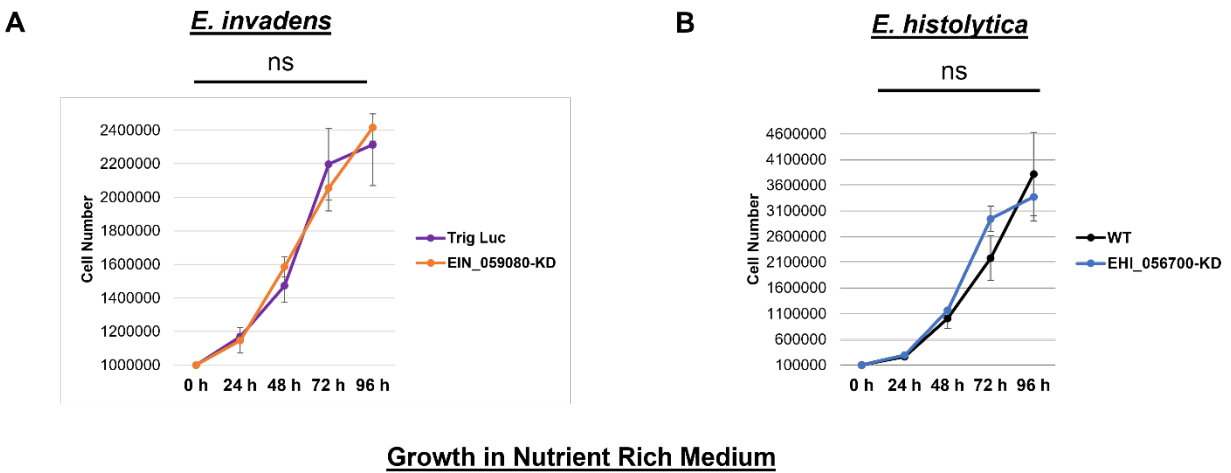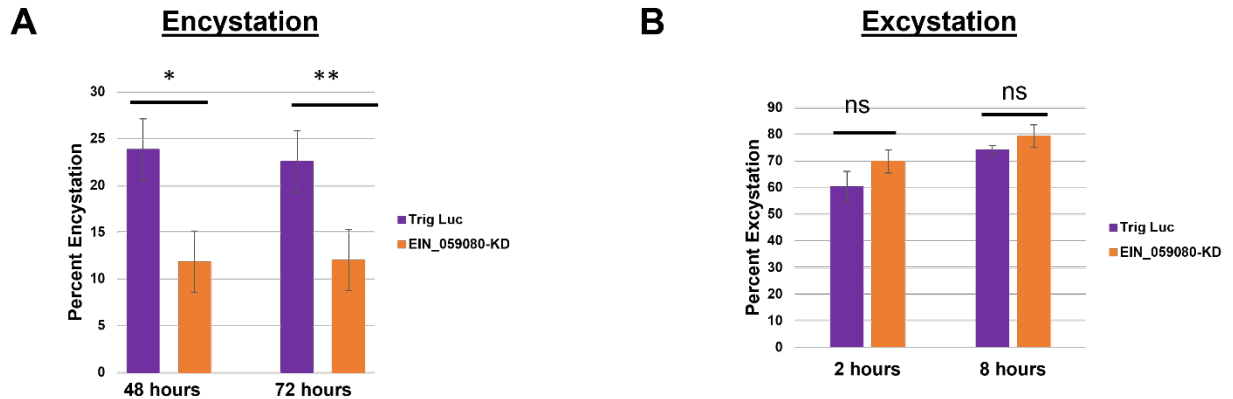
A E. invadens

B E. histolytica

Growth in Nutrient Rich Medium

Fig 3.3: Mutant trophozoites exhibit no growth defect compared to control trophozoites

A) Growth of Trig Luc (control) and EIN_059080-KD *E. invadens* parasites was assessed by inoculating 1,000,000 parasites into 13 mL of standard media. Parasites were enumerated after 24, 48, 72, and 96 h using an automated hemocytometer and Trypan blue exclusion. There is no significant difference in growth at any time point. B) After confirmation of gene knockdown, antibiotic selection was removed from EHI_056700-KD parasites to directly compare mutant parasites to WT parasites. Growth of WT and EHI_056700-KD *E. histolytica* parasites was assessed by inoculating 100,000 parasites into 13 mL of standard media. Parasites were enumerated after 24, 48, 72, and 96 h using an automated hemocytometer and Trypan blue exclusion. There is no significant difference in growth at any time point. Data represent the mean ± standard error of at least 3 separate trials (ns, *P*>0.05).

A   Encystation   **B**   Excystation

E. invadens

Fig 3.4: Encystation is significantly reduced in EIN_059080-KD parasites, while excystation is slightly increased.

A) Trig Luc (control) and EIN_059080-KD parasites were induced to encyst for either 48 or 72 h. Mature cysts were stained with Congo Red and quantified using flow cytometry. A significantly lower (*$P<0.05$; **$P<0.01$)) percent of EIN_059080-KD parasites encysted by 48 h and at 72 h compared to Trig Luc parasites. B) Trig Luc cells and EIN_059080-KD cysts were induced to excyst by incubation in excystation media for 2 or 8 h. The number of mature cysts was quantified before and after excystation and the decrease in the number of cysts represented the fraction (percent) of parasites that had excysted. The excystation rate of EIN_059080-KD was slightly (ns, $P>0.05$) higher than that of Trig Luc parasites at both 2 and 8 h. Data represent the mean ± standard error of at least 3 separate trials.

with human red blood cells (hRBCs) for 10 min, excess hRBCs were washed away, and parasites were lysed with formic acid. Heme was then measured spectrophotometrically (Powell et al., 2006). Compared to control parasites, EIN_059080-KD parasites possessed a significantly higher ($P<0.05$) rate of erythrophagocytosis (Fig 3.5A), while EHI_056700-KD parasites exhibited a significantly lower ($P<0.05$) rate of erythrophagocytosis (Fig 3.5B). To measure adhesion to host cells, Calcien-AM labeled parasites were incubated on a fixed monolayer of CHO cells for 30 min. Unadhered parasites were then washed away, and adhesion to host cells was measured spectrophotometrically (Powell et al., 2006). While adhesion to host cells was slightly higher ($P>0.05$) in EIN_059080-KD parasites compared to control cells (Fig 3.5C), adhesion was significantly lower ($P<0.01$) in EHI_056700 parasites compared to WT control parasites (Fig 3.5D).

Hypothetical proteins are involved in the stress response in *E. histolytica* and *E. invadens*

In the human host, *E. histolytica* experiences stress brought on by nutrient deprivation and the host immune response. To be a successful parasite, *E. histolytica* must counter the stress; therefore, understanding the stress response may uncover new drug targets. To determine if these hypothetical proteins are involved in the stress response, we exposed control and mutant *E. invadens* parasites to 1 M H_2O_2 or diluent for 1 h (Walters et al., 2022) and viability was assessed using Trypan blue exclusion and an automated hemocytometer. The difference in viability between control and treatment was then calculated. Parasites with reduced expression of EIN_059080 were significantly less viable than Trig Luc parasites when undergoing oxidative stress (Fig 5A). Mutants of the human pathogen were also exposed to oxidative stress (5 mM H_2O_2 for 3 h (Santos et al., 2020)) and viability was assessed. Like the *E. invadens* mutant, EHI_056700-KD parasites were more sensitive than control cells to oxidative stress (Fig. 3.6B). We also exposed the *E. histolytica* mutants to additional physiologically relevant stress conditions, nitrosative stress, or glucose deprivation. Control and mutant *E. histolytica* trophozoites were
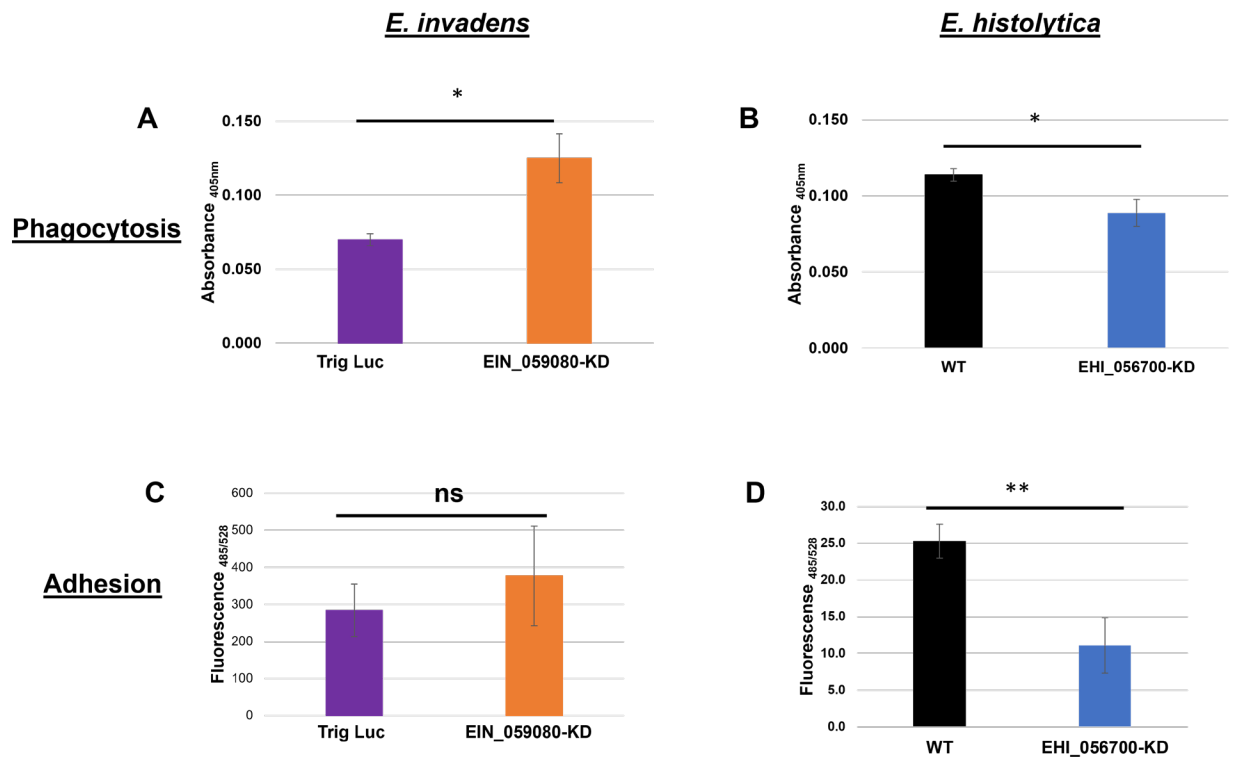
Fig 3.5: Virulence functions are increased in EIN_059080-KD parasites, while they are decreased in EHI_056700-KD parasites.

A,B) Control or mutant parasites were incubated with human red blood cells (hRBCs: amoeba ratio; 100:1) for 10 min, lysed, and spectrophotometrically analyzed for internalized heme at 405 nm. *E. invadens* amoebae with reduced expression of EIN_059080 (A) exhibited increased phagocytosis of hRBCs, while *E. histolytica* amoebae with reduced expression of EHI_056700 (B) exhibited reduced phagocytosis of hRBCs. The data represent the mean ± standard error of at least 3 separate trials (*$P<0.05$). C,D) Calcein AM-stained control or mutant parasites were incubated with fixed monolayers of Chinese Hamster Ovary (CHO) cells for 30 min. Unadhered parasites were rinsed off the monolayer of CHO cells and the level of adhesion (calcein-AM fluorescence) was measured by spectrofluorimetry using an excitation wavelength of 485 nm and an emission wavelength of 528 nm. EIN_059080-KD trophozoites exhibited a slightly higher adhesion to CHO cells than Trig Luc trophozoites (control) (ns, $P>0.05$), while EHI_056700-KD trophozoites exhibited significantly lower adhesion to CHO cells (**$P<0.01$). Data represent the mean ± standard error of at least 3 separate trials.
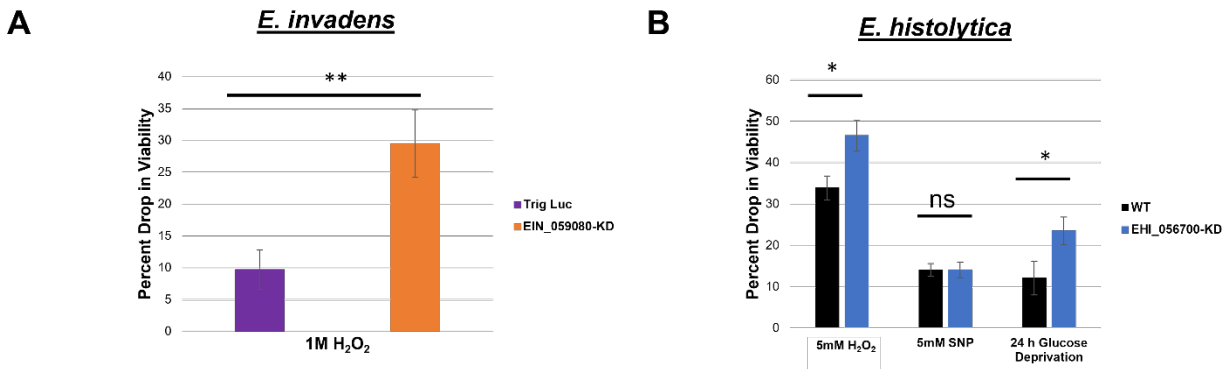
92

Fig 3.6: Mutant *E. invadens* and *E. histolytica* trophozoites are more susceptible to stress

A) Trig Luc (control) or EIN_059080-KD trophozoites were exposed to 1M H_2O_2 (oxidative stress) or ddH_2O (diluent) for 1 h at 25°C. Viability was assessed using Trypan blue exclusion and a Luna Automated Cell Counter. The percent drop in viability was calculated for each cell line by subtracting each H_2O_2 viability from the control viability (ddH_2O). EIN_059080-KD parasites exhibited a significantly higher decrease in viability when exposed to oxidative stress compared to those mutant parasites exposed to vehicle control, meaning EIN_059080-KD parasites were more sensitive to oxidative stress compared to control parasites (**P<0.01). B) After confirmation of gene knockdown, antibiotic selection was removed from EHI_056700-KD parasites to directly compare mutant parasites to WT parasites. WT or EHI_056700-KD parasites were exposed to 5mM H_2O_2 or ddH_2O (diluent) for 3 h at 37°C or, 5 mM sodium nitroprusside (SNP) (nitrosative stress) or ddH_2O (diluent) for 3 h at 37°C or ddH_2O, or glucose deprivation for 24 h. Viability was assessed as described above. EHI_056700-KD parasites were more sensitive to oxidative stress and glucose deprivation when compared to control (*P<0.05). There was no significant difference (ns, *P*>0.05) in viability for control or mutant parasites when exposed to nitrosative stress. Data represent the mean ± standard error of at least 3 separate trials.

exposed to 5mm H_2O_2 (Santos et al., 2020) 5 mM sodium nitroprusside (SNP) for 3 h (Santos et al., 2020), or glucose deprivation for 24 h (Tovy et al., 2011), and viability was assessed as described above. EHI_056700-KD parasites were more sensitive than control cells to glucose deprivation, but not to nitrosative stress (Fig 3.6B).

V.   DISCUSSION

In this study, we characterized two hypothetical proteins in the *Entamoeba* species to highlight their potential as drug targets. Compared to control parasites, *E. invadens* mutants with reduced expression of hypothetical protein, EIN_059080 had significantly reduced rates of encystation and erythrophagocytosis, and exhibited lower viability when exposed to oxidative stress, compared to control parasites. Interestingly, *E. histolytica* parasites with reduced expression of hypothetical protein EHI_057600 exhibited significantly increased rates of erythrophagocytosis and adhesion and were exhibited significantly less viable when exposed to oxidative stress and glucose deprivation. These data suggest that careful characterization of hypothetical proteins in the *Entamoeba* species will provide insight into mechanisms of stage conversion, virulence, and the stress response, which is critical for future drug development.

Hypothetical proteins present a promising reservoir of novel mediators of cellular processes critical to mediating the lifecycle of eukaryotic pathogens. Approximately 54% of *E. histolytica* genes and 66% of *E. invadens* genes are annotated as hypothetical proteins (Fig 3.1) (amoebadba.org). Similarly, substantial portions of the genome are unclearly annotated or annotated as hypothetical proteins for *Leishmania donovani* (65%)(Ravooru et al., 2014), *Toxoplasma gondii* (strain ME49; 48.6%)(Croken et al., 2014), and *Plasmodium falciparum* (30%)(Singh and Gupta, 2022).

Our data demonstrate that reduced expression of EIN_059080 correlates with significantly reduced encystation in *E. invadens* parasites (Fig 3.4A). This is not surprising as hypothetical proteins have previously been implicated in stage conversion in the *Entamoeba* (Manna et al.,

2018). RNA-Seq data showed the hypothetical proteins EIN_083100 and EIN_024000 are developmentally regulated in *E. invaden*s and are enriched in cysts (Manna et al., 2018). However, excystation was slightly increased in EIN_059080-KD parasites (Fig 3.4B). These results are interesting as EIN_059080 is primarily expressed at 2 h into the excystation program (Ehrenkaufer et al., 2013). Similarly, Mony et al., (2014) identified three hypothetical proteins as regulators of stumpy formation in *Trypanosoma brucei* (Mony et al., 2014). To gain further insight into the role of EHI_057600 in stage conversion, it will be necessary to characterize this process in EHI_056700-KD *E. histolytica* parasites. If reduced expression of EHI_056700 correlates with reduced encystation or excystation, it will support the idea that EHI_056700 represents an attractive drug target.

Erythrophagocytosis and adhesion to host cells, two important virulence functions, were found to be altered in EIN_059080-KD and EHI_057600-KD parasites (Fig 3.5). *E. invadens* parasites with decreased expression of EIN_059080 exhibited significantly increased phagocytosis of hRBCs, while adhesion to CHO cells was only slightly increased. Interestingly, *E. histolytica* parasites with decreased expression of EHI_056700 possessed significantly lower rates of phagocytosis and adhesion. Similarly, a *Trichomonas vaginalis* hypothetical protein TVAG_157210 (TvAD1) was found to play an integral role in parasite adherence to host cells (Molgora et al., 2021). Hypothetical proteins have been implicated in virulence in other protozoa as well. *In silico* analyses of hypothetical proteins from *P. falciparum* (Singh and Gupta, 2022), *Trypanosoma cruzi* (Silber and Pereira, 2012), and *Leishmania spp.* (Chávez-Fumagalli et al., 2017; Ravooru et al., 2014) are required for parasite virulence.

To be successful parasites, the *Entamoeba* species must be able to withstand stress within the reptilian and human hosts. To determine if hypothetical proteins play a role in the stress response, we exposed mutant *E. invadens* and *E. histolytica* parasites to various stresses. Parasites with reduced expression of EIN_059080 were significantly more susceptible to oxidative stress compared to control parasites. Additionally, EHI_056700-KD parasites were significantly

more susceptible to oxidative stress and glucose deprivation, but not to nitrosative stress. According to Rastew et al., (2013), most genes upregulated during oxidative and nitrosative stress are annotated as hypothetical proteins (Rastew et al., 2012). Since mutant parasites are more sensitive to physiologically relevant stress conditions such as oxidative stress and glucose deprivation, EHI_056700, may represent a potential drug target for the treatment of amoebiasis.

Hypothetical proteins are gaining attention as prospective targets for the treatment of other parasitic diseases. *Leishmania infantum* hypothetical protein, LiHyV, was identified as an antigen present in both promastigote and amastigote stages by an immunoproteomic approach (Martins et al., 2015). In a recent study by Aguttu et al., (2021) three hypothetical proteins were identified using computational methods and experimentally verified as a likely vaccine candidate against *P. falciparum* (Aguttu et al., 2021). Ultimately, our study underscores the importance of investigating and experimentally determining the function of hypothetical proteins in the *Entamoeba* species as they represent a novel pool of prospective drug targets.

VI.   Acknowledgements

VII.   Literature Cited

Aguttu, C., Okech, B.A., Mukisa, A., Lubega, G.W., 2021. Screening and characterization of hypothetical proteins of Plasmodium falciparum as novel vaccine candidates in the fight against malaria using reverse vaccinology. Journal of Genetic Engineering and Biotechnology 19. https://doi.org/10.1186/s43141-021-00199-y

Avron, b., stolarsky, t., chayen, a., mirelman, d., 1986. Encystation of *Entamoeba invadens* IP-1 is induced by lowering the osmotic-pressure and depletion of nutrients from the medium. The Journal of protozoology. 33, 522–525. https://doi.org/10.1111/j.1550-7408.1986.tb05655.x

Bercu, T.E., Petri, W. a, Behm, J.W., 2007. Amebic colitis: new insights into pathogenesis and treatment. Curr Gastroenterol Rep 9, 429–33.

Chávez-Fumagalli, M.A., Schneider, M.S., Lage, D.P., Machado-de-Ávila, R.A., Coelho, E.A.F., 2017. An in silico functional annotation and screening of potential drug targets derived from *Leishmania* spp. hypothetical proteins identified by immunoproteomics. Exp Parasitol. 176, 66–74. https://doi.org/10.1016/j.exppara.2017.03.005

Cherian, P.T., Wu, X., Yang, L., Scarborough, J.S., Singh, A.P., Alam, Z.A., Lee, R.E., Hurdle, J.G., 2015. Gastrointestinal localization of metronidazole by a lactobacilli-inspired tetramic acid motif improves treatment outcomes in the hamster model of *Clostridium difficile* infection. Journal of Antimicrob Chemo. 70, 3061–3069. https://doi.org/10.1093/jac/dkv231

Coppi, A., Eichinger, D., 1999. Regulation of *Entamoeba invadens* encystation and gene expression with galactose and N-acetylglucosamine. Mol. Biochem. Parasitol.102, 67–77. https://doi.org/10.1016/S0166-6851(99)00085-7

Croken, M.M., Qiu, W., White, M.W., Kim, K., 2014. Gene Set Enrichment Analysis (GSEA) of *Toxoplasma gondii* expression datasets links cell cycle progression and the bradyzoite developmental program. BMC Genom. 15. https://doi.org/10.1186/1471-2164-15-515

Diamond, Louis; Harlow, DR; Cunnick, C., 1978. A new medium for the axenic culture of *Entamoeba histolytica* and other *Entamoeba*. Trans R Soc Trop Med Hyg 72, 431–432.

Ehrenkaufer, G.M., Singh, U., 2012. Transient and stable transfection in the protozoan parasite Entamoeba invadens. Molecular and Biochemical Parasitology 184, 59–62. https://doi.org/10.1016/j.molbiopara.2012.04.007

Ehrenkaufer, G.M., Weedall, G.D., Williams, D., Lorenzi, H.A., Caler, E., Hall, N., Singh, U., 2013. The genome and transcriptome of the enteric parasite *Entamoeba invadens*, a model for encystation. Genome Biol. 14, R77. https://doi.org/10.1186/gb-2013-14-7-r77

Hendrick, H.M., Welter, B.H., Hapstack, M.A., Sykes, S.E., Sullivan, W.J., Temesvari, L.A., 2016. Phosphorylation of Eukaryotic Initiation Factor-2α during Stress and Encystation in *Entamoeba* Species. PLoS Path. 12, 1–14. https://doi.org/10.1371/journal.ppat.1006085

Ijaq, J., Chandrasekharan, M., Poddar, R., Bethi, N., Sundararajan, V.S., 2015. Annotation and curation of uncharacterized proteins- challenges. Frontiers in Genetics 6, 1–7. https://doi.org/10.3389/fgene.2015.00119

King, A. v, Welter, B.H., Koushik, A.B., Gordon, L.N., Temesvari, L.A., 2012. A Genome-Wide Over-Expression Screen Identifies Genes Involved in Phagocytosis in the Human Protozoan Parasite , *Entamoeba histolytica*. PLoS ONE 7. https://doi.org/10.1371/journal.pone.0043025

König, C., Honecker, B., Wilson, I.W., Weedall, G.D., Hall, N., Roeder, T., Metwally, N.G., Bruchhaus, I., 2021. Taxon-Specific Proteins of the Pathogenic *Entamoeba* Species *E. histolytica and E. nuttalli.* Frontiers in Cellular and Infection Microbiology 11, 1–10. https://doi.org/10.3389/fcimb.2021.641472

Luna-Nácar, M., Navarrete-Perea, J., Moguel, B., Bobes, R.J., Laclette, J.P., Carrero, J.C., 2016. Proteomic study of *Entamoeba histolytica* trophozoites, cysts, and cyst-like structures. PLoS ONE 11, 1–24. https://doi.org/10.1371/journal.pone.0156018

Manich, M., Hernandez-Cuevas, N., Ospina-Villa, J.D., Syan, S., Marchat, L.A., Olivo-Marin, J.C., Guillén, N., 2018. Morphodynamics of the actin-rich cytoskeleton in *Entamoeba histolytica*. Frontiers in Cellular and Infection Microbiology 8, 1–16. https://doi.org/10.3389/fcimb.2018.00179

Manna, D., Lentz, C.S., Ehrenkaufer, G.M., Suresh, S., Bhat, A., Singh, U., 2018. An NAD + -dependent novel transcription factor controls stage conversion in *Entamoeba*. Elife 7, 1–22. https://doi.org/10.7554/eLife.37912

Marchat, L.A., Hernández-de la Cruz, O.N., Ramírez-Moreno, E., Silva-Cázares, M.B., López-Camarillo, C., 2020. Proteomics approaches to understand cell biology and virulence of *Entamoeba histolytica* protozoan parasite. Journal of Proteomics 226, 103897. https://doi.org/10.1016/j.jprot.2020.103897

Martins, V.T., Duarte, M.C., Chávez-Fumagalli, M.A., Menezes-Souza, D., Coelho, C.S.P., de Magalhães-Soares, D.F., Fernandes, A.P., Soto, M., Tavares, C.A.P., Coelho, E.A.F., 2015. A *Leishmania*-specific hypothetical protein expressed in both promastigote and amastigote stages *of Leishmania infantum* employed for the serodiagnosis of, and as a vaccine candidate against, visceral leishmaniasis. Parasites and Vectors 8, 1–12. https://doi.org/10.1186/s13071-015-0964-5

Matthiesen J, Lender C, Haferkorn A, Fehling H, Meyer M, Matthies T, Tannich E, Roeder T, Lotter H, B.I., 2019. Trigger-induced RNAi gene silencing to identify pathogenicity factors of *Entamoeba histolytica*. FASEB Journal 33.

Molgora, B.M., Rai, A.K., Sweredoski, M.J., Moradian, A., Hess, S., Johnson, P.J., 2021. A novel T*richomonas vaginalis* surface protein modulates parasite attachment via protein:Host cell proteoglycan interaction. mBio 12, 1–17. https://doi.org/10.1128/mBio.03374-20

Mony, B.M., MacGregor, P., Ivens, A., Rojas, F., Cowton, A., Young, J., Horn, D., Matthews, K., 2014. Genome-wide dissection of the quorum sensing signalling pathway in *Trypanosoma brucei*. Nature 505, 681–685. https://doi.org/10.1038/nature12864

Morf, L., Pearson, R.J., Wang, A.S., Singh, U., 2013. Robust gene silencing mediated by antisense small RNAs in the pathogenic protist *Entamoeba histolytica*. Nucleic Acids Research 41, 9424–9437. https://doi.org/10.1093/nar/gkt717

Nagaraja, S., Cai, M.W., Sun, J., Varet, H., Sarid, L., Trebicz-Geffen, M., Shaulov, Y., Mazumdar, M., Legendre, R., Coppée, J.Y., Begley, T.J., Dedon, P.C., Gourinath, S., Guillen, N., Saito-Nakano, Y., Shimokawa, C., Hisaeda, H., Ankri, S., 2021. Queuine is a nutritional regulator of *Entamoeba histolytica* response to oxidative stress and a virulence attenuator. mBio 12, 1–28. https://doi.org/10.1128/mBio10.1128/mBio

Ng, Y.L., Olivos-García, A., Lim, T.K., Noordin, R., Lin, Q., Othman, N., 2018. *Entamoeba histolytica*: Quantitative proteomics analysis reveals putative virulence-associated differentially abundant membrane proteins. American Journal of Tropical Medicine and Hygiene 99, 1518–1529. https://doi.org/10.4269/ajtmh.18-0415

Powell, R.R., Welter, B.H., Hwu, R., Bowersox, B., Attaway, C., Temesvari, L.A., 2006. *Entamoeba histolytica*: FYVE-finger domains, phosphatidylinositol 3-phosphate biosensors, associate with phagosomes but not fluid filled endosomes. Experimental Parasitology 112, 221–231. https://doi.org/10.1016/j.exppara.2005.11.013

Ralston, K., Petri, W.A., 2011. Tissue Destruction and invasion by *Entamoeba histolytica*. Trends in Parasitology 27, 254–263. https://doi.org/10.1016/j.pt.2011.02.006.

Rastew, E., Vicente, J.B., Singh, U., 2012. Oxidative stress resistance genes contribute to the pathogenic potential of the anaerobic protozoan parasite, *Entamoeba histolytica*. International Journal for Parasitology 42, 1007–1015. https://doi.org/10.1016/j.ijpara.2012.08.006

Ravooru, N., Ganji, S., Sathyanarayanan, N., Nagendra, H.G., 2014. Insilico analysis of hypothetical proteins unveils putative metabolic pathways and essential genes in *Leishmania donovani*. Frontiers in Genetics 5. https://doi.org/10.3389/fgene.2014.00291

Santos, F., Marcial-Quino, J., Gómez-Manzo, S., Enríquez-Flores, S., Nequiz-Avendaño, M., Cortes, A., de la Luz León-Avila, G., Saavedra, E., Pérez-Tamayo, R., Olivos-García, A., 2020. Functional characterization and subcellular distribution of two recombinant cytosolic HSP70 isoforms from *Entamoeba histolytica* under normal and stress conditions. Parasitology Research 119, 1337–1351. https://doi.org/10.1007/s00436-020-06621-7

Sen, T., Verma, N.K., 2020. Functional annotation and curation of hypothetical proteins present in a newly emerged serotype 1c of Shigella flexneri: Emphasis on selecting targets for virulence and vaccine design studies. Genes (Basel) 11. https://doi.org/10.3390/genes11030340

Shirley, D.A.T., Farr, L., Watanabe, K., Moonah, S., 2018. A review of the global burden, new diagnostics, and current Therapeutics for amebiasis. Open Forum Infectious Diseases 5, 1–9. https://doi.org/10.1093/ofid/ofy161

Silber, A.M., Pereira, C.A., 2012. Assignment of Putative Functions to Membrane "Hypothetical Proteins" from the *Trypanosoma cruzi* Genome. The J. Membrane Biol. 245, 125–129. https://doi.org/10.1007/s00232-012-9420-z

Singh, G., Gupta, D., 2022. In-Silico Functional Annotation of *Plasmodium falciparum* Hypothetical Proteins to Identify Novel Drug Targets. Frontiers in Genetics 13, 1–10. https://doi.org/10.3389/fgene.2022.821516

Singh, N., Ojha, S., Bhattacharya, A., Bhattacharya, S., 2012. Stable transfection and continuous expression of heterologous genes in *Entamoeba invadens.* Mol. and Biochem. Parasitol. 184, 9–12. https://doi.org/10.1016/j.molbiopara.2012.02.012

Suresh, S., Ehrenkaufer, G., Zhang, H., Singh, U., 2016. Development of RNA interference trigger-mediated gene silencing in *Entamoeba invadens*. Infection and Immunity 84, 964–975. https://doi.org/10.1128/IAI.01161-15

Tovy, A., Hertz, R., Siman-Tov, R., Syan, S., Faust, D., Guillen, N., Ankri, S., 2011. Glucose starvation boosts *Entamoeba histolytica* virulence. PLoS Neglected Tropical Diseases 5. https://doi.org/10.1371/journal.pntd.0001247

Turab Naqvi, A.A., Rahman, S., Rubi, Zeya, F., Kumar, K., Choudhary, H., Jamal, M.S., Kim, J., Hassan, M.I., 2017. Genome analysis of *Chlamydia trachomatis* for functional characterization of hypothetical proteins to discover novel drug targets. International Journal of Biological Macromolecules 96, 234–240. https://doi.org/10.1016/j.ijbiomac.2016.12.045

Walters, H.A., Welter, B.H., Moss, H.C., Villano, M.A., Orobio-hurtado, R., Sullivan, W.J., Temesvari, L.A., 2022. Eukaryotic Initiation Factor 2 a Kinases Regulate Virulence Functions, Stage Conversion , and the Stress Response in *Entamoeba invadens*. mSphere XXXX. https://doi.org/10.1128/msphere.00131-22

Welter, B.H., Sehorn, M.G., Temesvari, L.A., 2017. Flow cytometric characterization of encystation in *Entamoeba invadens*. Molecular and Biochemical Parasitology 218, 23–27. https://doi.org/10.1016/j.molbiopara.2017.10.002

Wesel, J., Shuman, J., Bastuzel, I., Dickerson, J., Ingram-Smith, C., 2021. Encystation of *Entamoeba histolytica* in axenic culture. Microorganisms 9. https://doi.org/10.3390/microorganisms9040873

WHO & UNICEF, 2021. Progress on Household Drinking Water, Sanitation and Hygiene 200-2020, UNICEF journal.

Yang, Z., Zeng, X., Tsui, S.K.W., 2019. Investigating function roles of hypothetical proteins encoded by the *Mycobacterium tuberculosis* H37Rv genome. BMC Genomics 20, 1–10. https://doi.org/10.1186/s12864-019-5746-6

CHAPTER FOUR

TARGET ACQUIRED: TRANSCRIPTIONAL REGULATORS AS DRUG TARGETS FOR
PROTOZOAN PARASITES

Heather A. Walters [1,2] and Lesly A. Temesvari [1,2]

[1] Department of Biological Sciences

[2] Eukaryotic Pathogens Innovations Center (EPIC)

Clemson University

Clemson, South Carolina United States of America 29634

*Corresponding author

Lesly A. Temesvari (LAT)

Email: LTEMESV@clemson.edu

I.   Abstract

Protozoan parasites are single-celled eukaryotic organisms that cause significant human disease and pose a substantial health and socioeconomic burden worldwide. They are responsible for at least 1 million deaths, annually. The treatment of such diseases is hindered by the ability of parasites to form latent cysts, develop drug resistance, or be transmitted by insect vectors. Additionally, these pathogens have developed complex mechanisms to alter host gene expression. The prevalence of these diseases is predicted to increase as climate change leads to the augmentation of ambient temperatures, insect ranges, and warm water reservoirs. Therefore, the discovery of novel treatments is necessary. Transcription factors (TFs) lie at the junction of multiple signaling pathways in eukaryotes and aberrant TF function contributes to the progression of numerous human diseases, including cancer, diabetes, inflammatory disorders and cardiovascular disease. TFs were previously thought to be undruggable. However, due to recent advances, TFs now represent appealing drug targets. It is conceivable that TFs, and the pathways they regulate, may also serve as targets for anti-parasitic drug design. Here, we review TFs and transcriptional modulators of protozoan parasites and discuss how they may be useful in drug discovery. We also provide information on TFs that play a role in stage conversion of parasites, TATA box-binding proteins, and TFs and cofactors that participate with RNA polymerases I, II and III. We also highlight a significant gap in knowledge in that the TFs of some of parasites have been under investigated. Understanding parasite transcriptional pathways and how parasites alter host gene expression will be essential in discovering innovative drug targets.

II.   Introduction

Protozoan parasites are single-celled eukaryotic organisms that cause a variety of human diseases and pose a substantial health and socioeconomic burden worldwide (Burgess, 2017). Such pathogens (Table 4.1) are responsible for at least 1 million deaths, annually (Canon et al., 2018). Since these organisms are transmitted by insect vectors, or by contaminated food or

water, they present the highest burden in tropical and resource-poor countries that lack proper sanitation. Furthermore, climate change is increasing the endemic range of insect-vectors, thus increasing the spread of parasitic diseases to developed areas (Short et al., 2017). The World Health Organization (WHO) classifies some of the diseases caused by parasites (e.g., leishmaniasis, trypanosomiasis) as neglected tropical diseases, which cause severe illness in over 1 billion people. At least one of these diseases (i.e., cryptosporidiosis) is categorized as a class B bioterrorism agent by the Centers for Disease Control (CDC) and the National Institutes of Health (NIH). It is well-established that these diseases are difficult to treat due to evolved drug resistance and the ability of parasites to form latent, resistant cysts or oocysts (Schapp and Schilde, 2018). Overall, there is an urgent need to develop new therapeutics for this class of pathogens.

Drug resistance, latency, and virulence rely on exquisitely-controlled transcriptional programs in the parasite and sometimes, in the host. Thus, targeting transcription and the factors that regulate transcription is an attractive prospect in anti-parasitic drug design. Transcription factors (TFs) were once thought to be undruggable (Lambert et al., 2018). However, methodological advances including chromatin IP (ChIP)-

Table 4.1: Overview of protozoan parasites and their diseases

Disease	Kinetoplastids				Amoebozoa					Apicomplexans		
	Trichomoniasis	Chagas disease	African sleeping sickness	Leishmaniasis	Amoebiasis (amoebic dysentery)	Giardiasis	Primary amoebic meningoencephalitis	Amoebic keratitis and encephalitis	Amoebic encephalitis	Cryptosporidiosis	Toxoplasmosis	Malaria
Parasite	Trichomonas vaginalis	Trypanosoma cruzi	Trypanosoma brucei	Leishmania species	Entamoeba histolytica	Giardia intestinalis	Naegleria fowleri	Acanthamoeba castellani	Balamuthia mandrillaris	Cryptosporidium parvum	Toxoplasma gondii	Plasmodium falciparum
Reservoir	Sexually transmitted disease	Kissing bug	Tsetse fly	Sand fly	Contaminated food and water	Contaminated food and water	Contaminated food and water	Contaminated water	Contaminated water	Contaminated water	Contaminated food, cat litter, and soil	Mosquito
Prevalence	784,000 cases annually	10,000 death annually	60 million people currently at risk	1,000,000 cases annually	50 million cases annually	284 million cases annually	Rare-98% fatal	Rare	Rare	784,000 cases annually	25% of the world's population	>400,000 deaths annually
Endemic areas	Worldwide	Rural Latin and South America	Sub-Saharan Africa	Worldwide	Sub-Saharan Africa and southern Asia	Worldwide	Worldwide	Worldwide	Worldwide	Worldwide	Worldwide	Sub-Saharan Africa
Encystation or stage specific		No recent data			EhERM-BP[b]	TOP3β[b]	No recent data		No recent data		TgBFD1[b]	
TATA-box binding proteins (TBP)	TvTBPs		TbTBP[a]	LmTbp[a]	EhTBP1[b] EhTAF1	Giardia proteases GiTBP[a]		AcTBPs[a]		CpTBP[a]		PfTBP
RNA polymerase III cofactors			TbMaf1	LmBdp1[b]								
RNA polymerase II cofactors			TFII-like complexes		EhNF-Y[b] EhPC4 EhNF-Y[a]			AcTIF-IA				PfNF-YB
RNA polymerase I cofactors												
Modulators of host transcription			Indolepyruvate	Effector acting on c-myc Effector acting on XBP-1						RNA transcript Cdg7_FLc_1000 RNA transcript Cdg7_FLc_0220	TgTEEGR	

a Transcription factor identified, and characterized > 5 years ago and thus not included in this review
b knock out, knock down of gene expression, or inhibition of gene product resulted in decreased growth or decreased virulence

seq, RNA-seq, and genome editing, have moved TFs to the forefront of drug discovery (Papavassiliou and Papavassiliou, 2016; Lambert et al., 2018). This is important because TFs are implicated in numerous pathologies. For example, TFs represent 20% of identified oncogenes in cancer (Lambert et al., 2018). Additionally, dysregulation of GATA TFs are implicated in cardiac disease, aberrant levels of heat shock TF 1 (HSF1) are linked to several neurogenerative diseases, and upregulation of NF-κB is associated with inflammation disorders (Papavassiliou and Papavassiliou, 2016).

Therefore, targeting TFs may also be a viable approach to treat parasitic disease. Numerous ways to target transcription have been conceived (Lambert et al., 2018) (Figure 4.1). For example, small molecules can be used to physically block DNA-protein (Figure 4.1B) and protein-protein interactions (Figure 4.1C), TFs may also be targeted for degradation by ubiquitination or sumoylation (Figure 4.1D) or their expression can be controlled by blocking their own transcriptional modulators. (Figure 4.1E). The outcome of these approaches is a block in transcription of one or more essential genes.

This review summarizes the most recent data (≤ 5 years) on TFs in extracellular and intracellular parasites (Table 4.1). Indeed, each of these classes of parasites present different challenges when investigating drug targets. Given that both parasite and host transcription are important in virulence, we also discuss parasite-derived transcriptional modulators that alter host gene expression to promote parasite survival. Interestingly,
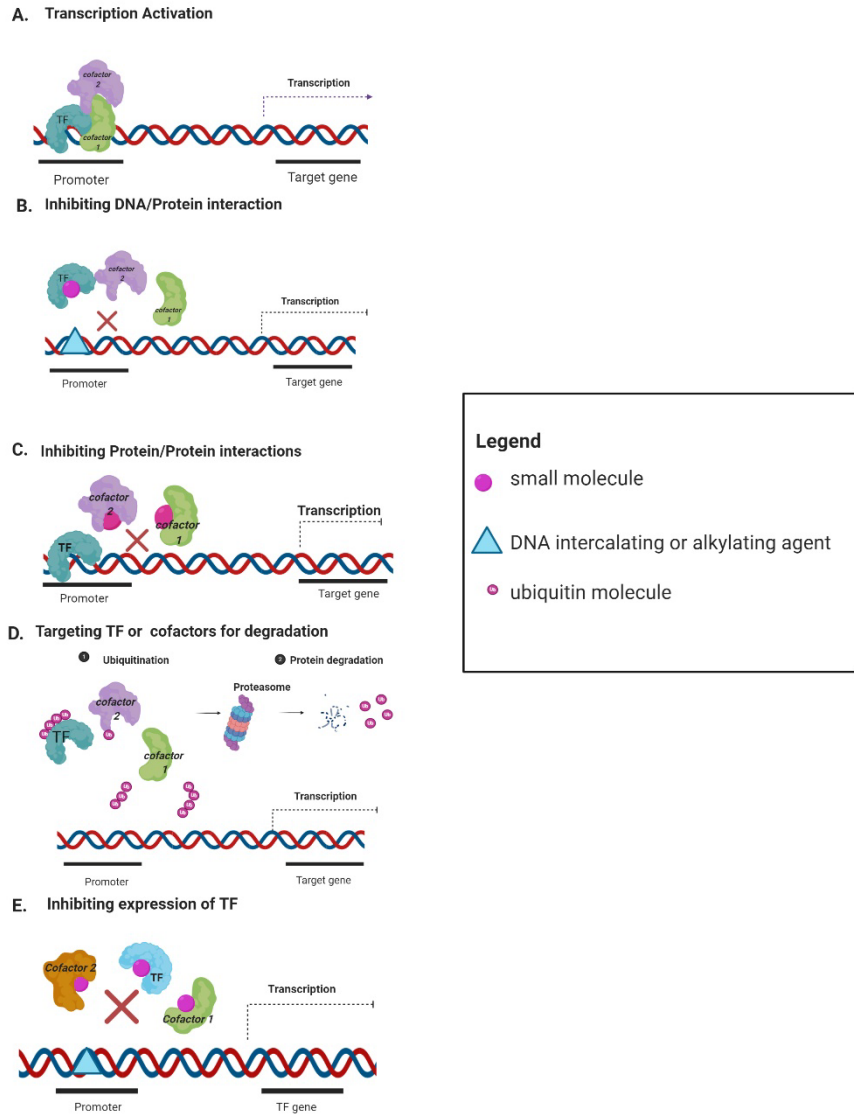
Figure 4.1: Mechanisms of Targeting Transcription Factors

A. A general representation of transcription is provided. TF is activated, binds to consensus sequence, recruits cofactors and RNA pol, resulting in transcription of the target gene. Mechanisms for targeting TFs include **B.** Inhibiting TF/DNA interactions using specific small molecules to block DNA-binding pockets within TF or using alkylating/intercalating agents or small molecule that binds to DNA consensus sequence, distorting shape or physically blocking TF binding **C.** Inhibiting TF/protein interactions using small molecules to block protein-protein binding sites. **D.** Marking TFs or necessary cofactors for degradation via ubiquitination or sumoylation. **E.** Controlling expression of TFs by inhibiting their own transcriptional modulators. Examples of TF targeting drugs include Ecteinasciden 743, which alkylates the minor groove of DNA, blocking NF-Y binding (Method B) (Lambert et al., 2018), triptolide, a plant-derived natural product, which blocks the assembly of TFIIIB with necessary cofactors (Method C) (Liang et al., 2019), mebendazole, which induces degradation of the TF, MYB (Method D) (Lambert et al., 2018), and vorinostat, an HDAC inhibitor, which is used to control overexpression of c-Myc in T-cell acute lymphoblastic leukemia (Method E) (Lambert et al., 2018). This illustration was created using BioRender (Toronto, Canada).

there is a paucity of recent information on transcriptional regulation in and by *Naegleria fowleri*, *Balamuthia mandrillaris*, and *Acanthamoeba castellani*. We further discuss this gap in knowledge in the conclusion. Finally, as a guide to the reader we include several tables. Table 4.1 provides an overview of protozoan parasites, prevalence, and TFs or modulators discussed. Table 4.2 describes parasite TFs, recently discovered, but reviewed elsewhere. Table 4.3 describes parasite modulators that act on host transcription that are also reviewed elsewhere. Finally, Table 4.4 summarizes the available evidence supporting the potential of these parasite TFs as drug targets.

III. Encystation- or Stage-Specific Transcription

Many parasites have a complex-multistage life cycle. *Entamoeba histolytica* (Manna et al., 2018), *Giardia intestinalis* (Sun et al*.,* 2020), and *Cryptosporidium spp*. (Ming et al., 2018) have two-stage life cycles, consisting of infective, environmentally stable cyst forms and pathogenic parasites. Specifically, these three pathogens encyst in the GI tract and are shed back into the environment. On the other hand, *Toxoplasma gondii* has both a sexual phase in the feline definitive host and an asexual phase in the human host (Hong et al., 2017). In the asexual phase, *T. gondii* tachyzoites, which are actively dividing, form cysts (bradyzoites) within muscle and brain tissue. This allows *T. gondii* to establish chronic infections (Hong et al., 2017). For all of these parasites, stage conversion is crucial for disease transmission and parasite pathogenesis. Understanding the transcriptional pathways that govern these mechanisms would significantly inform drug development (Schapp and Schilde, 2018).

Table 4.2: Transcription factors reviewed elsewhere. Parasitic transcription factors (TFs), which were described in the last 5 years, but are not reviewed here because they have been reviewed elsewhere. The table also includes a brief description of function and pertinent references.

Parasite	Transcription factor	Function	Reference
Toxoplasma gondii	AP2IX-4	Loss of AP2IX-4 results in a modest virulence defect and reduced cyst burden, regulates bradyzoite-specific genes	Bing et al., (2018); reviewed in Jeninga et al. (2019)
	AP2IV-3 and AP2IX-9	Tissue cyst formation decreased by disruption of the AP2IX-9 gene and enhanced by deletion of the AP2IV-3 gene, demonstrating that these factors have opposite functions in bradyzoite development	Reviewed in Jeninga et al. (2019)
	TgAP2XI-5 and TgAP2X-5	Cooperatively regulate virulence gene expression	Reviewed in Jeninga et al. (2019)
Plasmodium falciparum	AP2 TFs-ap2-o2, ap2-o3, ap2-o4,ap2-sp2, and ap2-sp3.5	TFs required for parasite transmission via mosquitos.	Reviewed in Josling et al. (2018).
	AP2-FG	Responsible for female-specific gene regulation, AP2-FG null parasites generate early females	Yuda et al. (2020)
	PfAP2Tel	AP2 DNA-binding domain that binds to telomeres could be responsible for	Sierra-Miranda et al. (2017).

		chromosome integrity	Reviewed in Jeninga et al. (2019)
	AP2-exp	Regulates clonally variant genes	Martins et al. (2017)
			Reviewed in Jeninga et al. (2019)
Plasmodium berghei	ApiAP2	Critical parasite virulence factor	Akkaya et al. (2020)

Table 4.3: Transcriptional modulators reviewed elsewhere. Parasitic transcriptional modulators that alter host gene expression, which were described in the last 5 years, but are not reviewed here because they have recently been reviewed elsewhere. The table also includes a brief description of function and pertinent references.

Parasite	Modulator	Function	Reference
Toxoplasma gondii	ROP16	Phosphorylates and inhibits host STAT3[a] and STAT6[a], resulting in activated macrophages (M2) that are less able to control parasite load	Chen et al. (2020) Reviewed in Hakimi et al. (2017)
	*Tg*IST	Required in all to block host IFN-γ[a] mediated STAT1[a] transcription in mouse and human cells	Olias et al. (2016); reviewed in Hakimi et al. (2017)
	MYR1	Required to deliver secreted effectors into the host cell and is required for virulence	Franco et al. (2016); reviewed in Hakimi et al. (2017)
	GRA24	Interacts with host MAP[a] kinase, promoting nuclear translocation and triggering a pro-	Pellegrini et al. (2017); reviewed in Hakimi et al. (2017)

		inflammatory response	
Plasmodium falciparum	_Pf_EMP1	Expressed on infected host RBC[a] surface, represses host cell immune response by repressing NF-κB[a]; already used as vaccine target	Sampaio et al. (2018)

[a]Abbreviations: STAT: Signal Transducer And Activator Of Transcription; IFN-γ: interferon-γ; MAP-mitogen activated protein; RBC: red blood cell; NF-κB: Nuclear factor-κB

Table 4.4: Summary of the available evidence supporting the potential of parasite transcription factors as drug targets.

Parasite	TF	NCBI Accession Number	KD[a] or KO[b]	Phenotype of Gene Disruption	Druggable Domains Modelled?	Small Molecule Binding (Empirical or Modeled)	Identity Shared with Human Ortholog	Human Ortholog Accession Number	Inhibition of Orthologs in Other Species
Encystation-specific TFs									
Entamoeba invadens	ERM-BP[1]	XP_00418 4544.1	KD	encystation decreased, cyst morphology altered, viability unaffected	NS	NS	none	N/A	N/A
Giardia intestinalis	TOP3β[2]	XP_00170 9794.1	KD	encystation and viability are decreased	NS	Norfloxacin reduces growth and cyst formation	28.73%[2]	NM_003935.5	Norfloxacin inhibits human protein[2]
Toxoplasma gondii	BFD1[3]	XM_0187 79152.1	KO	in vitro & in vivo differentiation is blocked	NS	NS	54.08% to human c-myb[d]	AAA52031.1	Mebendazole targets human myb for degradation[4]
TATA-box Binding Proteins									
Entamoeba histolytica	TBP[6]	XP_00191 4239.1	KD	decreased erythrophagocytosis[5]	interdomain region[6]	modelled binding of several molecules using flexible and rigid docking[6]	54.4%[5]	NM_003194	Hedamycin blocks human TBP from binding DNA[4]
Plasmodium falciparum	TBP[6]	XM_0013 51584.1	NS[c]	NS	NC-2 binding domain and N-ter stirrup region[6]	modelled binding of several molecules using flexible and rigid docking[6]	38.3%[6]	NM_003194	Pluramycin traps human TBP on promoter[4]
Trichomonas vaginalis	TBP1[7]	XP_00132 9427.1	NS	NS	NS	NS	44.75%[7]	NM_003194	Hypericin inhibit modification of human TBP[4]
T. vaginalis	TBP2[7]	XP_00130 0812.1	NS	NS	NS	NS	37.78%[7]	NM_003194	CC-1065 inhibits human TBP DNA binding[4]
E. histolytica	TAF1[8]	XP_65493 5.1	NS	NS	NS	NS	32%[8]	NM_004606	BI-2536 inhibits human TAF1[9]
E. histolytica	TRF1[5]	XP_65253 3.1	KD	unsuccessful, TRF1 may be essential	NS	NS	56% to human TBP[d]	NM_003194	NS
RNA Polymerase II & III Cofactors									
Leishmania major	Bdp1[10]	XP_00168 7246.1	KD	growth defect, RNA pol III transcription reduced	NS	NS	22.8%[10]	NM_018429	NS
Trypanosoma brucei	Maf1[11]	XP_84466 2.1	KD	RNA pol II transcription is increased, growth increases	NS	NS	15%[11]	NM_032272	NS
P. falciparum	NF-YB[12]	XP_00134 8144.1	NS	NS	NS	NS	60%[d]	NM_006166	ET743 inhibits human NF-Y DNA binding[4]
E invadens	NF-YC[13]	XP_00425 8893.1	KD	encystation decreased	NS	NS	low homology, conserved functional domains to human NF-YC	NM_014223	ET743 inhibits human NF-Y DNA binding[5]
E. histolytica	PC4[14]	XP_65387 8.1	NS	NS	NS	NS	39.34%[d]	NM_006713	AG-1031 inhibits human PC4[15]
T. brucei	TFL1/2[16]	XP_82819 7.1; XP_82961 5.1	KD	silencing either one halts cell growth after 48 h	NS	NS	none[16]	N/A	NS
RNA Polymerase I Cofactors									
E. histolytica	TIF1A[17]	XP_64912 9.1	NS	NS	NS	NS	21.29%[d]	NP_060897	aspirin induces degradation of TIF-1A in humans[19]
Acanthamoeba castellani	TIF1A[18]	ELR1367 6.1	NS	NS	NS	NS	37.3%[d]	NP_060897	aspirin induces degradation of TIF-1A in humans[19]

[a]KO, knockout; [b]KD, knockdown; [c]NS, not studied.
[d]Identity calculated from NCBI Blast (https://blast.ncbi.nlm.nih.gov/Blast.cgi).
References: [1]Manna et al., 2018; [2]Sun et al., 2020; [3]Waldman et al., 2020; [4]Lambert et al., 2018; [5]Narayanasamy et al., 2018; [6]Santiago et al., 2018; [7]Parra-Marín et al., 2019; [8]Avendaño-Borromeo et al., 2019; [9]Remillard et al., 2019; [10]Román-Carraro et al., 2019; [11]Romero-Meza et al., 2017; [12]Lima et al., 2017; [13]Manna et al., 2019; [14]de la Cruz et al., 2016; [15]Zhang et al., 2020; [16]Srivastava et al., 2018; [17]Srivastava et al., 2016; [18]Gogain and Paule, 2004; [19]Chen et al., 2018

Manna et al., (2018) identified ERM-BP (Encystation Regulatory Motif Binding Protein) that regulates encystation in the reptilian parasite, *E. invadens*. This parasite can encyst in culture and serves as a surrogate for the human pathogen, which cannot be induced to encyst in the laboratory. ERM-BP is conserved in all the *Entamoebae*. ERM-BP was identified by its ability to bind a consensus promoter motif in cyst-specific genes. It was demonstrated that ERM-BP resides in the nucleus and controls encystation in a NAD+-inducible fashion. Overexpression of ERM-BP led to increased encystation, while knocking down ERM-BP expression resulted in decreased encystation. Additionally, cysts that were produced in the ERM-BP knockdown cell line exhibited altered morphology suggesting that there was a defect in cyst wall synthesis. In support of this, the expression of cyst wall markers, chitinase and Jessie-3, was reduced in the knockdown cell line, suggesting that ERM-BP regulates a subset of cyst-wall specific genes. ERM-BP has no obvious canonical DNA-binding domain and additional structural analyses will be necessary to identify the DNA-binding pocket. Since this protein does not exist in the human host, small molecule inhibition at the DNA-binding region (Figure 4.1, Strategy B) may represent a novel therapy for amoebiasis, as blocking encystation would ultimately block transmission.

Topoisomerases (type I and II) are involved in cell growth and differentiation and are essential to overcome topological problems experienced by chromosomes during DNA replication, transcription, recombination, and mitosis (Sun et al., 2020). Sun and colleagues (2020) characterized *G. intestinalis* TOP3β, a type IA DNA topoisomerase. It was shown that the *Giardia* TOP3β homolog shared 28.73% identity and 41.32% similarity with the human counterpart. TOP3β expression increased during encystation and immunoprecipitation showed that TOP3β interacted with the promoters of cyst wall protein-1 (CWP-1) and MYB2 during stage conversion. The MYBs are a large family of functionally diverse TFs found in all eukaryotes. Overexpression of TOP3β led to increases in encystation and the expression of CWP and MYB2

genes (Sun et al., 2020). Conversely, mutation of the TOP3β protein led to cell lines that exhibited decreased encystation rates and significantly lower expression of both CWP and MYB2 genes. The authors also found that the topoisomerase inhibitor, norfloxacin, inhibited *G. intestinalis* growth and encystation. However, norfloxacin also inhibits human type IA topoisomerases. Therefore, a *Giardia*-specific norfloxacin alternative will be necessary if *Giardia* TOP3β is to be targeted for the treatment of giardiasis (Sun et al., 2020).

The MYB family of TFs, itself, has been implicated in stage conversion in the *Entamoebae* (Ehrenkaufer et al., 2009), *Giardia* (Sun et al., 2002), and *Plasmodium* (Gissot et al., 2005). In *Trichomonas vaginalis*, which is a parasite that lacks a latent stage, MYB-like TFs regulate expression of adhesion proteins that are critical for parasite-host interaction (Chu et al., 2018). More recently, a MYB-like protein, BFD1, which controls the switch between active tachyzoite to latent bradyzoite in *T. gondii*, has been described (Waldman et al., 2020). After invasion of host cells, tachyzoites replicate within the parasitophorous vacuole. During differentiation into bradyzoites (cysts), the parasitophorous vacuole is modified into a heavily glycosylated cyst wall, containing stage-specific proteins of unknown function. Stage conversion can be induced *in vitro* by various stimuli (alkaline pH, heat shock, or nutrient starvation), but mechanisms underlying this transition are largely unknown (Waldman et al., 2020). Waldman and colleagues (2020) demonstrated that BFD1 is a MYB-like TF that is necessary for differentiation *in vitro* and in mouse models of infection.

Using CRISPR-mediated technology, a knockout strain of *T. gondii* was generated (ΔBFD1). ΔBFD1 parasites did not differentiate and failed to form cysts in the brains of mice. However, the mortality and morbidity of mice infected ΔBFD1 was the same as those infected with wild-type or complemented parasites. Thus, BFD1 seems to be dispensable for the acute stage of the disease. *In vitro*, ΔBFD1 parasites developed normally throughout the tachyzoite cycle but failed to initiate bradyzoite gene expression and died under stress, instead of forming

latent cysts. Furthermore, overexpression of BFD1 was sufficient to induce stage conversion in 60% of parasites *in vitro*. Lastly, the authors found BFD1-binding sites near start sites of several bradyzoite-specific genes, including BFD1, itself. The authors stated that BFD1 could be the basis of therapeutics, as disrupting stage conversion would allow more effective immune clearance of tachyzoites (Waldman et al., 2020).

IV.   TATA-box binding proteins (TBPs)

TATA-box binding protein (TBP), a subunit of TFIID, is a general TF that is involved in transcription by multiple RNA polymerases including RNA polymerases II (RNA Pol II) and III (RNA Pol III) (Han and He, 2016) (Figure 4.2A, B). TBP binds to the canonical TATA box sequence (TATAWAW, where W represents either an A or T), which is found in many eukaryotic promoter elements (Han and He, 2016). TBP is also involved in transcription of genes that do not possess the TATA-box element (Para-Marrin et al.,
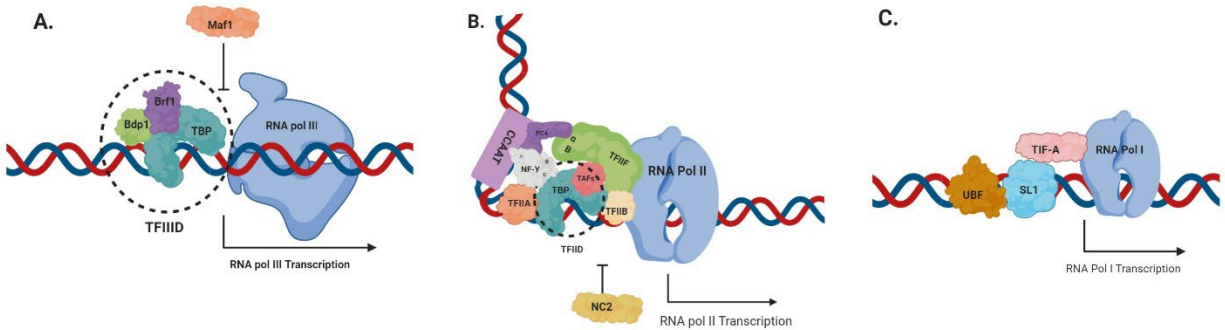
Figure 4.2: RNA Polymerases and their Cofactors

The illustrations are not inclusive of all known cofactors and their interactions. For clarity, only those proteins described in this review are incorporated in the diagrams. **A.** RNA Pol III transcribes short, abundant nonprotein-coding RNA transcripts such as tRNAs, 5S rRNAs, and other essential small RNAs. Recruitment of RNA Pol III to the DNA relies on proteins, which make up a pre-initiation complex. Among the proteins in this complex is TFIIIB, which consists of three subunits, the TATA-box binding protein (TBP), B Double Prime 1 (Bdp1), and Brf1. RNA Pol III transcription can be inhibited by Maf1. **B.** RNA Pol II transcribes precursor mRNAs, microRNAs and a majority of small nuclear RNAs (snRNAs). Like RNA Pol III, RNA Pol II also relies on TBP for promoter binding. However, TBP-related factors (TRFs) can also fill the role of TBP (not shown). TBP function also depends on TBP-associated factors (TAFs), which may be determinants of promoter selectivity. Transcription of genes by RNA Pol II also requires the protein complexes TFIIA, TFIIB, and TFIIF. The TFIIF complex binds to RNA Pol II and the TFIIB complex. The α and β subunits of TFIIF further interact with the transcription machinery by binding PC4, which interacts with Nuclear Factor Y (NF-Y). Nuclear Factor-Y (NF-Y) is a heterotrimeric TF, composed of three subunits. The A subunit interacts with PC4 and the B and C subunits interact with TBP. RNA Pol II transcription may be negatively regulated by NC2. **C.** RNA Pol transcribes all the rRNA genes except 5S rRNA. Upstream binding factor (UBF) adheres to the promoters of rDNA, which triggers the SL-1 binding. RNA Pol I, connected to TIF-1A, binds to the UBF/SL-1 complex. Finally, TIF-1A facilitates the interaction between RNA Pol I and SL-1, forming the pre-initiation complex. This figure was created using BioRender (Toronto, Canada).

2019). Human TBP possesses two domains: a divergent N-terminal sequence and a conserved 180 amino acid C-terminal DNA-binding domain, composed of two structural region repeats flanking a highly basic segment. This confers a saddle-like shape to the protein. The concave "straddles the DNA", whereas the convex surface is analogous to the "seat" of the saddle where TBP interacts with general TFs and other cofactors (Kim et al., 1993).

TBP is a key element that is indispensable to transcription and disrupting any of its interactions with other proteins, or blocking its function, could potentially lead to a lethal decrease in transcription (Figure 4.1, Strategy B and C). Given its fundamental requirement, TBP also has a low mutation rate. Therefore, the chance of acquiring resistance to TBP-targeting drugs is low (Santiago et al., 2019). TBPs have been identified in *E. histolytica* (Narayanasamy et al., 2018; Santiago et al., 2019), *Plasmodium falciparum* (Santiago et al., 2019), *A. castellani* (Chen et al., 2004), *Leishmania major* (Ivens et al., 2005), *Trypanosoma brucei* (Ibrahim, et al., 2009), *C. parvum* (Millership et al., 2004), *T. vaginalis* (Parra-Marrin et al., 2019), and *G. intestinalis* (Best et al., 2004).

Two TBPs exist in *E. histolytica* (EhTBP1 and EhTBP2), EhTBP2 is 100% identical to EhTBP1 and is endogenously silenced. EhTBP1 possesses the conserved TBP saddle like-structure and binds TATA-box promoter element and TATA-variants, which are noncanonical TBP-binding sites. Narayanasamy et al. (2018) found that EhTBP not only binds the TATA-box and TATA-variants, but also binds the GAAC-box, which is an unusual and novel core promoter found in 56% of *E. histolytica* genes. Knocking down expression of EhTBP1 (Verma et al., 2019; Narayanasamy et al., 2018) resulted in reduced phagocytosis and decreased expression of Hgl, a cell surface adhesin that controls parasite-host interaction. Although phagocytosis and parasite-host adhesion are important virulence functions, pathogenicity of the EhTBP1 knockdown strain has not been examined in an *in vivo* model of infection.

Using computational methods, Santiago et al. (2019) showed that *P. falciparum* TBP (PfTBP) and *E. histolytica* TBP (EhTBP) exhibited unique features that may be exploited for drug design. These features were specific to TBP's role in RNA Pol II-based transcription (Figure 4.2B). For example, the TFIIA-binding cavity was more open in PfTBP than in human TBP (hsaTBP), while the same domain in EhTBP was less open. A more open TFIIA binding site is potentially druggable because molecules (drugs) that fit into the PfTBP TFIIA binding domain, would not necessarily fit into hsaTBP. Computational modeling also showed that EhTBP and PfTBP possessed less-conserved and more open negative cofactor-2 (NC-2) binding sites compared to that of hsaTBP. NC-2 is a negative regulator of TBP. It binds to TBP and prevents the recruitment of TFIIA and TFIIB. Thus, the NC-2 binding site is another promising target (Santiago et al., 2019) (Figure 4.1, strategy B and C). In other systems, the strategy to target TBP has been to block its DNA-binding activity (Lambert et al., 2018). Currently, there are no known drugs that bind in the TFIIA- or NC-2-pocket of TBP. Given the uniqueness of these sites in the parasites, discovering and designing such drugs would be a novel and attractive line of research.

Parra-Marín et al. (2019) characterized two TBP proteins in *T. vaginalis*. TvTBP1 and TvTBP2 are 45.16% identical to each other and are both actively expressed in the parasite. GST-pull down assays showed that TvTBP1 interacts with IBP39, a protein exclusive to *T. vaginalis* that is part of the pre-initiation complex. Typical TATA-box sequences have not been identified in the *T. vaginalis* genome, but electrophoretic mobility shift assays (EMSAs) showed that both TvTBPs bind to the promoters of genes that are transcribed by multiple RNA polymerases. This was not surprising since *P. falciparum* and *E. histolytica* TBPs are known to also bind TATA-variants (Narayanasamy et al., 2018; Santiago et al., 2019). Furthermore, TvTBPs possessed the conserved saddle-like tertiary structure and the canonical carboxy-terminal domain of the TBP superfamily. HsaTBP contains four phenylalanine residues that are required for TATA-box

binding. Parra-Marín et al. (2019) showed that in TvTBP1, two of the phenylalanine residues were substituted with tyrosine residues and in TvTBP2, one of the phenylalanine residues was replaced with isoleucine. If such amino acid substitutions alter DNA-binding pocket shape or openness, compared to that of hsaTBP, the TvTBP DNA-binding sites may serve as drug targets. Importantly, TvTBP1 does not complement a *S. cerevisiae* strain lacking TBP, suggesting that it may contain sufficiently divergent structure, which would be ideal for drug targeting.

 E. histolytica also possesses EhTBP-associated factor 1 (EhTAF1) (Avendaño-Borromeo et al., 2019) and TBP-related factor 1 (EhTRF1) (Narayanasamy et al., 2018). In humans, TAF1 binds TBP and has been shown to have a central role in gene expression (Avendaño-Borromeo et al., 2019). A human homolog of TRF1 does not seem to exist; however, in *Drosophila melanogaster*, TRF1 regulates a subset of specialized genes involved in embryogenesis. In humans TRF2 selectively regulates TATA-less promoters (Narayanasamy et al., 2018). Avendaño-Borromeo and colleagues (2019) found that EhTAF1 coprecipitates with EhTBP and EhTRF1. Interestingly, EhTAF1 does not have an apparent TBP-binding domain or a zinc knuckle domain, which is involved in DNA binding (Avendaño-Borromeo et al., 2019). Since the structure of EhTAF1 differs from the structure of the human counterpart, disrupting the association of EhTBP with EhTAF1, by targeting a unique domain within EhTAF1, could be a valuable therapeutic strategy (Figure 4.1, Strategy C). A similar strategy could be used for EhTRF1, especially since a human homolog does not seem to exist and the authors were not able to knock down TRF1 gene expression in parasites (Narayanasamy et al., 2018).

<center>V. RNA Polymerase III Cofactors</center>

 RNA Pol III is specialized for transcribing short, abundant nonprotein-coding RNA transcripts such as tRNAs, 5S rRNAs, and other essential small RNAs (reviewed in Turowski and Tollervey, 2016). Recruitment of RNA Pol III to the DNA relies on proteins, which make up a pre-

<center>118</center>

initiation complex. Among the proteins in this complex is TFIIIB, which consists of three subunits, the TATA-box binding protein (TBP), B Double Prime 1 (Bdp1), and Brf1 (Figure 4.2A). RNA Pol III transcription can be inhibited by Maf1, which blocks the interaction between TFIIIB and the polymerase, itself. Homologs to many of these RNA Pol III transcription partners have been identified in parasites.

B Double Prime 1 (Bdp1)

Bdp1 contains a SANT domain, which is a highly conserved 50 amino acid sequence present in proteins involved in transcriptional regulation (Ferrari et al., 2004; Román-Carraro et al., 2019). Román-Carraro and colleagues (2019) identified and characterized a Bdp1 homolog in *Leishmania major* (LmBdp1). Sequence alignment of LmBdp1 with other Bdp1 homologs demonstrated that LmBdp1 contains an extended SANT domain (characterized by 5 α-helices), flanked by an N-linker region and a long arm. Interestingly, the long arm is predicted to occur in all Bdp1 orthologues, except the human protein. The N-linker region is required for interacting with the minor groove of DNA, while the long arm interacts with Brf1 (Román-Carraro et al., 2019).

When attempting to produce a double knockout of LmBdp1, using targeted gene replacement, Román-Carraro and colleagues (2019) found that *L. major* possesses a third copy of the LmBdp1 gene. In this mutant, known as DKO+1, LmBdp1 expression was reduced by 70% and growth was reduced compared to single knockout and wild type parasites. This suggests that LmBdp1 is an essential gene. Transcription by RNA Pol III was also decreased in DKO+1 cells. ChIP assays revealed that LmBdp1 binds to Pol III promoters, such as those that drive expression of U2, U4, and some snRNAs (Román-carraro et al., 2019). Since LmBdp1 appears to be essential for TFIIIB-based recruitment of RNA Pol III and differs structurally from the human homolog, LmBdp1 may be a suitable target for drug development.

Maf1

Maf1 is a negative regulator of TFIIIB and acts by associating with the C160 subunit of RNA Pol III and with the third subunit of TFIIIB, Brf1. Ultimately, this interaction prevents recruitment of TBP and represses transcription. Romero-Meza et al. (2017) identified a Maf1 homolog in *T. brucei* (TbMaf1) which is encoded by two genes, whose products share 95.8% identity. While TbMaf1 and human Maf1 shared only 15% amino acid identity, they both possessed three conserved domains of unknown function, named: A, B, and C. The linker region between domains A and B was not conserved and was specific to each species. Since domains A, B, and C are conserved, TbMaf1 is predicted to possess the same tertiary structure as human Maf1, suggesting that they have similar functions. Romero-Meza et al. (2017) showed that TbMaf1 localizes to the nucleus, controls cell growth, and is a negative regulator of transcription. However, altering levels of TbMaf1 expression did not affect the levels of TbTBP, as seen in mammalian cells (Romero-Meza et al., 2017).

<div align="center">V.   RNA Polymerase II Cofactors</div>

RNA polymerase II (RNA Pol II) is required for the synthesis of precursor mRNAs, microRNAs and a majority of small nuclear RNAs (snRNAs). Like RNA Pol III, RNA Pol II also relies on TBP for promoter binding. However, TBP-related factors (TRFs) can also fill the role of TBP in a tissue-specific fashion (Narayanasamy et al., 2018). TBP function also depends on TBP-associated factors (TAFs), which may be determinants of promoter selectivity. Transcription of genes by RNA Pol II also requires the protein complexes TFIIA, TFIIB, TFIID, TFIIE, TFIIF and TFIIH. The TFIIF complex binds to RNA pol II and the TFIIB complex, as illustrated in Figure 4.2B (Schweikhard et al., 2014). The α and β subunits of TFIIF further interact with the transcription machinery by binding PC4 (Akimoto et al., 2014) a single-strand DNA binding protein, which also interacts with

Nuclear Factor Y (NF-Y).   Nuclear Factor-Y (NF-Y) is a heterotrimeric TF, composed of three subunits: A, B, and C) (Manna et al., 2019). The A subunit interacts with PC4 and the B and C subunits interact with TBP. RNA Pol II transcription may be negatively regulated by NC2.

Nuclear Factor Y

Lima and colleagues (2017) characterized *P. falciparum* NF-YB (PfNF-YB). *P. falciparum* merozoites invade red blood cells (RBCs) and develop asexually through ring, trophozoite, and schizont stages. PfNF-YB was expressed mainly in the schizont stage. Chromatin IP (ChIP) identified 297 target genes that were putatively regulated by PfNF-YB. These genes were known to play roles in protein translation, protein folding, intracellular transport, cell redox homeostasis and metabolism. A conserved CCAAT motif was found in 140 of the Pf NF-YB-regulated genes. Of the other 157 putative target gene promoters, 45 exhibited at least 80% homology in a motif consisting of 5 bases upstream and downstream of the CCAAT core. The authors proposed 5 PfNF-YB-binding consensus sequences; however, the interaction of PfNF-YB with these sequences was not specifically tested. Overall, these data suggest that PfNF-YB may represent an anti-malarial candidate, which would specifically act on the schizont stage (Lima et al., 2017).

Manna et al. (2019) identified all three NF-Y subunits in *E. invadens* (EiNF-Y) and found that it regulates stage conversion. While divergent from human homologs, all three subunits exhibited conservation in domains necessary for DNA-binding and subunit interactions. For example, human NF-YC specifically interacts with TBP and this region was conserved in the *Entamoeba* counterpart. However, *E. invadens* NF-YC also contained a unique N-terminal sequence. Expression analyses revealed EiNF-YA was constitutively expressed in trophozoites and cysts, while NF-YB and NF-YC were only expressed during encystation. Both EiNF-YA and EiNF-YC bound the CCAAT consensus motif and were localized to cyst nuclei. Importantly, when expression of EiNF-YC was knocked down, encystation efficiency was decreased. Reduction of

EiNF-YC expression did not alter the level of NF-YA protein, but instead caused mislocalization of NF-YA. Thus, correct localization of EiNF-YA seems to depend on EiNF-YC (Manna et al., 2019). A search of AmoebaDB (www.amoebadb.org) reveals that the human pathogen, *E. histolytica*, also possesses all three subunits (NF-YA: EHI_054140, NF-YB: EHI_168220, NF-YC:EHI_076830), which seem to be equally expressed in both trophozoites and cysts. Thus, *E. histolytica* NF-Y is likely to play an important role in transcription throughout the entire life cycle of this parasite, making it an attractive drug target.

Positive Cofactor 4 (PC4)

A homolog of PC4 was identified in *E. histolytica* (EhPC4) (de la Cruz et al., 2016). EhPC4 contains a conserved DNA-binding domain and is predicted to fold into a tertiary structure containing four β-sheets and one α-helix, which is similar to the human ortholog. Overexpression of wild type EhPC4 led to a significant increase in cell proliferation and DNA replication, without a decrease in viability. de la Cruz et al. (2016) also found that EhPC4-overexpressing cells contained multiple giant nuclei and only 10% of the mutant cells completed cytokinesis compared to 80% of control cells. Transcriptomic analysis revealed that 328 genes were significantly modulated in the transgenic cells; these genes were predicted to be involved in cellular processes such as metabolism, cell division, and signal transduction. A previous study (de la Cruz et al., 2014) demonstrated that EhPC4 facilitated parasite migration and destruction of colonic epithelium. Taken together, these two studies suggest that this TF may be vital for parasite viability and virulence, and ultimately, may represent a valuable drug target.

Transcription factor II F (TFIIF)

Srivastava et al. (2018) identified two TFIIF-like RNA Pol II-binding proteins in *T. brucei*, named TFL1 and TFL2 (TFIIF-like). These two proteins shared little sequence similarity with other

known TFIIF proteins. Modeling determined that these proteins contain a winged helix domain, like that of mammalian TFIIF, and conditional silencing of either TFL1 or TFL2 halted cell growth after 48 hours of induction. The authors also showed TFL1 and TFL2 are localized to the nucleus and interact with each other to form a heteromeric TFL complex.

Trypanosome genomes contain arrays of tandemly linked genes that are transcribed polycistronically by RNA Pol II. Pre-mRNAs are modified by *trans* splicing of a spliced leader RNA (SLRNA) and polyadenylation. TFL1 or TFL2 silencing reduced SLRNA transcription *in vitro*, SLRNA abundance *in vivo,* and the formation of the preinitiation complex at SLRNA promoters *in vivo* (Srivastava et al.*,* 2018). Thus, it is conceivable that blocking TFL complex-DNA interactions (Figure 4.1, Strategy B), or blocking TFL1-TFL2 interactions (Figure 4.1, Strategy C) may serve to counter trypanosomiasis.

VI. RNA Polymerase I Cofactors

RNA polymerase I (RNA Pol I) is responsible for transcribing all the rRNA genes except 5S rRNA, which is synthesized by RNA Pol III (see above). It accounts for over 50% of the total RNA synthesized in a cell (Russel and Zomerdijk, 2006). Three initial steps are critical for pre-rRNA synthesis (reviewed in Jin and Wou, 2016). First, an upstream binding factor (UBF) adheres to the promoters of rDNA, which triggers the subsequent recruitment of SL-1, also known as TIF-1B. Second, RNA Pol I, connected to TIF-1A, binds to the UBF/SL-1 complex. Finally, TIF-1A facilitates the interaction between RNA Pol I and SL-1, forming the pre-initiation complex (Figure 4.2C.). The phosphorylation status of TIF-1A determines its ability to interact with the transcription machinery.

Transcription Initiation Factor IA (TIF-1A)

TIF-1A, which is essential to RNA Pol I function, has been described in *E. histolytica* (Srivastava et al., 2016) and *A. castellani* (Gogain and Paule, 2005). Both EhTIF-1A and AcTIF-

1A were shown to bind RNA Pol I. EhTIF-1A has the expected nucleolar localization and, phosphorylation of AcTIF-1A regulates its function. Together, these studies support the authenticity of TIF-1A homologs and the conservation of the rRNA transcription machinery in these parasites (Gogain and Paule, 2005; Srivastava et al., 2016). While some RNA pol I subunits have been identified in *T. brucei (*Srivastava et al., 2016*)*, TIF-IA has yet to be identified in this parasite.

VIII.   Modulation of Host Transcription

Hijacking host cells and controlling the immune response ensures parasite survival. To achieve this, several parasites possess transcriptional modulators that alter host transcription. Accordingly, this is another way in which transcription may be targeted for anti-parasitic therapy.

Manipulation of host NF-κB

NF-κB is a family of conserved dimeric TFs that include such subunits as p65, Rel B, c-Rel, p50, or p52. NF-κB can exist as different forms including transcription-activating (e.g., p65-p50) or transcription-repressing (e.g., p50-50) dimers. Inactive NF- κB exists as a dimer in the cytoplasm bound to IκB. Stress from such stimuli as free radicals, pathogens, or UV radiation, results in phosphorylation of IκB, which causes the release of the NF-κB dimer. NF- κB subsequently moves to the nucleus, where it binds to promoters and affects the transcription of genes associated with immunity, cellular growth, and apoptosis. NF-κB is also important in controlling parasitic infections since it also controls the production of nitric oxide (NO) by macrophages (Calegari-Silva et al., 2018; Kumar et al., 2018).

Leishmania amazonensis is the causative agent of cutaneous and diffuse cutaneous leishmaniasis. After invasion of macrophages, the parasite can induce IFN1-β expression and inhibit NO production in the host cell via suppression of NF-κB. *L. amazonensis* also induces expression of superoxide dismutase (SOD-1), which favors parasite growth, by protecting it from

oxidative stress. Dias-Teixeira et al., (2016) discovered that endoplasmic reticulum (ER) stress makes macrophages more susceptible to *L. amazonensis* infection through the activation of the host TF, X-box binding protein-1 (XBP-1).

In mammalian cells, the integrated ER stress response consists of 3 signaling pathways that work to restore cell homeostasis during stress. These include the transcription factor, ATF-6, the ER-resident transmembrane nuclease, IRE1, and a PKR-like ER kinase (PERK). Once activated by ER stress, IRE1 splices an intron from cytoplasmic XBP-1-encoding mRNA, which is subsequently translated to produce active XBP-1. Active XBP-1 translocates to the nucleus and induces the expression of inflammatory molecules such as IL-6, IL-1β, and IFN-1β (Dias-Teixeira et al., 2016). Macrophages that were treated with thapsagargin, an inducer of ER stress, exhibited increased *L. amazonensis* burden compared to untreated control cells.

qPCR showed *L. amazonensis* infection induces expression and nuclear translocation of host XBP-1 and chromatin immunoprecipitation (ChIP) demonstrated that XBP-1 binds to the promoter of IFB1-β. When expression of XBP-1 was knocked down in macrophages, intracellular levels of NO were significantly increased, and *L. amazonensis* infection was significantly reduced. Furthermore, when XBP-1 knockdown cells were treated with an antioxidant, parasite growth was significantly increased. Taken together, these data indicate that infection of macrophages with *L. amazonensis* activates host cell XBP-1, which plays a critical role in infection by increasing host IFB1-β expression and by protecting the parasites from oxidative stress (Dias-Teixeira et al., 2016). However, the mechanism by which *L. amazonensis* activates XBP-1 remains unclear.

Another research group demonstrated that *L. amazonensis* suppresses NO production via another mechanism, namely upregulation of histone deacetylase-1 (HDAC-1) (Calegari-Silva et al., 2018). Changes in gene expression can occur post-translationally by modification of

histones. NF-κB subunits are known to interact with histone acetylases (HATs) and HDACs, which in turn modify local histones leading to alterations in gene expression. Previous studies have shown that NF-κB recruits HDAC-1 to repress expression of pro-inflammatory genes (Williams et al., 2006; Elsharkawy et al., 2010; and Collins et al., 2014) Calegari-Silva et al. (2018) found *L. amazonensis* infection induces upregulation of macrophage HDAC-1 expression in cell culture and in human clinical samples. Furthermore, the authors showed that HDAC-1 is recruited to the iNOS promoter, forms a complex with NF- κB, and ultimately represses macrophage production of NO, which, in turn, increases parasite survival. Additionally, Calegari-Silva et al. (2018) silenced HDAC-1 in host macrophages prior to infection with *L. amazonensis* and observed decreased parasite load, compared to controls. The mechanism by which *L. amazonensis* upregulates HDAC-1 in host cells is unclear.

L. donovani, the causative agent of visceral leishmaniasis, also affects host NF-κB. During infection of host cells, the parasite activates host hypoxia inducible factor-1α (HIF-1α), a hypoxia-induced TF, and induces a 2.8-fold increase in host microRNA (miRNA), miR-210. This ultimately downregulates host NF-κB activity (Kumar et al*., 2018).   Silencing of HIF-1α in macrophages and subsequent infection with *L. donovani* led to a significant decrease of miRNA-210 expression, suggesting that miRNA-210 expression is HIF-1α-dependent. Parasite infectivity and parasite load were also significantly decreased in HIF-1α-silenced and miRNA-silenced macrophages compared to control macrophages, suggesting these effectors are critical for parasite survival (Kumar et al., 2018).

Importantly, miRNA-210 appeared to be a negative regulator of NF-κB activation. The level of NF-κB p50-p65 dimer was equivalent in both the cytoplasm and nucleus of macrophages before and after *L. donovani* infection. However, in miRNA-210-silenced cells, *L. donovani* infection induced the translocation of p50-p65 into the nucleus.   Additionally, proinflammatory

cytokines were significantly increased and anti-inflammatory cytokines were significantly decreased in infected miRNA-210-silenced macrophages compared to infected control macrophages. Oxidative and nitrosative species were also increased in infected miRNA-210-silenced macrophages compared to infected control macrophages. Taken together, these data imply that *L. donovani* infection induces expression of HIF-1α in host macrophages via an unknown mechanism, which induces expression of miRNA-210, and subsequently inhibits activation of NF-κB and the production of pro-inflammatory cytokines. Ultimately, this allows *L. donovani* to survive and successfully establish infection (Kumar et al., 2018).

T. gondii is also able to manipulate host NF-κB controlled genes by releasing effectors. There are two types of *T. gondii* secreted effectors, those secreted from the apical rhoptry organelle (ROP proteins) and those secreted from dense granules (GRA proteins). Both types of effectors rewire host gene expression to promote parasite survival (Braun et al., 2019). One such GRA is TEEGR (*Toxoplasma* E2F4 associated EZH2 inducing Gene Regulator) (Braun et al., 2019). Host cells infected with a knockout (Δteegr) strain of *T. gondii* exhibited upregulation of 784 genes (human fibroblasts, HFFs) or 1529 genes (human astrocytes) when compared to host cells infected with the wildtype strain. Once exported into the host cell, TEEGR localizes to the host nucleus, forms a complex with host E2F3 and E2F4 TFs, and upregulates E2F4- and E2F3-dependent gene expression. One such upregulated host gene, EZH2, is a subunit of Polycomb repressive complex 2, which mediates epigenetic silencing of host gene expression. Once expressed, EZH2 represses transcription of a subset of NF-κB-regulated cytokines, thereby strongly contributing to the host immune response and promoting parasite persistence in mice (Braun et al., 2019).

G. intestinalis is another pathogen that can modulate host NF-kB signaling to avoid the host inflammatory response. It is well-established that NF-κB regulates transcription of

inflammatory genes, such as nitric oxide synthase (NOS) and cyclooxygenase 2 (COX-2) during infection (Faria et al., 2020). *G. intestinalis* may counter the inflammatory response through the action of proteases (Faria et al., 2020). Macrophages were exposed to *Giardia* and then to lipopolysaccharide (LPS), a component of gram-negative bacterial cell walls, which induces an NF-kB-mediated inflammatory response. Pretreatment with *Giardia* led to a diminished LPS-induced production of NOS and COX-2. The effect seemed to be mediated by *Giardia*-induced proteolytic cleavage of the NF-kB subunit, p65, because protease inhibitors nullified the effect. Furthermore, the effect seemed to be contact-mediated since it was diminished when *Giardia* trophozoites were prevented from directly interacting with the macrophages using a transwell co-culture system. Since *Giardia* is an extracellular pathogen, the authors posited that *Giardia* proteases were likely delivered to the host cell by extracellular vesicles (Faria et al., 2020). Thus, *Giardia* may modulate the host inflammatory response by inhibiting NF-κB, which, in turn, would inhibit important signaling pathways of the host innate immune response.

Manipulation of host c-Myc

c-Myc is a eukaryotic TF that regulates many genes involved in cell growth and cell cycle progression and is activated by mitogenic signals such as serum starvation or epidermal growth factor (Dominguez-Sola et al, 2007; Miller et al., 2012). *L. donovani* can enhance its own survival by upregulating host c-Myc expression, which subsequently represses host miRNA expression (Colineau et al., 2018). Colineau and colleagues (2018) infected human monocyte-derived macrophages with *L. donovani* and measured miRNA expression. Forty-six total miRNAs were detected in infected cells and 19 of these were significantly downregulated compared to those in uninfected macrophages. Dicer and Drosha are miRNA processing proteins (Li and Patel, 2016). Expression of Drosha was upregulated at 48 hours post *L. donovani* infection (Colineau et al., 2018). Reduced expression of the 19 miRNAs depended on host c-Myc, since c-Myc silencing or pharmacological inhibition of c-Myc reversed the phenotype. c-Myc silencing also reduced

intracellular survival of *L. donovani*, demonstrating that c-Myc is essential for parasite pathogenesis. How c-Myc is upregulated by *L. donovani* remains elusive. However, given the plethora of genes regulated by c-Myc, *L. donovani* could modulate the expression of many host genes to its advantage (Colineau et al., 2018).

Manipulation of other host pathways

While in the human bloodstream, *T. brucei* parasites import high levels of host tryptophan and phenylalanine, which are required for many cellular functions including energy production, cell cycle progression, cell bioenergetics, and differentiation (Marchese et al., 2018). McGettrick and colleagues (2016) showed that once imported into the parasites, amino acids are metabolized by transamination. A byproduct of this transamination is the aromatic ketoacid, indolepyruvate. *T. brucei* excretes high levels of this ketoacid into the host bloodstream. Indolepyruvate inhibits host HIF-1α, decreasing expression of IL-1β, allowing the parasite to evade immune clearance (McGettrick et al., 2016). Transamination is facilitated by the *T. brucei* cytoplasmic aspartate aminotransferase, TbcASAT. RNAi-based silencing of TbcASAT expression resulted in a decrease in aromatic ketoacid secretion and reduced growth of the parasite. This further supports the role of ketoacids in manipulation of host transcription and parasite virulence.

In addition to using metabolites to affect host transcription, parasites can also use RNA. *C. parvum* is an intracellular parasite that invades host intestinal epithelial cells. At the onset of infection, epithelial cells release chemokines, which recruit immune cells. These immune cells release NO and antimicrobial peptides, such as DEFB1, which can kill the parasite or inhibit parasite growth. Ming and colleagues (2018) found that delivery of the parasite RNA, Cdg7_FLc_1000, to the host nucleus, downregulates DEFB1 gene expression in host cells. Transgenic host cells expressing Cdg7_FLc_1000 or *C. parvum*-infected cells exhibited

decreased levels of DEFB1, compared to untransfected or uninfected cells. Treating host cells with Cdg7_FLc_1000 siRNAs, prior to *C. parvum* infection, reversed the effect on DEFB1 expression. Furthermore, parasite burden was decreased in cells where expression of Cdg7_FLc_1000 was reduced. Overall, the data show that Cdg7_FLc_1000 is an important secreted effector of *C. parvum* that may serve as a target for anti-cryptosporidiosis therapy (Ming et al., 2018).

Another RNA delivered into host cell nuclei by *C. parvum* is Cdg2_FLc_0220. Zhao and colleagues (2018) found that 46 host genes were upregulated, and 8 host genes were downregulated in parasite-infected human intestinal epithelium (INT) cells. Similar changes in gene expression were seen when Cdg2_FLc_0220 was exogenously expressed in INT cells. The upregulated gene set included interleukins, their receptors, and inflammatory response mediators. DAZ-interacting zinc finger protein 1 (DZIP1) was the most significantly downregulated host gene. Not much is known about the function of DZIP1L, but it has been shown to localize to centrioles and interact with septin2, a protein implicated in cytoskeleton function. To clarify the mechanism by which *C. parvum* uses Cdg2_FLc_0220 to suppress host gene expression, Zhao et al. (2018) measured G9a enrichment near the DZIP1L gene locus. G9a is a histone methyltransferase that mediates transcriptional repression of human genes and has previously been implicated in *C. parvum* suppression of host gene expression (Artal-Martinez de Narvajas et al., 2013; Tong et al., 2013; Fan et al., 2015). G9a was enriched near the DZIP1L gene. Silencing of G9a in host cells reduced the effect of infection on DZIP1L expression. Lastly, pull down assays showed that Cdg2_FLc_0220 physically associates with G9a. These data suggest that parasite suppression of host DZIP1L is dependent on delivery of Cdg2_FLc_0220 and its interaction with host G9a.

IX.   Concluding Remarks and Future Perspectives

In this review, we have highlighted a number of TFs that regulate parasite transcription and we have described mechanisms by which parasites regulate host transcription (Table 4.1). Additional TFs and transcriptional modulators, not discussed here, have been reviewed elsewhere (Tables 4.2, 4.3). The idea of targeting transcription and TFs for drug therapy was long considered a "Sysyphean task" (Papavassiliou and Papavassiliou, 2016). However, recent methodological advances have revealed that TFs are, indeed, targetable. Thus, the TFs and transcriptional modulators of protozoan parasites represent attractive drug targets as they are vital in parasitic virulence. The empirical and modelling data discussed within this review (and summarized in Table 4.4) support the idea that targeting these TFs and transcriptional modulators may be a viable treatment approach.

Many components of the transcription machinery described in this review have already been explored as targets for drug design in other systems (Figure 4.1). For example, inhibition of human NF-κB has been explored for the treatment of osteoarthritis (reviewed Rigoglou and Papavassiliou, 2013). Additionally, the guanine alkylating anti-neoplastic drug, pluramycin (Lambert et al., 2018), and the kinase inhibitors, Hypericin, Rottlerin, and SP600125 (Schug, 2011), have been used to inhibit TBP. Ecteinascidin 743 (Et743; trabectedin, Yondelis), a DNA minor groove alkylating drug, has been used to block NF-Y DNA binding (Lambert et al., 2018) and triptolide, a plant-derived natural product, blocks assembly of TFIIIB (Liang et al., 2019). Vorinostat, an HDAC inhibitor, could be used to control overexpression of c-Myc in T-cell acute lymphoblastic leukemia (Lambert et al., 2018). Lastly, the small molecule, AG-1031 inhibits PC4 (Zhang et al., 2020). Given that parasites are eukaryotes, many of the TFs described in this review are, to some extent, homologous to those in the human host (Table 4.4). Therefore, it is conceivable that existing TF-targeting drugs may be re-purposed for the treatment of parasitic infections.

A common and important readout in drug screens is inhibition of parasite growth. However, it is easy to envision high throughput screens that specifically target certain cellular functions. For instance, Ahyong and colleagues (2016) used the MMV Malaria box to screen for drugs that inhibit translation in *P. falciparum* (Ahyong et al., 2016). Perhaps similar high throughput approaches may be used to screen small molecule libraries to find drugs that interrupt TF-DNA or TF-cofactor binding. Indeed, such a high throughput screen was used to identify drugs that inhibit the interaction between the human TF, ERG, and its cofactor, EWS (Nicholas et al., 2020). Computer modeling, such as that done for *E. histolytica* and *P. falciparum* TBP (Santiago et al., 2019), will accelerate such high throughput approaches.

That parasites are eukaryotes also complicates drug discovery because it is necessary that drugs maximally inhibit the parasite, while minimally affecting the host. Therefore, it is imperative that state-of-the-art technology be used to identify novel domains, functions, and structural features in conserved parasite TFs or evolutionarily divergent TFs. We highlighted several TFs (e.g., EhTBP, PfNF-Y, TgBFD1, TbMAF1) that were homologous to host TFs, but nevertheless, possessed unique regions or unique functions. An example of an evolutionary divergent class of TFs are the AP2 TFs. These are found in apicomplexan parasites and are so named because they contain a Apetala2 DNA binding domain (Jeninga, et al., 2019). While weakly similar proteins have been identified in plants, homologs do not exist in the human host. Apicomplexan AP2 TFs can either bind DNA promoters directly or bind and influence chromatin modifiers. The *T. gondii* genome contains 67 AP2 TFs, *P. falciparum* contains 27, and *Cryptosporidium spp*. possess 17. These TFs control vital processes within these pathogenic parasites and their unique DNA binding domains make them an attractive drug target as they are not found within the human host. AP2 TFs have recently been reviewed in detail (Jeninga et al., 2019). Therefore, they are not further discussed in this review.

It is notable that there was a scarcity of recent studies on TFs or effectors from *Naegleria fowleri*, *Balamuthia mandrillaris*, or *Acanthamoeba castellani*. While infections with these amoebae are rare, incidence is increasing (Mungroo et al., 2019), as a result of escalation of global temperatures and an increase in warm water reservoirs. These parasitic amoeba cause devasting and mostly fatal (90%) brain infections (Mungroo et al., 2019). Therefore, the lack of data on a potential drug target, namely TFs, is alarming and represents a significant gap in knowledge.

Since targeting TFs is a novel treatment approach for parasitic infections, three-dimensional modeling, and tests for small molecule binding (summarized in Table 4.4), have yet to be conducted for most parasite TFs. Thus, this field of research is wide-open and should yield new and interesting drug targets. As the information about TFs and other transcriptional effectors grows, especially for those that regulate virulence, their value as drug targets should become more evident. To maximize the discovery of drugs for any potential target, it will be necessary to identify DNA-binding pockets (if applicable), target DNA sequences (if applicable), cofactors, and the relationship between structure and function. Such knowledge will drive the development of novel anti-parasitic agents that are so desperately needed today.

X.   Acknowledgments

XI.   References

Ahyong, V., Sheridan, C. M., Leon, K. E., Witchley, J. N., Diep, J., & Derisi, J. L. (2016). Identification of *Plasmodium falciparum* specific translation inhibitors from the MMV Malaria Box using a high throughput *in vitro* translation screen. Malar J. 15, 173.

Akimoto, Y., Yamamoto, S., Iida, S., Hirose, Y., Tanaka, A., Hanaoka, F., & Ohkuma, Y. (2014). Transcription cofactor PC4 plays essential roles in collaboration with the small subunit of general transcription factor TFIIE. Genes to Cells. 19(12), 879–890.

Akkaya, M., Bansal, A., Sheehan, P. W., Pena, M., Molina-Cruz, A., Orchard, L. M., Cimperman, C. K., Qi, C. F., Ross, P., Yazew, T., Sturdevant, D., Anzick, S. L., Thiruvengadam, G., Otto, T. D., Billker, O., Llinás, M., Miller, L. H., & Pierce, S. K. (2020). A single-nucleotide polymorphism in a *Plasmodium berghei* ApiAP2 transcription factor alters the development of host immunity. Sci. Adv. 6(6), 1–14.

Artal-Martinez de Narvajas, A., Gomez, T. S., Zhang, J.-S., Mann, A. O., Taoda, Y., Gorman, J. A., Herreros-Villanueva, M., Gress, T. M., Ellenrieder, V., Bujanda, L., Kim, D.-H., Kozikowski, A. P. Koenig, A., & Billadeau, D. D. (2013). Epigenetic Regulation of Autophagy by the Methyltransferase G9a. Mol. Cell. Biol. 33(20), 3983–3993.

Avendaño-Borromeo, B., Narayanasamy, R. K., García-Rivera, G., Labra-Barrios, M. L., Lagunes-Guillén, A. E., Munguía-Chávez, B., Castañón-Sánchez, C. A., Orozco, E., & Luna-Arias, J. P. (2019). Identification of the gene encoding the TATA box-binding protein-associated factor 1 (TAF1) and its putative role in the heat shock response in the protozoan parasite *Entamoeba histolytica*. J. Parasitol. Res. 118(2), 517–538.

Best, A. A., Morrison, H. G., McArthur, A. G., Sogin, M. L., & Olsen, G. J. (2004). Evolution of eukaryotic transcription: Insights from the genome of *Giardia lamblia*. Genome Res. 14(8), 1537–1547.

Bing, X., Gerlach, J., Loeb, G., & Buchon, N. (2018). *Toxoplasma gondii* AP2IX-4 regulates gene expression during bradyozoite development. mSphere 2(2), 1–18.

Braun, L., Brenier-Pinchart, M. P., Hammoudi, P. M., Cannella, D., Kieffer-Jaquinod, S., Vollaire, J., Josserand, V., Touquet, B., Couté, Y., Tardieux, I., Bougdour, A., & Hakimi, M. A. (2019). The *Toxoplasma* effector TEEGR promotes parasite persistence by modulating NF-κB signaling via EZH2. Nat. Microbiol. 4(7), 1208–1220.

Burger K., Muhl B., Harasim T., Rohrmoser M., Malamoussi A., Orban M., Kellner M., Gruber-Eber A., Kremmer E., Holzel M., Eick D. Chemotherapeutic drugs inhibit ribosome biogenesis at various levels. J. Biol. Chem. 285 (16), 12416–12425.

Burgess, S. L., Gilchrist, C.A., Lynn, T.C., and Petri, W. A. 2017. Parasitic Protozoa and Interactions with the Host Intestinal Microbiota. Infect. Immun. 85 (8), 1-12.

Calegari-Silva, T. C., Vivarini, Á. C., Pereira, R. de M. S., Dias-Teixeira, K. L., Rath, C. T., Pacheco, A. S. S., Silva, G. B. L., Pinto, C. A. S., dos Santos, J. V., Saliba, A. M., Corbett, C. E. P., de Castro Gomes, C. M., Fasel, N., & Lopes, U. G. (2018). *Leishmania amazonensis* downregulates macrophage iNOS expression via Histone Deacetylase 1 (HDAC1): a novel parasite evasion mechanism. Eur. J. Immun. 48(7), 1188–1198.

Cannon, M. V., Bogale, H., Rutt, L., Humphrys, M., Korpe, P., Duggal, P., Ravel, J., & Serre, D. (2018). A high-throughput sequencing assay to comprehensively detect and characterize

unicellular eukaryotes and helminths from biological and environmental samples. Microbiome 6(1), 1–11.

Carpio, A., Romo, M. L., Parkhouse, R. M. E., Short, B., & Dua, T. (2016). Parasitic diseases of the central nervous system: Lessons for clinicians and policy makers. Expert Rev. Neurother. 16(4), 401–414.

Chen, J., Lobb, I. T., Morin, P., Novo, S. M., Simpson, J., Kennerknecht, K., Von Kriegsheim, A., Batchelor, E. E., Oakley, F., & Stark, L. A. (2018). Identification of a novel TIF-IA-NF-κB nucleolar stress response pathway. Nucleic Acids Res. 46(12), 6188–6205.

Chen, L., Christian, D. A., Kochanowsky, J. A., Phan, A. T., Clark, J. T., Wang, S., Berry, C., Oh, J., Chen, X., Roos, D. S., Beiting, D. P., Koshy, A. A., & Hunter, C. A. (2020). The *Toxoplasma gondii* virulence factor ROP16 acts in cis and trans and suppresses T cell responses. J. Exp. Med. 217(3), 1-16.

Chen, L., Peng, Z., & Bateman, E. (2004). In vivo interactions of the *Acanthamoeba* TBP gene promoter. Nucleic Acids Res. 32(4), 1251–1260.

Chu, C. H., Huang, Y. H., Liu, H. W., Hsu, H. M., & Tai, J. H. (2018). Membrane localization of a Myb3 transcription factor regulated by a TvCyP1 cyclophilin in the parasitic protozoan *Trichomonas vaginalis*. FEBS J. 285(5), 929–946.

Colineau, L., Lambertz, U., Fornes, O., Wasserman, W. W., & Reiner, N. E. (2018). c-Myc is a novel *Leishmania* virulence factor by proxy that targets the host miRNA system and is essential for survival in human macrophages. J. Biol. Chem. 293(33), 12805–12819.

Collins, P. E., Kiely, P. A. and Carmody, J. R., Inhibition of transcription by B cell leukemia 3 (Bcl-3) protein requires interaction with nuclear factor κB (NF-κB) p50. J. Biol. Chem. 2014. 289: 7059–7067.

de la Cruz, O. H., Marchat, L. A., Guillén, N., Weber, C., Rosas, I. L., DÍaz-Chávez, J., Herrera, L., Rojo-Domínguez, A., Orozco, E., & López-Camarillo, C. (2016). Multinucleation and Polykaryon Formation is Promoted by the EhPC4 Transcription Factor in *Entamoeba histolytica*. Sci. Rep. 6 (2015), 1–12.

de la Cruz, O. H., Muñiz-Lino, M., Guillén, N., Weber, C., Marchat, L. A., López-Rosas, I., Ruíz-García, E., Astudillo-de la Vega, H., Fuentes-Mera, L., Álvarez-Sánchez, E., Mendoza-Hernández, G., & López-Camarillo, C. (2014). Proteomic profiling reveals that EhPC4 transcription factor induces cell migration through up-regulation of the 16-kDa actin-binding protein EhABP16 in *Entamoeba histolytica*. J. Proteomics 111, 46–58.

Devlin, J.R., Hannan, K.M., Hein, N., Cullinane, C., Kusnadi, E., Ng, P.Y., George, A.J., Short, J., Bywater, M.J., Poortinga, G., Sanij, E., Kang, J., Drygin, D., O'Brien, S., Johnstone, R.W., McArthur G.A., Hannan, R.D., Pearson, R.B. Combination Therapy Targeting Ribosome Biogenesis and mRNA Translation Synergistically Extends Survival in MYC-Driven Lymphoma. Cancer Discov. 2016; 6, 59–70.

Dias-Teixeira, K. L., Calegari-Silva, T. C., Dos Santos, G. R. R. M., Dos Santos, J. V., Lima, C., Medina, J. M., Aktas, B. H., & Lopes, U. G. (2016). The integrated endoplasmic reticulum stress response in *Leishmania amazonensis* macrophage infection: The role of X-box binding protein 1 transcription factor. FASEB J. 30(4), 1557–1565.

Dominguez-Sola, D., Ying, C. Y., Grandori, C., Ruggiero, L., Chen, B., Li, M., Galloway, D. A., Gu, W., Gautier, J., & Dalla-Favera, R. (2007). Non-transcriptional control of DNA replication by c-Myc. Nature 448(7152), 445–451.

Ehrenkaufer, G. M., Hackney, J. A., & Singh, U. (2009). A developmentally regulated Myb domain protein regulates expression of a subset of stage-specific genes in *Entamoeba histolytica*. Cell. Microbiol. 11(6), 898–910.

Elsharkawy, A. M., Oakley, F., Lin, F., Packham, G., Mann, D. A. and Mann, J. (2010).The NF-κB p50:p50: HDAC-1 repressor complex orchestrates transcriptional inhibition of multiple pro-inflammatory genes. J. Hepatol. 53, 519–527

Fan, J., Xing, Y., Wen, X., Jia, R., Ni, H., He, J., Ding, X., Pan, H., Qian, G., Ge, S., Hoffman, A. R., Zhang, H., & Fan, X. (2015). Long non-coding RNA ROR decoys gene-specific histone methylation to promote tumorigenesis. Genome Biol. 16(1), 1–17.

Faria, C. P., Neves, B. M., Lourenço, Á., Cruz, M. T., Martins, J. D., Silva, A., Pereira, S., & Sousa, M. (2020). *Giardia lamblia* Decreases NF-κB p65RelA Protein Levels and Modulates LPS-Induced Pro-Inflammatory Response in Macrophages. Sci. Rep. 10(1), 1–17.

Ferrari, R., Rivetti, C., Acker, J., & Dieci, G. (2004). Distinct roles of transcription factors TFIIIB and TFIIIC in RNA polymerase III transcription preinitiation. PNAS. 101(37), 13442–13447.

Franco, M., Panas, M. W., Marino, N. D., Lee, M. W., Buchholz, K. R., Kelly, F. D., Bednarski, J. J., Sleckman, B. P., Pourmand, N., & Boothroyd, C. (2016). A Novel Secreted Protein, MYR1, Is Central to *Toxoplasma's* Manipulation of Host Cells. MBio. 7(1), 1–16.

Ghoshal, K., Jacob, S.T. (1997). An alternative molecular mechanism of action of 5-fluorouracil, a potent anticancer drug. Biochem. Pharmacol. 53, 1569–1575.

Gissot M, Briquet S, Refour P, Boschet C, Vaquero C. PfMyb1, a *Plasmodium falciparum* transcription factor, is required for intra-erythrocytic growth and controls key genes for cell cycle regulation. J. Mol. Biol. 346(1), 29-42.

Gunther, J., Shafir, S., Bristow, B., & Sorvillo, F. (2011). Short report: Amebiasis-related mortality among United States residents, 1990-2007. Am. J. Trop. Med. Hyg. 85(6), 1038–1040.

Hakimi, M., Olias, P., & Sibley, L. (2017). *Toxoplasma* Effectors Targeting Host Signaling and Transcription. Clin. Microbiol. Rev. 30(3), 615–645.

Han, Y., & He, Y. (2016). Eukaryotic transcription initiation machinery visualized at molecular level. Transcription. 7(5), 203–208.

Hong, D.P., Radke, J. B., & White, M. W. (2017). Opposing Transcriptional Mechanisms Regulate *Toxoplasma* Development. mSphere 2(1), 1–15.

Huang, B. (2009). Metapocket: A meta approach to improve protein ligand binding site prediction. OMICS 13(4), 325–330.

Ibrahim, B. S., Kanneganti, N., Rieckhof, G. E., Das, A., Laurents, D. V., Palenchar, J. B., Bellofatto, V., & Wah, D. A. (2009). Structure of the C-terminal domain of transcription factor IIB from *Trypanosoma brucei*. Proc. Natl. Acad. Sci. USA 106(32), 13242–13247.

Ivens, A. C., Peacock, C. S., Worthey, E. A., Murphy, L., Aggarwal, G., Berriman, M., Sisk, E., Rajandream, M. A., Adlem, E., Aert, R., Anupama, A., Apostolou, Z., Attipoe, P., Bason,

N., Bauser, C., Beck, A., Beverley, S. M., Bianchettin, G., Borzym, K., Myler, P. J. (2005). The genome of the kinetoplastid parasite, *Leishmania major*. Science 309(5733), 436–442.

Jeninga, M. D., Quinn, J. E., & Petter, M. (2019). Apiap2 transcription factors in apicomplexan parasites. Pathogens 8(2), 1–24.

Jin, R., & Zhou, W. (2017). TIF-IA: an oncogenic target of pre-ribosomal RNA synthesis. Biochim. Biophys. Acta. 176(12), 139–148.

Josling, G. A., Williamson, K. C., & Llinás, M. (2018). Regulation of Sexual Commitment and Gametocytogenesis in Malaria Parasites. Annu. Rev. Microbiol. 72(1), 501–519.

Kerry, L. E., Pegg, E. E., Cameron, D. P., Budzak, J., Poortinga, G., Hannan, K. M., Hannan, R. D., & Rudenko, G. (2017). Selective inhibition of RNA polymerase I transcription as a potential approach to treat African trypanosomiasis. PLoS Negl.Trop. Dis. 11(3), 1–24.

Kim, J. L., Nikolov, D. B., & Burley, S. K. (1993). Co-crystal structure of TBP recognizing the minor groove of a TATA element. Nature 365(6446), 520–527.

Kumar, V., Kumar, A., Das, S., Kumar, A., Abhishek, K., Verma, S., Mandal, A., Singh, R. K., & Das, P. (2018). *Leishmania donovani* activates hypoxia inducible factor-1α and miR-210 for survival in macrophages by downregulation of NF-κB mediated pro-inflammatory immune response. Front. Microbiol. 9(385) 1–14.

Lambert, M., Jambon, S., Depauw, S., & David-Cordonnier, M. H. (2018). Targeting transcription factors for cancer treatment. Molecules 23(6), 1479.

Li, S., & Patel, D. J. (2016). Drosha and Dicer: Slicers cut from the same cloth. Cell Res. 26(5), 511–512.

Liang, X., Xie, R., Su, J., Ye, B., Wei, S., Liang, Z., Bai, R., Chen, Z., Li, Z., & Gao, X. (2019). Inhibition of RNA polymerase III transcription by Triptolide attenuates colorectal tumorigenesis. J. Exp. and Clin. Cancer Res. 38(1), 1–13.

Lima, W.R., Martins, D.C., Parreira, K.S. Genome-wide analysis of the human malaria parasite *Plasmodium falciparum* transcription factor PfNF-YB shows interaction with a CCAAT motif. Oncotarget 8(69), 113987–114001.

Lin, B., Su, L., Weng, S., Pan, Y., Chan, N., Li, T., Wang, H., & Sun, C. (2013). DNA Topoisomerase II Is Involved in Regulation of Cyst Wall Protein Genes and Differentiation in *Giardia lamblia*. PLoS Neg. Trop. Dis. 7(5), 1-20.

Liu, H., Yang, J., Li, L., Weimei, S., & Yuan, Xiaoliang and Wu, L. (2016). The Natural Occurring Compounds Targeting Endoplasmic Reticulum Stress. J. Altern. Complement Med. 2016(4), 333–335.

López-Camarillo, C., López-Rosas, I., Ospina-Villa, J. D., & Marchat, L. A. (2014). Deciphering molecular mechanisms of mRNA metabolism in the deep-branching eukaryote *Entamoeba histolytica*. Wiley Interdiscip. Rev. RNA 5(2), 247–262.

Mahajan, P.B. (1994). Modulation of transcription of rRNA genes by rapamycin. Int. J. Immunopharmacol. 16, 711–721.

Manna, D., Lentz, C.S., Ehrenkaufer, G.M., Suresh, S. , Bhat, A., Singh, U. An NAD + -dependent novel transcription factor controls stage conversion in *Entamoeba*, Elife 7 (2018) 1–22.

Manna, D., & Singh, U. (2019). Nuclear Factor Y (NF-Y) Modulates Encystation in *Entamoeba*. MBio 10(3), 1–13.

Marchese, L., Nascimento, J., Damasceno, F. S., Bringuad, F., Michels, P., & Silber, A. (2018). The Uptake and Metabolism of Amino Acids, and Their Unique Role in the Biology of Pathogenic Trypanosomatids. Pathogens 7(36), 1–45.

Martins, R. M., Macpherson, C. R., Claes, A., Scheidig-Benatar, C., Sakamoto, H., Yam, X. Y., Preiser, P., Goel, S., Wahlgren, M., Sismeiro, O., Coppée, J. Y., & Scherf, A. (2017). An ApiAP2 member regulates expression of clonally variant genes of the human malaria parasite *Plasmodium falciparum*. Sci. Rep. 7(1), 1–10.

McGettrick, A. F., Corcoran, S. E., Barry, P. J. G., McFarland, J., Crès, C., Curtis, A. M., Franklin, E., Corr, S. C., Mok, K. H., Cummins, E. P., Taylor, C. T., O'Neill, L. A. J., & Nolan, D. P. (2016). *Trypanosoma brucei* metabolite indolepyruvate decreases HIF-1α and glycolysis in macrophages as a mechanism of innate immune evasion. Proc. Natl. Acad. Sci. USA 113(48), E7778–E7787.

McIlwee, B. E., Weis, S. E., & Hosler, G. A. (2018). Incidence of endemic human cutaneous leishmaniasis in the United States. JAMA Dermatol. 154(9), 1032–1039.

Menard, D., & Dondorp, A. (2017). Antimalarial drug resistance: a threat to malaria elimination. Cold Spring Harbor Perspect. Med. 7(7), 1–24.

Miller, D. M., Thomas, S. D., Islam, A., Muench, D., & Sedoris, K. (2012). c-Myc and cancer metabolism. Clin. Cancer Res. 18(20), 5546–5553.

Millership, J. J., Waghela, P., Cai, X., Cockerham, A., & Zhu, G. (2004). Differential expression and interaction of transcription co-activator MBF1 with TATA-binding protein (TBP) in the apicomplexan Cryptosporidium parvum. Microbiol. 150(5), 1207–1213.

Ming, Z., Gong, A. Y., Wang, Y., Zhang, X. T., Li, M., Dolata, C. E., & Chen, X. M. (2018). Trans-suppression of defense DEFB1 gene in intestinal epithelial cells following *Cryptosporidium parvum* infection is associated with host delivery of parasite Cdg7_FLc_1000 RNA. Parasitol. Res. 117(3), 831–840.

Mungroo, M. R., Anwar, A., Khan, N. A., & Siddiqui, R. (2019). Brain-eating Amoebae Infection: Challenges and Opportunities in Chemotherapy. Mini Rev. Med. Chem. 19(12), 980–987.

Narayanasamy, R. K., Castañón-Sanchez, C. A., Luna-Arias, J. P., García-Rivera, G., Avendaño-Borromeo, B., Labra-Barrios, M. L., Valdés, J., Herrera-Aguirre, M. E., & Orozco, E. (2018). The *Entamoeba histolytica* TBP and TRF1 transcription factors are GAAC-box binding proteins, which display differential gene expression under different stress stimuli and during the interaction with mammalian cells. Parasites Vectors 11(1), 1–16.

Nicholas, T. R., Meng, J., Greulich, B. M., Morris, T. S., & Hollenhorst, P. C. (2020). A high-throughput screen identifies inhibitors of the interaction between the oncogenic transcription factor ERG and the cofactor EWS. PLoS ONE 15(9), 1–13.

Olias, P., Etheridge, R. D., Zhang, Y., Holtzman, M. J., & Sibley, L. D. (2016). *Toxoplasma* Effector Recruits the Mi-2/NuRD Complex to Repress STAT1 Transcription and Block IFN-γ-Dependent Gene Expression. Cell Host Microbe 20(1), 72–82.

Panas, M. W., Naor, A., Cygan, A. M., & Boothroyd, J. C. (2019). *Toxoplasma* controls host cyclin E expression through the use of a novel myr1-dependent effector protein, HCE1. MBio 10(2), 1–18.

Papavassiliou, K. A., & Papavassiliou, A. G. (2016). Transcription Factor Drug Targets. J. Cell. Biochem. 117(12), 2693–2696.

Parra-Marín, O., Rosas-Hernández, L., López-Pacheco, K., Franco, B., Ibáñez-Escribano, A., Hernández, R., & López-Villaseñor, I. (2019). An in vitro characterization of the *Trichomonas vaginalis* TATA box-binding proteins (TBPs). Parasitol. Res. 118(10), 3019–3031.

Pellegrini, E., Palencia, A., Braun, L., Kapp, U., Bougdour, A., Belrhali, H., Bowler, M. W., & Hakimi, M. A. (2017). Structural Basis for the Subversion of MAP Kinase Signaling by an Intrinsically Disordered Parasite Secreted Agonist. Structure 25(1), 16–26.

Raskatov, J. A., Meier, J. L., Puckett, J. W., Yang, F., Ramakrishnan, P., & Dervan, P. B. (2012). Modulation of NF-κB-dependent gene transcription using programmable DNA minor groove binders. Proc. Natl. Acad. Sci. 109(4), 1023–1028.

Remillard, D., Buckley, D. L., Seo, H. S., Ferguson, F. M., Dhe-Paganon, S., Bradner, J. E., & Gray, N. S. (2019). Dual Inhibition of TAF1 and BET Bromodomains from the BI-2536 Kinase Inhibitor Scaffold. ACS Med. Chem. Lett. 10(10), 1443–1449.

Rigoglou, S., & Papavassiliou, A. G. (2013). The NF-κB signaling pathway in osteoarthritis. The Int. J. Biochem. Cell Biol. 45(11), 2580–2584.

Román-carraro, F.C., Florencio-mart, L.E., Romero-meza, G., Nepomuceno-mej, T., Carrero, JC., Arroyo, R., Ortega-lópez, J., Manning-cela, RG., Mart,S. (2019). TFIIIB Subunit Bdp1 Participates in RNA Polymerase III Transcription in the Protozoan Parasite *Leishmania major*. Biomed Res. Int. 2019, 1-14.

Romero-Meza, G., Vélez-Ramírez, D. E., Florencio-Martínez, L. E., Román-Carraro, F. C., Manning-Cela, R., Hernández-Rivas, R., & Martínez-Calvillo, S. (2017). Maf1 is a negative regulator of transcription in *Trypanosoma brucei*. Mol. Microbiol. 103(3), 452–468.

Russell, J., & Zomerdijk, J. C. B. M. (2006). The RNA polymerase I transcription machinery. Biochem. Soc. Symp. 73(73), 203–216.

Sampaio, N. G., Emily Marie Eriksson, & Schofielda, L. (2018). *Plasmodium falciparum* PfEMP1 Modulates Monocyte/ Macrophage Transcription Factor Activation and Cytokine and Chemokine Responses. Infect. Immun. 86(1), 1–14.

Santiago, Á., Razo-Hernández, R. S., & Pastor, N. (2019). The TATA-binding Protein DNA-binding domain of eukaryotic parasites is a potentially druggable target. Chem. Biol. Drug Des. 95(1), 130–149.

Schaap, P., & Schilde, C. (2018). Encystation: The most prevalent and under investigated differentiation pathway of eukaryotes. Microbiol. 164(5), 727–739.

Schug, T. T. (2011). Targeting transcription through inhibition of TBP. Oncotarget 2(1–2), 5–7.

Schweikhard, V., Meng, C., Murakami, K., Kaplan, C. D., Kornberg, R. D., & Block, S. M. (2014). Transcription factors TFIIF and TFIIS promote transcript elongation by RNA polymerase II by synergistic and independent mechanisms. Proc. Natl. Acad. Sci. USA 111(18), 6642–6647.

Short, E. E., Caminade, C., & Thomas, B. N. (2017). Climate Change Contribution to the Emergence or Re-Emergence of Parasitic Diseases. Infect. Dis. 10, 1-7

Sierra-Miranda, M., Vembar, S. S., Delgadillo, D. M., Ávila-López, P. A., Herrera-Solorio, A. M., Lozano Amado, D., Vargas, M., & Hernandez-Rivas, R. (2017). PfAP2Tel, harboring a non-canonical DNA-binding AP2 domain, binds to *Plasmodium falciparum* telomeres. Cell. Microbiol. 19(9), 1-12.

Srivastava, A., Badjatia, N., Lee, J. H., Hao, B., & Günzl, A. (2018). An RNA polymerase II-associated TFIIF-like complex is indispensable for SL RNA gene transcription in *Trypanosoma brucei*. Nucleic Acids Res. 46(4), 1695–1709.

Sun, C. H., Palm, D., McArthur, A. G., Svärd, S. G., & Gillin, F. D. (2002). A novel Myb-related protein involved in transcriptional activation of encystation genes in Giardia lamblia. Mol. *Microbiol.* 46(4), 971–984.

Sun, C. H., Weng, S. C., Wu, J. H., Tung, S. Y., Su, L. H., Lin, M. H., & Lee, G. A. (2020). DNA topoisomerase IIIβ promotes cyst generation by inducing cyst wall protein gene expression in *Giardia lamblia*. Open Biol. 10(2), 1-19.

Tong, X., Zhang, D., Buelow, K., Guha, A., Arthurs, B., Brady, H. J. M., & Yin, L. (2013). Recruitment of histone methyltransferase g9a mediates transcriptional repression of fgf21 gene by e4bp4 protein. J. Biol. Chem. 288(8), 5417–5425.

Turowski, T. W., & Tollervey, D. (2016). Transcription by RNA polymerase III: Insights into mechanism and regulation. Biochem. Soc. Trans. 44(5), 1367–1375.

Verma, K., & Datta, S. (2019). Heavy subunit of cell surface Gal/GalNAc lectin (Hgl) undergoes degradation via endo-lysosomal compartments in *Entamoeba histolytica*. Small GTPases 10(6), 456–465.

Waldman, B. S., Schwarz, D., Wadsworth, M. H., Saeij, J. P., Shalek, A. K., & Lourido, S. (2020). Identification of a Master Regulator of Differentiation in *Toxoplasma*. Cell 180(2), 359-372.

Williams, S. A., Chen, L. F., Kwon, H., Ruiz-Jarabo, C. M., Verdin, E. and Greene, W. C. (2006). NF-κB p50 promotes HIV latency through HDAC recruitment and repression of transcriptional initiation. EMBO J. 25(1), 139– 49.

Yuda, M., Kaneko, I., Iwanaga, S., Murata, Y., & Kato, T. (2020). Female-specific gene regulation in malaria parasites by an AP2-family transcription factor. Mol. Microbiol. 113(1), 40–51.

Zhang, W., Petrovic, J. M., Callaghan, D., Jones, A., Cui, H., Howlett, C., & Stanimirovic, D. (2006). Evidence that hypoxia-inducible factor-1 (HIF-1) mediates transcriptional activation of interleukin-1β (IL-1β) in astrocyte cultures.pdf. J. Neuroimmun. 174, 63–73.

Zhang, Y., Pavlov, A., Malik, S., Chen, H., Kim, N., Li, Z., Zhang, X., DePamphilis, M. L., Roeder, R. G., & Ge, H. (2020). Efficacy of a small molecule inhibitor of the transcriptional cofactor PC4 in prevention and treatment of non-small cell lung cancer. PLoS ONE 15(3), 1–16.

Zhao, G. H., Gong, A. Y., Wang, Y., Zhang, X. T., Li, M., Mathy, N. W., & Chen, X. M. (2018). Nuclear delivery of parasite Cdg2_FLc_0220 RNA transcript to epithelial cells during *Cryptosporidium parvum* infection modulates host gene transcription. Vet. Parasitol. 251, 27–33.